



**Università
degli Studi
di Ferrara**



**DOCTORAL COURSE IN
"EARTH AND MARINE SCIENCE (EMAS) "**

CYCLE XXXIII

COORDINATOR Prof. COLTORTI MASSIMO

**Marine environmental observation
through autonomous robotic platforms**

Scientific/Disciplinary Sector (SDS) GEO/02

Candidate

Dott. Ferretti Roberta

Supervisor

Prof.ssa Ivaldi Roberta
Ing. Caccia Massimo
Prof. Coltorti Massimo

(signature)

(signature)

Years 2017/2020

Contents

Abstract	7
Introduction.....	9
1 Kongsfjorden (Svalbard): a critical and key area for marine research	11
1. 1 Climate and meteorology	
1.1.1 Interactions between lower atmosphere and the fjord system	
1.2 Physical oceanography	
1.3 Geomorphology and geology	
1.3.1 Submarine glacial landforms and ice sheets characteristics	
1.4 Glaciers and freshwater supply of Kongsfjorden	
1.4.1 Ice loss processes: meltwater discharge and calving events	
1.4.2 Evolution of the coastline	
1.4.3 Focus on two tidewater glaciers: Kronebreen and Blomstrandbreen	
1.5 Suspended particulate matter and sedimentation processes	
1.5.1 Water Column	
1.5.2 Sediments	
1.6 Underwater radiation regime	
1.7 Gaps of knowledge and research priorities	
1.7.1 The Abiotic Environment	
1.7.2 Land-Sea-Ice-Atmosphere Interactions	
1.7.3 Additional remarks	
2 Metrology for marine environmental monitoring: observation requirements and essential variables	35
2.1 Essential Climate Variables – ECV	
2.2 Essential Ocean Variables - EOVS	
2.2.1 EOVS – Physics	
2.2.2 EOVS – Biogeochemistry	
2.2.3 EOVS – Cross Disciplinary	
2.2.4 Support variables	

- 2.3 Metrological requirements for ECV and EOVS observations
- 2.4 Essential Arctic Variables – EAV
- 2.5 Positioning and range measurements in the context of metrology
 - 2.5.1 Positioning for autonomous vehicles in air
 - 2.5.2 Underwater positioning for autonomous vehicles
 - 2.5.3 Range measurements: seabed bathymetry and ice morphology
- 2.6 Limitation due to critical environments

3 Methods and technologies for observation and monitoring in harsh Arctic environment 53

- 3.1 The need for autonomous platforms to observe the marine Arctic areas
- 3.2 The environment as driver of technological innovation and new observation methods
 - 3.2.1 The PROTEUS USSV example
- 3.3 The “data-driven” acquisition campaigns of the CNR-INM Group
 - 3.3.1 Sea surface and air column characterization – 2017 UVASS campaign
 - 3.3.2 Water column, sea surface and air column characterization - 2018 Campaign

4 Svalbard Field Data 73

- 4.1 Kongsbreen Glacier
- 4.2 Conwaybreen Glacier
- 4.3 Blomstrandbreen Glacier
- 4.4 Air data analysis
 - 4.4.1 Kongsbreen
 - 4.4.2 Blomstrandbreen

5 Scoglio d’Affrica (Northern Tyrrhenian Sea): seabed gas emission observations 123

- 5.1 Geological and morphostructural setting of the area
- 5.2 Magnetic anomalies
- 5.3 Introduction on methane emissions
 - 5.3.1 Gas seeps in the Tyrrhenian Sea: occurrence and distribution
 - 5.3.2 Scoglio d’Affrica emission site
 - 5.3.3 The discovered Mud Volcano: geochemistry and origin of methane at Scoglio d’Affrica

6 Methods and technologies for seabed gas emissions observation and monitoring in Northern Tyrrhenian Sea	139
6.1 The need for an integrated observing system to study seabed gas emissions in the Tyrrhenian Sea	
6.2 Integrated seabed gas emissions observing system: the contribution of marine robotics	
6.2.1 e-URoPe operations and acquisition procedures during the 2019 “Scoglio d’Affrica” campaign	
7 Seabed gas emissions in the Scoglio d’Affrica area: data collection and analysis	149
7.1 Morpho-acoustic data	
7.2 e-URoPe dives and video data acquisition	
7.2.1 Time synchronisation of the data	
7.2.2 Data analysis and emissions points identification	
7.3 Rapid environmental assessment: map of gas emissions points	
8 Discussion of transient phenomena observations in Svalbard and Northern Tyrrhenian Sea	169
8.1 Oceanographic processes from tidewater glacier in Kongsfjorden	
8.2 Shallow water gas emissions in the Scoglio d’Affrica	
9 Concluding remarks	189
Bibliography	193
Acknowledgments	209

Abstract

The main objective of the research activity described in this thesis is the development of methodologies and procedures to carry out observing operations of transient phenomena in critical marine environments through the use of autonomous robotic platforms for the acquisition of physical and bio-geo-chemical parameters and for the seabed characterisation.

The particularity of this work consists in a strong connection with metrology together with observing methodologies, based on robotic platforms, adjustable according to the specific marine environment being studied, in order to obtain results that are reliable, reproducible and comparable with those obtained through the classic monitoring methodologies. The environments in which the tests were executed are particularly dynamic, sensitive and fragile areas where it is necessary to study and apply particular methodologies to observe phenomena strongly localised in space and requiring very high resolutions, in time. Moreover, the critical conditions may present some risks not only for the data acquisition but also for the instrumentation and the operators. This is the case, for instance, of polar marine environment in the proximity of tidal glaciers and of Tyrrhenian Sea in areas characterized by seabed degassing activities, where monitoring procedures using robotic platforms can allow the safe observation of not repeatable and not completely predictable events.

Chapter 1 deals with the description of the complexity of the Svalbard environment, highlighting its role as a critical but at the same time a key environment for marine research. In particular the focus is on the description of the climate and meteorology, the physical oceanography, the geomorphology and geology of the Kongsfjorden. Moreover, a description of the tidewater glacier and the processes of meltwater supply in the fjord system is reported.

Chapter 2 gives an introduction of the metrology principles, necessary for the environmental observations. The Essential Climate Variables (ECV) are described, paying particular attention to Ocean (EOV) and Arctic (EAV) ones. Furthermore, the problem of positioning and measuring the range in the context of metrology is addressed. This is a crucial point, especially when acquisition operations take place in critical environments such as the Arctic.

Chapter 3 deals with describing the methodologies and technological solutions adopted for observations in the Arctic area. In particular, the reasons that lead to the choice of the use of robotic platforms in this area are highlighted. The environment and its limitations are the factors that drive the development of new technologies and the use of new observation methods. In this context, the PROTEUS robotic vehicle is described, and the data acquisition campaign carried out in 2018 in the Kongsfjorden by CNR-INM (Italian National Research Council - INstitute of Marine engineering), in collaboration with other research institutes, is illustrated. Sampling of water and acquisition of physical and bio-geo-chemical parameters along the water and air column took place near the fronts of four tidewater glaciers. In chapter 4 the analysis of these data is performed in order to characterise particular processes that occur near the front of these glaciers: analysing specific variables, such as temperature, salinity, turbidity, chlorophyll-a, it was possible to identify the distribution of the water masses and the presence, in some points, of the plume of meltwater coming from the glacier, before the mixing with the water of the fjord and the detection of particular surface

water named “Sill Surface Water”.

In chapter 5 the seabed gas emissions phenomena in the Northern Tyrrhenian sea are introduced. In particular a description of the area from a geographical, geological and morphostructural point of view is depicted together with the introduction of the seabed methane emissions. The complexity of these kind of events requires to have an integrated observation system which allows to characterise the area from different points of view, also with the introduction of marine robotic platforms. In particular, the use of the CNR-INM robotic platform e-URoPe during a campaign organized in June 2019 by the Italian Hydrographic Institute in collaboration with other research centers, like the University of Ferrara, is described in chapter 6. During this campaign, e-URoPe was used for the collection of video images in a sub-area of interest of the larger area inspected with the high resolution MBES from ship (ITS Magnaghi, Italian Navy Ship) and from support boats. In chapter 7 the collected data are analysed with the purpose of georeferencing the video images acquired with the ROV and integrating them with the acoustic data from MBES in order to create a map of the emission points in the area of the Scoglio d’Affrica. The data were then integrated with the results of the geochemical analysis on the gases sampled during some previous campaigns held in the same areas. Furthermore, the ROV data were used to enrich the morphological and geochemical information known in literature: this allowed to obtain insight information on the temporal and spatial evolution of gaseous emissions in the area of the Scoglio d’Affrica.

Chapter 8 discusses the results obtained during the data analysis phase, in relation to what is known in the literature, and shows the novelties with respect to the state of the art: the observation of stratification processes of the water masses near the tidewater glacier in Svalbard, highlighting internal effects due to the morphology with an unprecedented level of detail, and the study of the evolution of seabed gas emission processes in shallow areas of Tyrrhenian Sea, integrating ROV video and acoustic MBES data with geochemical and morphological data. In chapter 9 the concluding remarks of this work are described, highlighting how it provides an approach to the observation of transient phenomena in critical environment, focused on the measurements, the quality of the data and their interpretation. Future technological and scientific developments are also mentioned.

Introduction

Enhancing the marine environmental monitoring and prediction capabilities will increase our ability to respond adequately to major challenges and efficiently preserve both the environment and the ecosystems. Nevertheless, due to the risky and difficult marine environment, more than 80% of the oceans are presently still unexplored and unmapped (Dañobeitia et al., 2020). Moreover, in specific marine environment there is the presence of transient phenomena, particular events that occur in very localized points in space and in time intervals that are very short. The transient character of these events is related to the fact that they are not repeatable and not completely predictable. Despite the obvious practical difficulties, there is considerable interest in the observation and identification of these phenomena, both from the point of view of marine sciences and for the possible consequences in terms of hazards they can generate.

In this work the focus is on transient phenomena that occur in dynamic, sensitive, and fragile areas, often difficult or impossible to reach due to prohibitive environmental and climatic situations that make them critical, and the traditional methods of observations inadequate. For all these reasons, the trend in marine observations goes towards an increasing application of autonomous buoys, moorings, autonomous underwater vehicles (AUVs), and unmanned aerial vehicles (UAVs) (Vihma et al., 2019). Robotic systems are increasingly being utilized as fundamental data-gathering tools by scientists, providing effective solutions to collect high quality data in hazardous environment, mitigating risks and allowing the overcome of some limitations typical of traditional surveys.

These distinctive features require the development of dedicated observation procedures, which on the one hand consider the constraints imposed by the environment in which operations take place, and on the other hand, can satisfy the requests in terms of spatial and temporal resolution and accuracy, necessary to record these transient events. In parallel with the development of specific observation procedures, it is necessary to use instruments and tools that can overcome the limitations associated with traditional methods of observing critical marine environment. In this perspective, the use of autonomous robotic platforms characterized by ease of assembly and adaptability, equipped with instrumentation capable of operating even in demanding working conditions, is of fundamental importance. The critical environmental conditions may present some risks for the data acquisition but can also constitute a limit from a metrological point of view: very often it is not possible to perform repeated measurements due to adverse conditions and therefore measurements referring to the observations of different phenomena are paired even if they are not directly comparable from a metrological point of view. In this context, it is essential to apply multidisciplinary and coordinated measurement procedures to gather data that have metrological traceability thus ensuring compatibility.

This thesis shows the use of robotic technologies and the ability to acquire accurate scientific data in hostile environment, where it is not possible to use standard sampling and investigation techniques. The particularity of this work consists in a strong connection with metrology together with observing methodologies adjustable according to the specific marine environment being studied, to measure accurate variables in cost effective and safe way and to obtain results that are

reliable, reproducible, and comparable with those obtained through the classic monitoring methodologies. An original part of this work is the collection of data concentrated on a very short time scale within which instantaneous and strongly localized in space phenomena occur but with consequences on the environment that also extend over longer time scales.

Two case studies are described: water mass stratification with possible presence of plume of meltwater from glaciers in Svalbard and seabed methane emissions in the Tyrrhenian sea. The critical conditions to which the measuring instruments are subject, the dangers to which operators may be exposed, the constraints on data acquisition operations in the two environments chosen as case studies are certainly different. In the case of the Arctic, the main difficulties are related to possible malfunctions of the instruments due to the low temperatures in which they work, the operators are exposed to risks related to the sudden detachment of pieces of ice from the fronts of the glacier and in general there are constraints on the possibility of manoeuvring also linked to restrictions in navigation inside the fjord near the glaciers. As for the case of the Tyrrhenian Sea, the working conditions are more standard as regards the temperature in which the instruments operate but there are still critical issues related to the safety of navigation and operators in an area that can be subject to violent gas explosions from the seabed, with consequent leakage of material mixed with gas even above sea level. Furthermore, the limitations on ship operations in this area are related to the low depth of the seabed and the inability to reach the place of interest for the observation. Although each of the two environments has specific criticality linked to the particular working conditions, both are subject to the presence of transient phenomena, which require very high performance from the operators and instruments in terms of spatial and temporal resolution. For these reasons, the approach followed for the observation and study of these phenomena was common to both case studies: specific observation methodologies, using autonomous vehicles and procedures strictly connected to the principles of metrology and adapted to the particular environment, made it possible to achieve important results with high effectiveness, overcoming various practical difficulties. In particular, the collection of data near the front of tidewater glaciers in the Arctic environment gives the possibility to study the processes of stratification of water generated from glacial melting in an area unexplored and unsampled before, due to the dangerousness related to calving events. Investigations of the oceanographic parameters were conducted at a small scale with high accuracy and precision. Similar requirements on the data quality are necessary to study the evolution in time of the emission points in the Northern Tyrrhenian Sea, where seabed gas emissions phenomena take place. A robotic platform, characterised by peculiar geo-referencing tools with elevated accuracy, was employed to map the gas emissions points using the video images acquired in an area difficult to assess due to possible violent and explosive degassing activity. The data acquired allow to enrich the morphological and geochemical information known in the literature, obtaining in-depth information on the temporal and spatial evolution of gaseous emissions in the Scoglio d'Affrica area.

The thesis addresses the two case studies separately, describing the specificity of each environment, the procedures implemented for data collection and subsequent analysis to enhance the results obtained in each area. The scientific discussion and the concluding remarks deal with giving a general view of the valuable results obtained, comparing them with what is already present in the literature, highlighting the important advances obtained in terms of observation of transient phenomena in hostile environment with innovative techniques, focused on the measurements, the quality of the data and their interpretation.

Chapter 1

Kongsfjorden (Svalbard): a critical and key area for marine research

The Arctic Ocean is undergoing a rapid warming process. In the past few decades, Arctic average temperatures increased at twice the rate observed in the rest of the world (A.C.I.A, 2004).

The current climate changes and their impacts make it imperative to increase our knowledge of climate–ocean–glacier systems: Arctic fjords can provide valuable information on this as these high latitude regions are undergoing rapid and considerable alterations due to climate change (IPCC, 2014) and one of the most evident consequences of long-term climate warming is the retreat of glaciers (Halbach et al., 2019). The amplified climatic warming at northern high latitudes makes Svalbard glaciers prime targets for understanding not only glacial dynamics but also the effects of ongoing climate change on glaciers, oceans, and ecosystems (Lindbäck et al., 2018).

Numerous investigations of Svalbard fjords have demonstrated that these possess sediment archives that allow us to reconstruct environmental changes and establish baseline values for change in the Arctic. In particular the Kongsfjorden–Krossfjorden system (Figure 1.1) is a natural archive that provides reference values for polar marine sedimentary environments as, within the last two millennia, the glaciers on Svalbard fluctuated repeatedly and the Kongsfjorden–Krossfjorden system has gone through significant environmental change (Husum et al., 2019).

Kongsfjorden, and more generally Svalbard environment, is strongly influenced by the presence of marine terminating glaciers. Glaciers that flow into the sea and terminate in an ice cliff from which icebergs are discharged are called tidewater glaciers (Van Der Veen, 1996) and the breakage of icebergs from the cliff is termed “calving”. They constitute more than 60% of the total ice–covered area. Examples of tidewater glaciers in the Kongsfjorden are Kronebreen and Kongsvegen at the head of the fjord, and Conwaybreen and Blomstrandbreen on its northern coast (Svendsen et al., 2002).

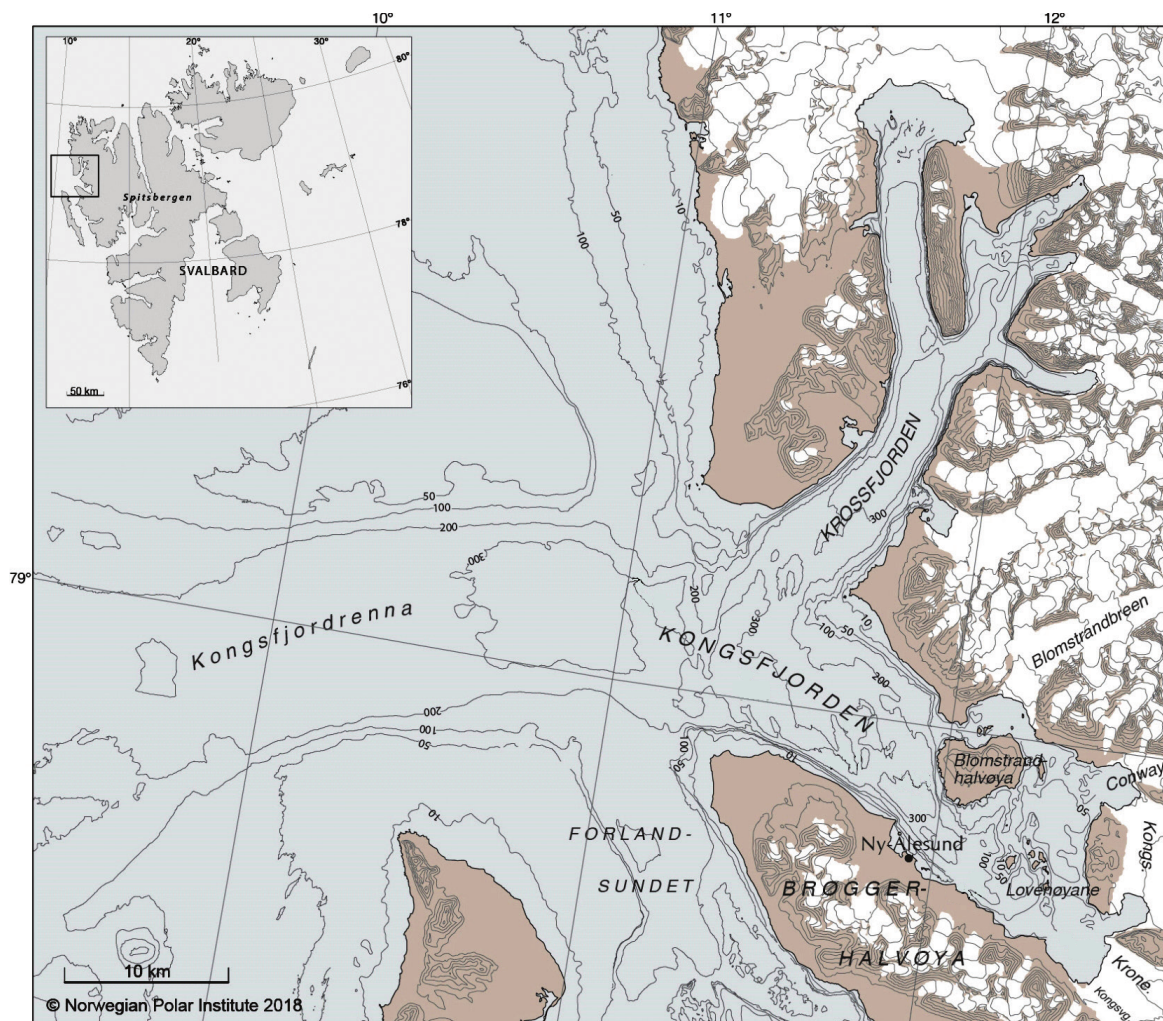


Figure 1.1 - Bathymetric map showing the system formed by Kongsfjorden and Krossfjorden. Depths are given in meters. Names of some of the tidewater glaciers have been abbreviated as follows: “Conway” is Conwaybreen, “Kongs” is Kongsbreen, “Krone” is Kronebreen and “Kongsvg” is Kongsvegen. Source: Husum et al. (2019).

Moreover Kongsfjorden is characterized not only by large environmental gradients driven by melt water processes along the edges of tidewater glaciers but also by the inflow of relatively warm Atlantic Water from the West Spitsbergen Current (WSC), the main heat source for the European Arctic (Figure 1.2) (Husum et al., 2019). This feature is due to the fact that Kongsfjorden is an open fjord, without a sill, and is connected to Fram Strait, a gateway to the Arctic Ocean, through the trough Kongsfjordrenna, which extends from the fjord to the shelf break.

For these reasons, Svalbard represents a border area between the Atlantic Ocean, characterized by warmer salty waters, and the Arctic Waters (AW), characterized by low salinity and high concentrations of suspended solids (Hop et al., 2019). Interactions between forces governing the fjord circulation, coupled with the complex bottom topography and coastline, result in a complicated flow pattern and distribution of different water masses within the fjord system (Svendsen et al., 2002). The seasonal variation in freshwater input creates a very stable stratification in summer and very weak stratification in winter. Atmospheric heating during summer and cooling during winter enhance this effect. The upper layer circulation in summer is confined to a shallow surface layer (Svendsen et al., 2002). Advection of Transformed Atlantic Water (TAW) into the

fjord is important for its seasonal oceanographic dynamics, as well as for its biological communities. Even though the Atlantic signal extends throughout the fjord, the inner fjord is considered mostly Arctic with regard to physical and biological characteristics. The inner fjord basin is largely influenced by run-off from tidal glaciers, which create gradients in freshwater influence and sediment load towards the middle of the fjord. Because of the dual Atlantic and Arctic inputs, the fjord houses pelagic and benthic communities that comprise a mixture of boreal and Arctic flora and fauna (Hop et al., 2019). In light of the above, the climate changes will most likely influence the fjord system from two directions - the ends opening out into the sea and the inner ends abutting the glaciers - rendering the fjord system a sensitive indicator of climate change phenomena (Svendsen et al., 2002).

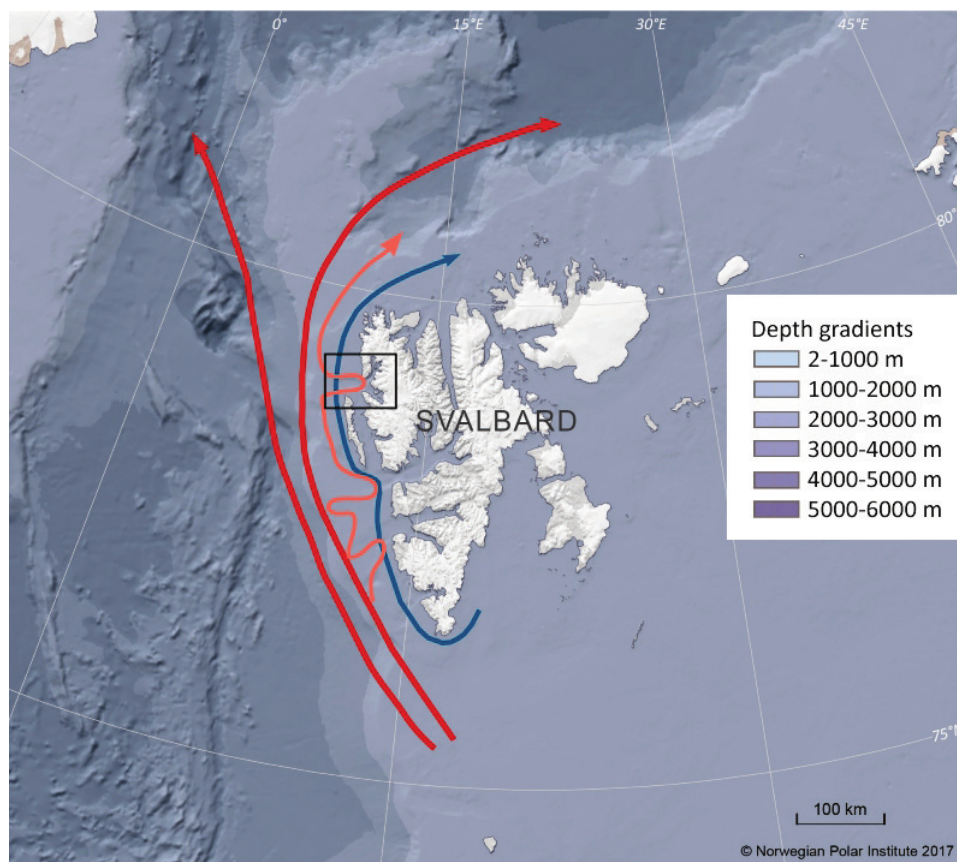


Figure 1.2 - Index map showing Svalbard and dominating current systems. The red lines are branches of the West Spitsbergen Current. The pink line is the Spitsbergen Trough Current. The blue line is the Spitsbergen Polar Current. The black square shows the location of the Kongsfjorden–Krossfjorden system. Source: Husum et al. (2019).

The Kongsfjorden area has a rich history of research and monitoring activities, much of which are associated with the currently research stations at Ny-Ålesund (Figure 1.3) (Hop et al., 2019), and these data are useful for an overview of the system at a global level (geological, geophysical, geochemical, micro-biological, etc...) so that we can study how various phenomena influence each other and what effects they can produce. Long term observations are fundamental to distinguish between seasonal variability and climate-induced changes. An overview of the Kongsfjorden system will be made below to illustrate its characteristics from different points of view.



Figure 1.3 – Ny-Ålesund research stations from above. (Photo: Jürgen Graeser)

1. 1 Climate and meteorology

The climate of Svalbard is strongly influenced by the atmospheric general circulation, the annual variation in light conditions, Arctic sea ice extent and ocean currents. The most common wind direction on Spitsbergen is always along valleys or fjords from inland to the sea, and the prevailing winds are from the north-east to the south-east sectors, except during summer.

The wind conditions in Kongsfjorden are to a large extent governed by orographic steering of the large-scale wind fields and katabatic winds transporting cold dense air from the inland glaciers to the warmer fjords (Svendsen et al., 2002). The most prominent feature is the main wind direction

from east/south-east (around 110°) which is present throughout the whole year, but with highest wind velocity in the cold period between autumn and spring. A second frequently observed wind direction is from south-west (around 225°), related to katabatic outflow from the Brøggerbreen glaciers channeled along the slopes of the Zeppelin mountain range south of Ny-Ålesund. While all other wind directions occur likewise all year around, wind from the North (around $0^\circ/360^\circ$) is almost exclusively observed during the summer period, with velocities less than 5 m/s. This wind from the fjord in the North towards the mountain in the South is likely to be a sea breeze formed by increasing temperature differences between the land and water, especially as it occurs only during the snow-free period of polar day (Maturilli et al., 2013).

The solar radiation exhibits a clear seasonal trend, with high values in spring and summer, and near-zero values from November to January, i.e. during the polar night, as expected due to the location of the fjord. Air temperature modulates the surface ice melting, and hence also the englacial and subglacial water drainage network. Similar to solar radiation, air temperature also showed clear seasonal oscillations, with higher values in summer (up to 12°C) and lower values in winter (down to a minimum of -24.4°C).

Rainfalls showed a typical seasonal pattern with more frequent events during warmer seasons, especially in early September (D'Angelo et al., 2018).

The knowledge of the seasonal and inter-annual trend of the climatic and meteorological conditions of the fjord is fundamental because these conditions influence numerous physical, chemical and biological processes that take place in the fjord such as, for example, water masses stratification and circulation, calving and submarine melting of glacier, nutrient supply and primary production.

1.1.1 Interactions between lower atmosphere and the fjord system

The recent change in the atmospheric circulation favors an increased advection of moist and warm air from the lower latitude Atlantic region, causing atmospheric warming over Svalbard. This is valid not only for surface temperatures, but for the entire troposphere (Van den Heuvel et al., 2020). Melting of sea ice and other climate change effects influence also the marine ecosystem, including phytoplankton and their productivity. As phytoplankton are also emitting biogenic vapors into the atmosphere, these changes may have consequences to atmospheric chemistry, secondary aerosol (solid or liquid particles suspended in the air) formation and clouds. Low-level clouds above Arctic sea ice and open waters play an important climatic role that is connected to the characteristics of the sea ice. Above highly reflecting ice surfaces, low-level clouds decrease the radiative cooling of the surface which keeps the ice warmer than it would be without clouds. The formation of clouds depends on the prevailing meteorological conditions, but the optical properties of clouds are determined by both their micro- and macro-physical characteristics. So there are strong interactions and associated feedbacks between aerosol – cloud – sea ice loss – climate.

Black carbon aerosol may also affect the physical and radiative properties of clouds or, when deposited on the ground, impact the regional radiation balance by reducing snow and ice surface albedo.

In this context it is of fundamental importance to measure atmospheric parameters along the vertical profile. Recent technological development has enabled production of small, low-cost sensors with capabilities similar to those used in the laboratory. These sensors can be installed on balloons or small unmanned aerial vehicles, allowing direct measurements in the lower atmosphere.

Supplementing the traditional infrastructure for the vertical probing of atmospheric variables with drones, unmanned aerial vehicles, and balloons will not only enhance the understanding of the Arctic atmosphere, but also facilitate the use and interpretation of remote sensing observations (Van den Heuvel et al., 2020).

1.2 Physical oceanography

A generally accepted classification of water masses in the Nordic seas defines the characteristic values of the AW transported by the West Spitsbergen Current as temperature $> 3\text{ }^{\circ}\text{C}$ and salinity > 34.9 PSU. A considerable portion of the AW entering Kongsfjorden mixes with another type of water, Arctic Water (ArW), while it crosses the continental shelf, and consequently differs significantly from the water at the core of the WSC; this is called the Transformed Atlantic Water (TAW). Although the TAW also derives partly from ArW, it has a relatively higher temperature than the Arctic Ocean, which leads to the creation of particular physical conditions within the enclosed part of the Kongsfjorden. Moreover, an extremely low temperature ($T < -1.4^{\circ}\text{C}$) water mass was found near the glacier walls: this water derives from ice melting and winter convection, and is characterized by high salinity values (> 34.4 PSU). As it derives from winter convections, it was classified as Winter Cooled Water (WCW). In the inner basin of Kongsfjorden it is also possible to find a Surface Water (SW) that is characterized by low salinity: it derives from snow, ice and glacier melt (Svendsen et al., 2002).

The current interest in the Kongsfjorden is primarily based on the fact that this fjord is particularly suitable as a site for exploring the impacts of possible climate changes as they will most likely influence its partially closed water body from both ends: the outer fjord influenced by oceanographic conditions and the inner fjord influenced by large tidal glaciers. Alteration of melting of the glaciers will change the run-off pattern, and temperature and/or salinity changes in the adjacent Atlantic and Arctic water will cause changes in the fjords through exchange processes (Svendsen et al., 2002).

In this context, documented and projected alterations in the physico-chemical environment in the Kongsfjorden system include:

- atmosphere and ocean warming;
- decrease of winter sea-ice cover;
- glacier retreat;
- higher terrestrial run-off resulting in increasing nutrient, sediment and soil-associated contaminant loads;
- ocean acidification;
- changes in light climate, particularly ultraviolet B exposure.

1.3 Geomorphology and geology

The system formed by Kongsfjorden and Krossfjorden is located on the western coast of Spitsbergen (Svalbard) between $78^{\circ} 40'$ and $77^{\circ} 30'$ N and $11^{\circ} 3'$ and $13^{\circ} 6'$ E. The southern arm of

the system, Kongsfjorden, is oriented from south-east to north-west. Kongsfjorden is 20 km long and its width varies from 4 to 10 km, reached at the mouth between Kvadehuken and Kapp Guissez. The bathymetry of the fjord is complex (Figure 1.1), with sills, basins and glacially streamlined exposed rock basement (Howe et al., 2019) and there is a well-marked inner fjord with relatively shallow water, less than 100 m deep (Svendsen et al., 2002). Kongsfjorden is situated on a major tectonic boundary between the Tertiary fold-thrust belt of western Spitsbergen to the south-west and the Northwestern Basement Province of Svalbard to the north-east (Bergh et al., 2000; Svendsen et al., 2002).

Landforms around Kongsfjorden are shaped by glacial activity. The Kongsfjorden area shows a more complete glacial sedimentary record—back to ages older than Eemian (the last interglacial)—than most other places in Svalbard.

The area is characterized by a contrast between the alpine relief and coastal platforms. Active glacial, hydro-glacial, periglacial and coastal processes influence the landscape. In front of terrestrial glaciers streams rework the moraine deposits. The rivers form braided drainage systems that create wide sandurs with a number of small channels that are seasonally active, and with coarse fluvial deposits and limited vegetation. The main sedimentation source is from the subglacial meltwater discharge from the tidewater glaciers. Rates of silt/clay sedimentation (unconsolidated sediments) at the ice front are $> 10 \text{ cm a}^{-1}$ (Svendsen et al., 2002).

Concerning the seabed morphology, since 1980 acoustic seafloor data have been collected from Kongsfjorden by a number of workers to document the glaciomarine sedimentary environments and their depositional chronology. The processed images of the multibeam bathymetry show that the seabed morphology is highly variable throughout Kongsfjorden, with the central and outer part dominated by outcrops of bedrock, presumably Devonian-age conglomerates and sandstones with a thin ($< 10 \text{ m}$) sediment cover (Howe et al., 2019).

1.3.1 Submarine glacial landforms and ice sheets characteristics

The submarine landforms, produced at the base and margin of past ice sheets, remain well preserved on the seafloor in fjords and on high-latitude continental shelves after the retreat of the ice that produced them. The development of multi-beam echo sounding over the past two decades, coupled with high-accuracy GPS positioning, has allowed morphological mapping of the seafloor at an unprecedented level of detail. The study of submarine glacial landforms is useful not only to reconstruct the evolution of ice sheets during different glacial interglacial cycles but also to recover different types of information:

- maximum extent of grounded ice sheets: it can be derived from ice-marginal retreat moraines and from grounding-zone wedges (GZWs) which are typically transverse-to-flow of ice;
- flow direction: the fact that many subglacial landforms are elongate, with long axes orientated in the direction of past ice flow, means that flowlines within past ice sheets can be reconstructed. The orientation of the ploughmarks also gives information on the routes followed by the icebergs and on the direction of the ocean currents;
- dynamics of ice sheets: the distribution and nature of submarine glacial landforms can also be used to infer aspects of the past dynamics of ice sheets, in particular on past ice-flow velocities (fast or slow flowing ice);

- style and rate of ice-terminus retreat: where mega-scale glacial lineations (MSGs) are preserved undisturbed along all or part of a trough, this provides an indication that deglacial ice retreat was rapid. On the contrary, where series of small transverse-to-flow retreat ridges are present in cross-shelf troughs, this indicates the slow retreat of a grounded ice margin;
- conditions and phenomena at the ice-bottom interface: the beds of modern ice sheets, and the ice streams that drain the bulk of their mass to the ocean, are overlain by several kilometers of ice, making high-resolution geophysical investigations of the ice-bed interface difficult. By contrast, well-preserved submarine landforms and sediments on formerly ice-covered continental shelves provide a window onto this interface that is much easier to study using swath-bathymetric and seismic-reflection equipment deployed from research vessels. In Figure 1.4 different examples of glacial landforms are shown (Dowdeswell, 2016).

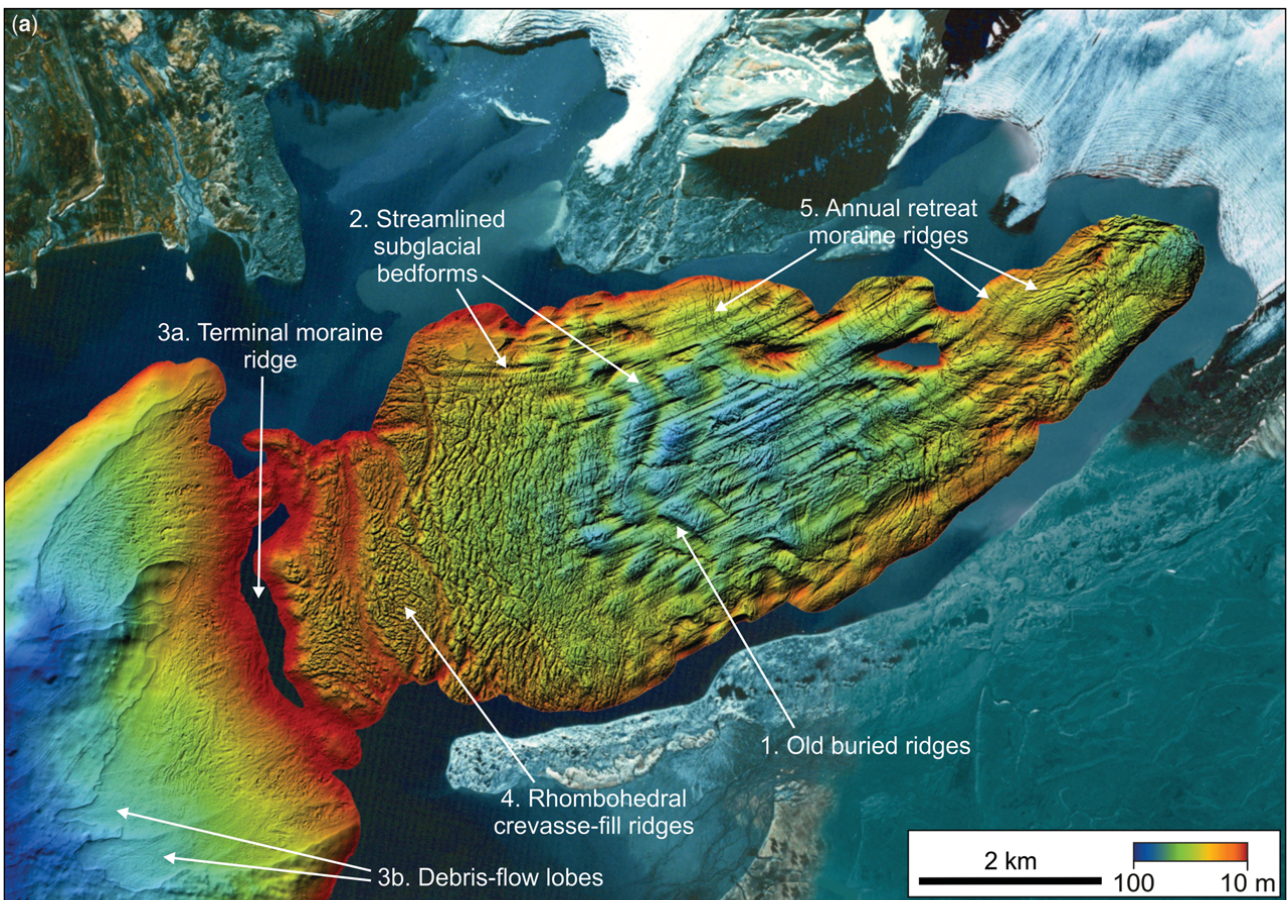


Figure 1.4 - The varying preservation of glacial landforms in marine environments after deglaciation less than 100 years ago. Multibeam-bathymetric image of the seafloor of Borebukta in western Svalbard, adjacent to two tidewater glaciers. Five types of glacial landforms (1, oldest, to 5, youngest) are superimposed, illustrating a very well-preserved assemblage of submarine landforms (modified from Dowdeswell, 2016).

As for the Svalbard, the seafloor close to the retreating termini of a number of surge-type glaciers, especially the tidewater glaciers, is characterised by distinctive sets of submarine glacial landforms: complex subglacially formed sedimentary ridges, a few metres in height and spaced a few hundred metres apart, provide a reticulate or box-work pattern on the seafloor and are sometimes referred to

as rhombohedral moraines (Figure 1.5, left). These sets of submarine glacial landforms are interpreted to have formed at the base of largely stagnant ice, as soft subglacial sediment is squeezed up into basal crevasses. This process is inferred to take place particularly at the termination of the active, fast-flowing stage of the surge cycle in surge-type glaciers (Dowdeswell, 2016).

Today, turbid meltwater plumes are observed regularly in summer beyond many tidewater glaciers in Svalbard. The meltwater and suspended sediments making up these plumes, and providing sediments to build ice-proximal fans, are derived from the mouths of subglacial channels at the base of tidewater ice cliffs. Tidewater glaciers in these areas exhibit varying degrees of ice-surface melting that dominate the basal hydrological system and its development over a given summer. Tunnels valleys and eskers (Figure 1.5, right), along with ice-proximal fans that are sometimes linked to so-called beads within esker systems, are indicators of relatively mild climatic conditions during Quaternary full-glacial periods. At these times, modeling suggests that the mid-latitude margins of ice sheets experienced abundant surface melting that contributed to the formation of subglacial channels which filled with sorted and sometimes relatively coarse-grained sediments as discharge waned (Dowdeswell, 2016).

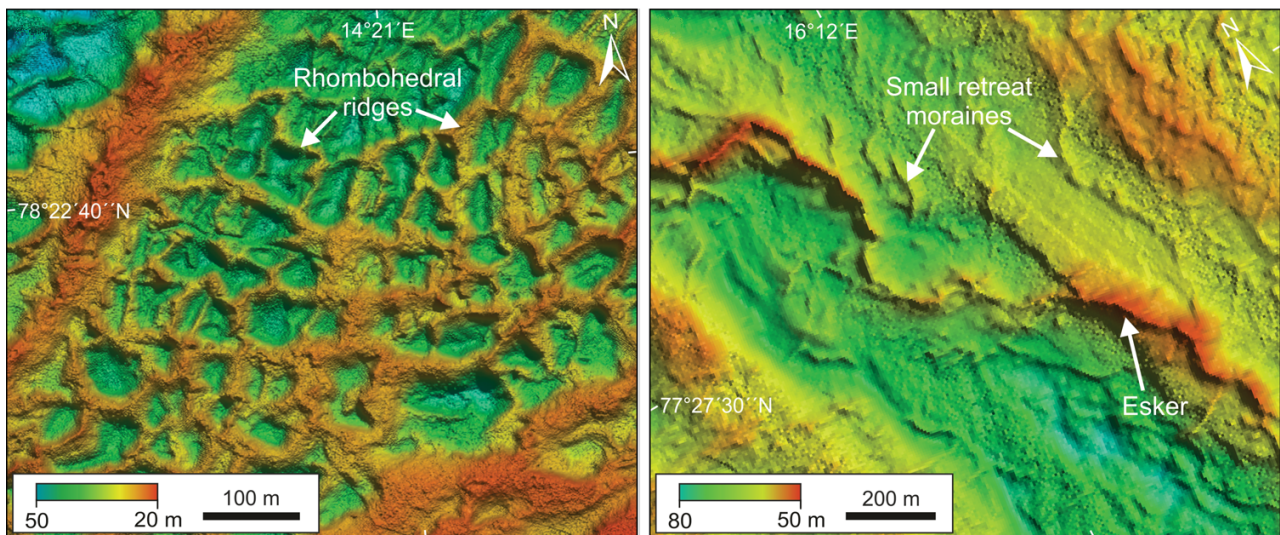


Figure 1.5 – Left: submarine examples of non-streamlined subglacial landforms: rhombohedral pattern of crevasse-fill ridges in a Svalbard fjord. Right: submarine examples of landforms produced by subglacial meltwater: an esker, with small transverse ridges superimposed on it, in Svalbard fjord (Source: Dowdeswell, 2016).

The volume of several submarine glacial and related landforms discussed above, together with the estimated time that they take to build up, is plotted in Figure 1.6. Marine-geophysical observations of area and thickness are available to characterize the approximate volume of each submarine landform type, but less control is available on the time taken for such landforms to develop, so this axis is therefore less closely constrained. It can be observed that the volume of specific glacial and related submarine landforms, and the time needed for their formation, scale together. The relationship is explained, in part at least, because the development of many different subglacial and ice-proximal landforms is related to the rate of transport and delivery of deformable till at the base of glaciers and ice sheets. Where ‘catastrophic processes’, such as iceberg-calving events or

outburst floods of meltwater, are involved, the time frame is obviously very short, but the volumes of sediment deposited or reworked are usually less than about a cubic kilometer and often only small fractions of that volume (Dowdeswell, 2016).

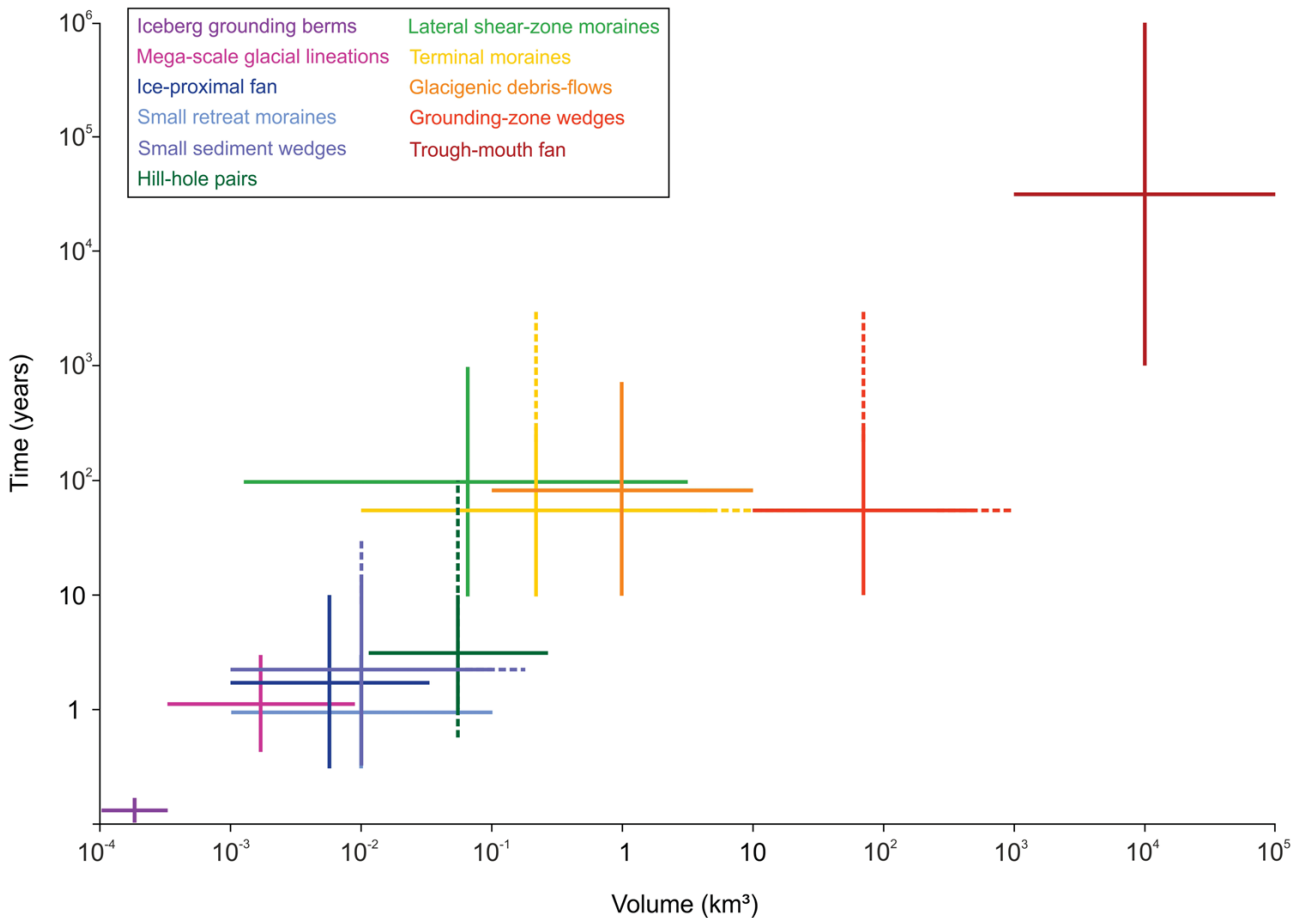


Figure 1.6 –Graph showing the estimated range in volume of several submarine glacial landforms and the approximate timescales over which they build up. Note the order-of-magnitude scales. Source: Dowdeswell, 2016.

Short-term observations of critical events, therefore, involve relatively small volumes of ice. However, these observations can be related to the effects of long-term events (long timescale) through the study of morphological formations involving large volumes and large spaces. In this context, examination of the glaciomarine sedimentary record at increasingly high resolution is important also because it has revealed the complexity of ice-sheet dynamics during retreat from full-glacial ice at the shelf edge. Cross-cutting relationships between glacial landforms, often produced over just a few thousand years or less, imply shifting interactions and feedbacks between sea-level rise, warming climate and the changing relationship between mass loss by iceberg production and meltwater runoff as deglaciation proceeds across shelves and fjords of varying depths (Dowdeswell, 2016).

1.4 Glaciers and freshwater supply of Kongsfjorden

The main glacierised area consists of the large glacier complex in the inner part of the fjords, with several calving fronts at the head of the fjords. Like most of Svalbard's glaciers, glaciers in the Kongsfjorden basin are subpolar or polythermal, which means that parts are temperate (above or close to zero) where meltwater can be present and parts are cold (below zero) (Svendsen et al., 2002).

The tidewater glaciers both retreat and advance much faster. The maximum extent is more difficult to locate precisely, but can be mapped from sub-sea moraines and direct observations. For example the maximum extent of Blomstrandbreen occurred at an unknown date probably before 1861 and the maximum extent of Kronebreen in 1869 was about 11 km beyond the present day front (Svendsen et al., 2002).

The four main sources for freshwater run-off are glacier ablation, snowmelt, and summer rainfall and ice calving. The main freshwater input to the fjord occurs in the summer season, mainly as melting of snow and ice. The inflow comes from point sources such as outlet channels from the glaciers (Svendsen et al., 2002). Among the effects of the climate changes, the following are of particular interest for the specific research covered by this thesis.

1.4.1 Ice loss processes: meltwater discharge and calving events

The rate of ice loss from a tidewater glacier terminus is the sum of that due to calving, and that due to submarine melting, and is commonly referred to as the frontal ablation rate.

To investigate the controls on measured frontal ablation rates we explore a variety of environmental variables that have previously been associated with calving behavior. These include local weather data (air temperature and precipitation), sea-surface temperature (SST), fjord ice presence and water temperatures at depth in the glacier fjords (henceforth 'sub-surface temperatures') (Luckman et al., 2015). Moreover, how a glacier responds to combination of the listed factors is site specific and is not uniform through space or time. As for the Kongsfjorden, for example, it does not have a pronounced sill meaning the barrier to warm water intrusion is less prominent here than in other locations. There is also a seasonal aspect to the intrusion of Atlantic water. For example, some studies suggest a geostrophic control mechanism for intrusion, whereby a density front at the mouth of the fjord is reduced gradually during spring as the fjord water is modified. This leads to a situation where Atlantic water is able to intrude (Holmes, 2018).

The meltwater inflow generally starts in June, peaks in July-August and ends around September (Dowdeswell, 2016). The glacier meltwater and associated sediment particle load create strong freshwater and turbidity gradients from the inner to the outer part of the fjord (Svendsen et al., 2002). Tidewater glaciers melt along their front where the ice is in contact with warmer fjord water (Schild et al., 2018) and this melt is amplified by local meltwater plumes, which transport large volumes of meltwater from sub- or englacial drainage systems into the fjord (Syvitski, 1989). When subglacial low-density water enters the fjord at the base of the glacier, it rises towards the surface, entraining large volumes of ambient fjord water (Holland et al., 1999; Morton et al., 1956) and can lead to a continuous upwelling of nutrients (Meire et al., 2017). The mineralogical characteristics of the particles eroded by the glacier and contained within the meltwater runoff depend on the

lithology of the underlying bedrock (Ashley, 2002; Halbach, 2019; Hodder et al., 2007; Smith, 1978). The strong correlation between frontal ablation rate and ocean temperature at Kronebreen is indicative of melt-driven convection at the ice–ocean interface, which is highly sensitive to ambient ocean temperature. This opens up the possibility of being able to predict the response of many tidewater glaciers to oceanographic forcing. For this reason, there is a growing need to assess subsurface temperatures at tidewater glacier margins to evaluate the relative prevalence of melt undercut versus other calving processes (Luckman et al., 2015).

The presence of these focused, concentrated discharges of sediment-rich meltwater from large tidal glaciers create steep environmental gradients in sedimentation and salinity along the length of this fjord. The glacial inputs cause reduced biomass and diversity in the benthic community in the inner fjord (Hop et al., 2002) and can strongly influence the ecosystem of the fjord, with subsequent consequences for the benthos and biogeochemistry of the system (Howe et al., 2019). We know that meltwater discharge from tidewater glaciers impacts the adjacent marine environment, for example the glacier meltwater discharge impacts phytoplankton production in the fjord through the reduction of ambient light levels caused by high suspended matter content close to the glacier fronts (Halbach, 2019). Nevertheless the mechanisms and underlying dynamics through which meltwater runoff and subglacial discharge from tidewater glaciers influence marine primary production remain poorly understood, as we still lack data from close proximity to glacier fronts.

The continuous retreat of tidewater glaciers will cause them to eventually terminate on land. The transition from tidewater to land-terminating glaciers may, thus, reduce the input of nutrients to the surface layer with negative consequences for summer productivity (Halbach, 2019). A future Kongsfjorden without tidewater glaciers is likely to have a number of implications. The removal of glacier front plumes should make the overall fjord circulation less dynamic during the summer months, in particular in the innermost fjord basin. As glacier front plumes disappear and subsurface transport towards the glacier fronts decreases, the volume of plankton brought towards the glacier fronts will be reduced. These areas might therefore become less prominent as feeding hotspots for birds, fish and seals preying on zooplankton. The present day vertical redistribution of water masses brings up nutrients to the euphotic zone, which likely sustains primary production after the spring bloom. Light limitation due to high concentrations of suspended sediments inhibits photosynthesis in the vicinity of the glacier fronts, but the cumulative nutrient resupply driven by the numerous tidewater glaciers around Svalbard likely has an effect on coastal productivity (Torsvik et al., 2019).

1.4.2 Evolution of the coastline

Climate warming affects tidewater glaciers through changes in the surface mass balance components, the dynamic response of glaciers, and the influence of warmer water on the ice cliff – ocean water interface. Generally, increased production of icebergs is a result of the dynamic response of glaciers terminating in the ocean to a warmer environment.

Inter–annual variations in the rate of terminus position changes of tidewater glaciers have to be surveyed carefully and their effects separated from those of seasonal fluctuations (winter advance and summer retreat). Published data confirm a general recession of tidewater glaciers in Svalbard (Błaszczuk et al., 2009).

Since the last glacial, the Kongsfjorden–Krossfjorden system has gone through significant environmental change from being filled by a fast-flowing ice stream (Ottesen et al., 2007) to becoming an open fjord, still influenced by tidewater glaciers (Husum et al., 2019).

The tidewater glaciers of Svalbard experience phases of retreat and readvance with subsequent inter-annual seasonal (winter-summer) movement. In addition, some Svalbard tidewater glaciers can experience phases of active surging whereby the glacier front can advance several kilometers, the glacier becomes heavily crevassed and the rate of iceberg calving subsequently increases (Howe et al., 2019). Swath bathymetry of the seafloor of the inner part of Kongsfjorden reveals characteristic landform assemblages of moraines, crevasse-squeeze ridges and glacial lineations that reflect different stages of glacier advance, stagnation or retreat due to climatic forcing or surges caused by internal glacier dynamic (e.g., Forwick et al., 2015).

While tidewater glacier fronts are not reliable as climate indicators, they are nevertheless important to fjord circulation and ecosystems. Since more than half of Svalbard’s ice area terminates in tidewater glacier fronts, a significant part of the glacier melt and rainfall on Svalbard enters the ocean at these fronts; this has a significant influence on the ocean circulation, particularly in constricted bays or fjords (Lydersen et al., 2014). The increased glacier melting and sediment flux from both the glaciers and the coast into the fjord will affect the natural habitats and the ecosystem, with impacts on all trophic levels. Changes of glacier dynamics may also affect planktic and nektic fauna in the water column, in addition to seabirds and marine mammal (Husum et al., 2019).

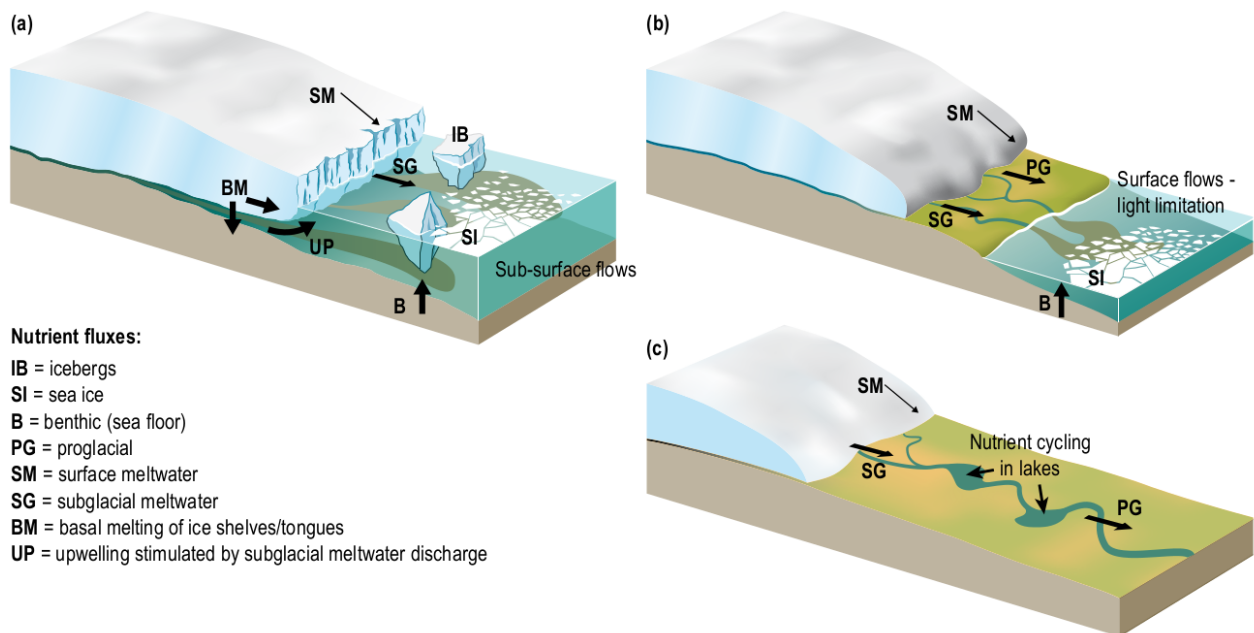


Figure 1.7 - Potential shifts in nutrient fluxes with landward retreat of marine-terminating glaciers (a) at different stages (b and c) – Source: IPCC, Special Report on the Ocean and Cryosphere in a Changing Climate, 2019

Utilizing Landsat imagery estimates of glacial retreat were obtained and indicates that, for example, Conwaybreen has a glacial rate of 47 m/yr and Kongsbreen 250 m/yr. Among others, Kronebreen has experienced the greatest retreat, about 11 km during the last 150 years, yielding an average

retreat rate of 75 m/year; approximately one third of this retreat has occurred just in the last 20 years (Torsvik et al., 2019).

The distribution and movement of some glacier fronts in the region have also been mapped using surface vessels, yet the innermost part of these fjords and the glacier front environments have not been subject to detailed bathymetric and oceanographic surveys. Given the highly dynamic and potentially hazardous nature of the calving front of many glaciers, most direct observations have been made from surface vessels, which for obvious reasons of safety maintain a safe recommended distance (typically > 200 m) (Kohler et al., 2007). The use of an autonomous underwater vehicle (AUV) can both mitigate this risk and collect high quality data almost directly from the active glacial front (Husum et al., 2019).

The evolution of the coast in Kongsfjorden can also be linked to the retreat of terrestrial glaciers and the development of the prodeltas (submarine parts of the deltas), representing a significant volume of sediments deposited directly into the fjord (Bourriquen et al., 2016). However, sediment supply from prodeltas is rarely considered, as they are located close to the land and mainly between 5 and 25 m of water depth, providing challenging conditions for mapping. The quantification of the evolution of the submarine prodeltas has been estimated from side-scan sonar mosaics, revealing that their extent expanded by ca. 40 000 m² from 2009 to 2012 (Bourriquen et al., 2016; Husum et al., 2019).

These observations demonstrate the inter-relationships between bathymetry and hydrography in the glacial front environment. Bathymetric setting can influence local hydrographic conditions and hence lead to glacial front melt (Howe et al., 2019). Long-term studies of coastline changes in Kongsfjorden are therefore needed to quantify and constrain models to measure the impact of the climate warming on the whole Kongsfjorden ecosystem.

It is not yet possible to forecast accurately tidewater front retreat in response to changes in the climatic forcing. However, using historic observations of front positions (Figure 1.8), and glacier bed mapping data which define the extent of the glacier bed below sea level (Lindbäck et al., 2018), we can estimate that full retreat onto land could occur over time-scales of up to decades or a century or two. For example, both Kongsbreen North and Kronebreen (Figure 1.8) have retreated through about half of their submarine bed length since 1860; if the retreat rate were to continue at the same rate, both glaciers would terminate on land sometime after 2100. On the other hand, Blomstrandbreen and Conwaybreen are both near their submarine limits; they likely will terminate on land much sooner, perhaps within a few years to a decade (Hanssen-Bauer et al., 2019).

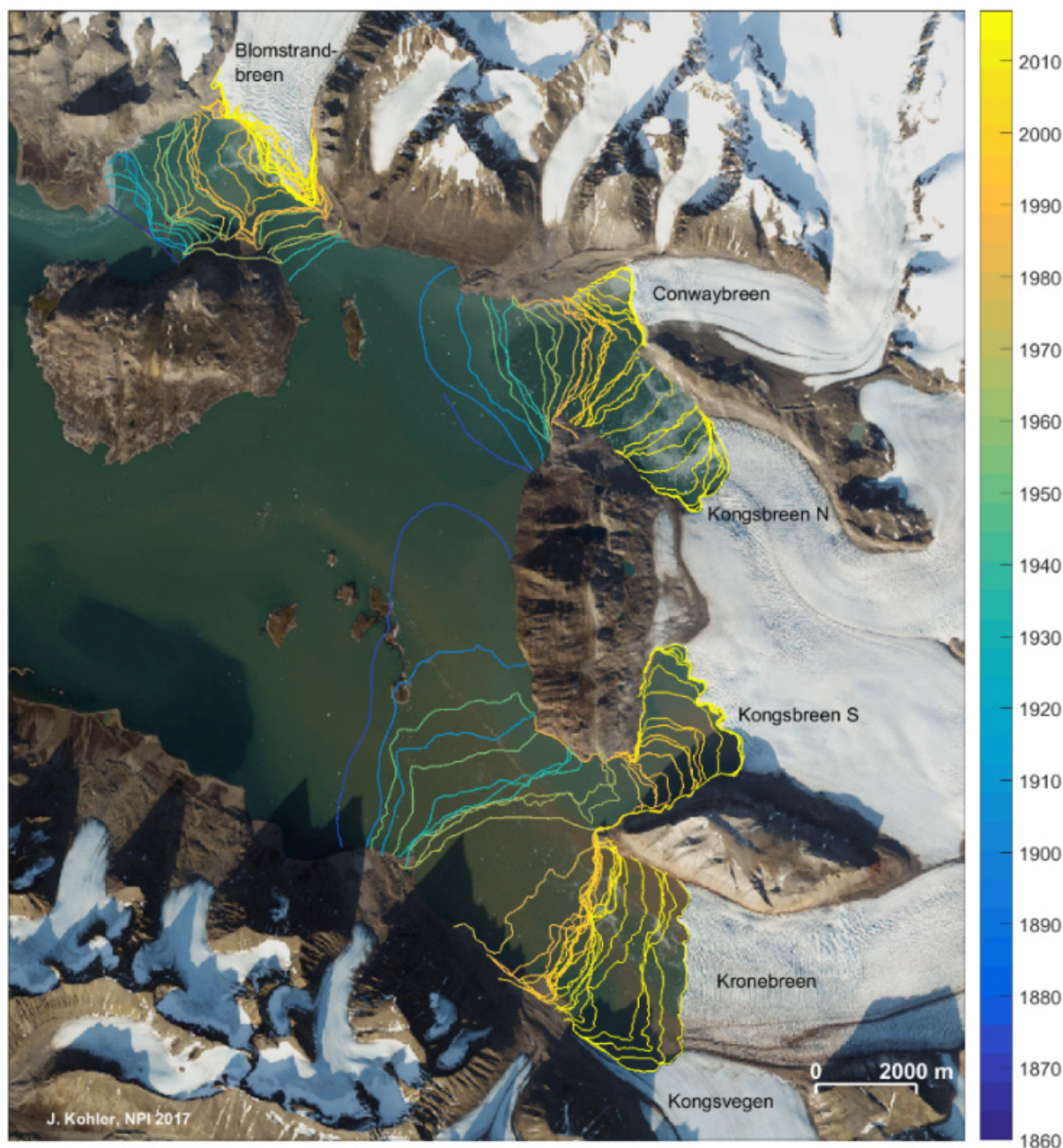


Figure 1.8 - Front positions of tidewater glaciers in Kongsfjorden. Source: Hanssen-Bauer et al. (2019).

Speed-up, thinning, and retreat of marine terminating glaciers are all inherently interlinked and the key research aim is to determine what caused this dynamical change. Ice-ocean interactions are an area of increasing research due to their importance for the issue of glacial mass balance and, as a consequence, sea level rise. This is because elevated mass losses at a marine terminating glacier can have impacts on glacier dynamics and set in motion a positive feedback which leads to further mass loss (Favier et al., 2014). As previously stated, some factors that can affect the dynamics of glaciers and their extent are listed below:

- atmospheric warming leading to increased surface melt and thinning;

- ocean temperatures are of great importance for glacial retreat rates as the intrusion of warm and saline Atlantic water into fjords is thought to be a key driver of retreat;
- local wind patterns related to larger scale atmospheric processes are a key driver of circulation within fjords and can drive different water masses in or out of the fjord (Straneo et al., 2010; Sundfjord et al., 2017);
- internal fjord processes are also of importance. For example, run-off from glaciers or rivers, vertical stratification of waters, and the seasonal warming of surface waters (related to stratification) all have an influence on fjord circulation (Cottier et al., 2005).
- site specific bathymetry: narrow and shallow parts of a fjord ('pinning points') exert a greater resistance to glacier flow, and are associated with reduced retreat rates. Wide and deep parts of a fjord are, conversely, associated with elevated retreat rates (Carr et al., 2015). Variations in bathymetry across a glacier front may also lead to spatial variations in retreat rate.

All these factors concerning the ice-ocean interactions highlights the complex web of processes which occur at glacier terminal locations and explains why there are still gaps in our knowledge (Holmes, 2018).

1.4.3 Focus on two tidewater glaciers: Kronebreen and Blomstrandbreen

Now the discussion will focus on Kronebreen and Blomstrandbreen, two particular glaciers of the Kongsfjorden. The insight into these two glaciers is due to the fact that they are the ones in front of which the experimental data acquisition campaigns, discussed in the following chapters, took place.

Kronebreen is a polythermal outlet glacier in the vicinity of Ny-Ålesund at 78°N, Svalbard, that is fed by Holtedahlfonna (together 295 km²) and Infantfonna (77 km²) and encompasses an elevation range of 0–1400 m a.s.l. (Nuth et al., 2013). Kronebreen surged in 1868 or 1869 and until 1995 the glacier had retreated 10–11 km from its maximum extent (Svendsen et al., 2002). The retreat was interrupted by a surge of the neighboring Kongsvegen in 1948 with a major advance of 4 km. The glacier terminus position has been generally retreating since the middle of the 20th century. It remained steady since the 1990s but has recently experienced a rapid retreat of more than 1 km between 2012 and 2016. As of 2018, the retreat is ongoing.

As a rule, the total glacier mass balance is calculated by adding climatic mass balance (including surface and subsurface processes of internal accumulation and refreezing) and frontal ablation (including calving flux, melt and sublimation of the calving face). Frontal ablation is the most difficult quantity to estimate but it has been observed that Kronebreen has a greater frontal ablation rate, compared with other glaciers in the area (Deschamps-Berger et al., 2019). This fact may be due to the proximity of Kongsfjorden to the WSC and the deep channel that supports a greater exchange of Atlantic-origin waters during summer and autumn causing a more direct and open connection between this glacier terminus and the source of warm water. In addition, Kronebreen has a large ablation area and will therefore experience higher summer melt-water discharges. These factors will encourage more efficient sub-aqueous melting and may help to explain the higher calving rates at Kronebreen.

On shorter timescales, frontal ablation may be influenced by other factors. For instance, spikes in frontal ablation rates at Kronebreen occasionally coincide with terminus velocity peaks causing the

frontal ablation rate to respond more strongly to ice dynamics (Luckman et al., 2015; Schellenberger et al., 2015).

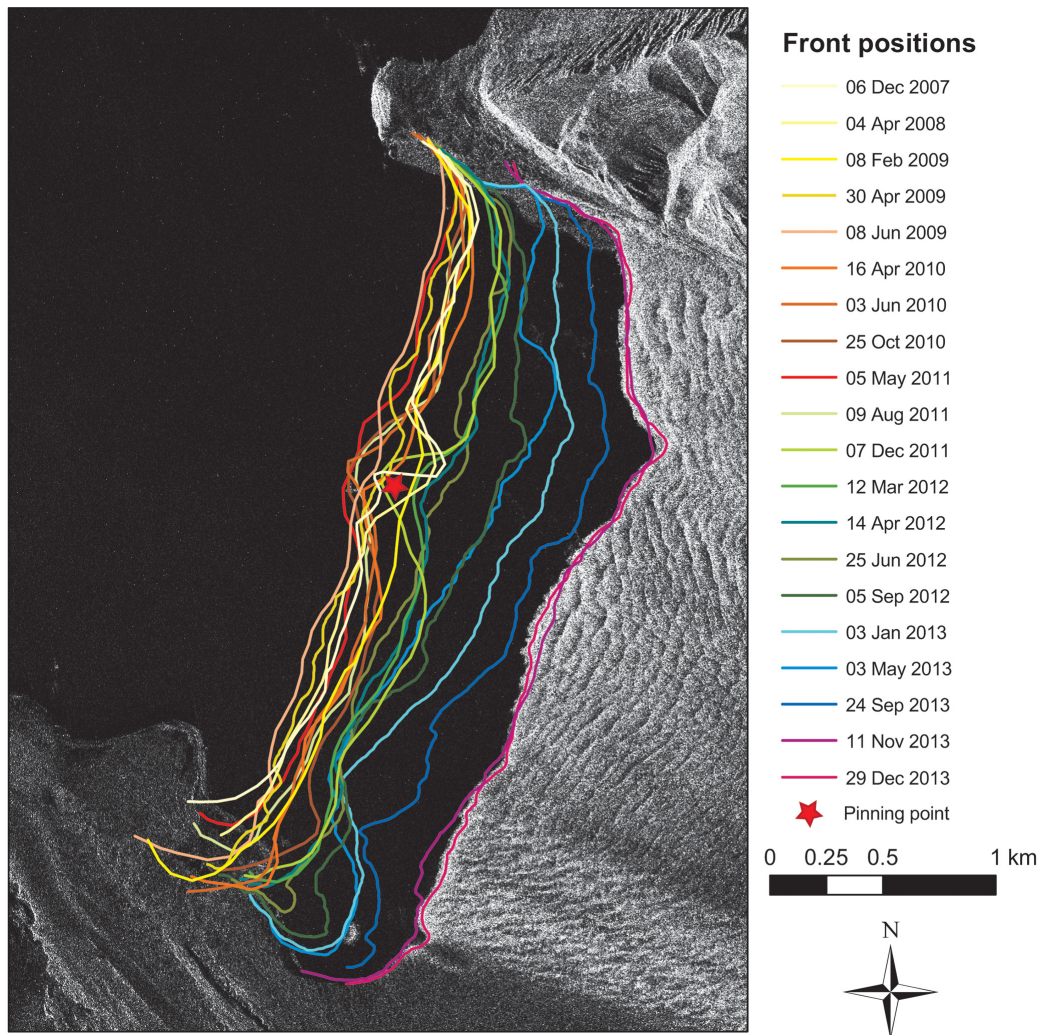


Figure 1.9 - Selected calving front positions of Kronebreen between December 2007 and December 2013. Background image RS-2 UF of 29 December 2013.– Source: Schellenberger et al. (2015).

Blomstrandbreen is an approximately 18-km-long tidewater glacier located in northwest Spitsbergen, that drains toward the southwest from Isachsenfonna into Kongsfjorden. Blomstrandbreen is fed by a number of smaller tributary glaciers, resulting in a total drainage area of approximately 90 km². It is known to be a surge-type glacier, which is relatively common for glaciers on Svalbard, with documented surges between 1911 and 1928, throughout the 1960s, and from 2007 onward. Surging glaciers exhibit cyclical activity with a quiescent phase of stagnation and slow ice flow, and an active phase of increased ice velocities. A surge often causes frontal advances and longitudinal extension that led to severe crevassing and calving if the terminus ends in fjord waters. After a surge event, the glacier returns to a quiescent state until the next surge, which

generally occurs decades to centuries later. The average retreat rate of Blomstrandbreen in the western channel from 1966 to 2009 is 55 m yr⁻¹. However, the bathymetric data reveal that intermoraine spacing is highly variable, with some sets of moraines being closely spaced (within 5 m), and some ridges being separated by more than 55 m (Burton et al., 2016).

The island of Blomstrandhalvøya in central Kongsfjorden was connected to the mainland of Spitsbergen by Blomstrandbreen and became an island between 1990 and 1994, when its connection by glacier ice to the mainland of Spitsbergen was broken. Nowadays a 4-km-wide bay, referred to as Nordvågen, which consists of two distinct main channels, separates Blomstrandbreen and Spitsbergen (Burton et al., 2016).

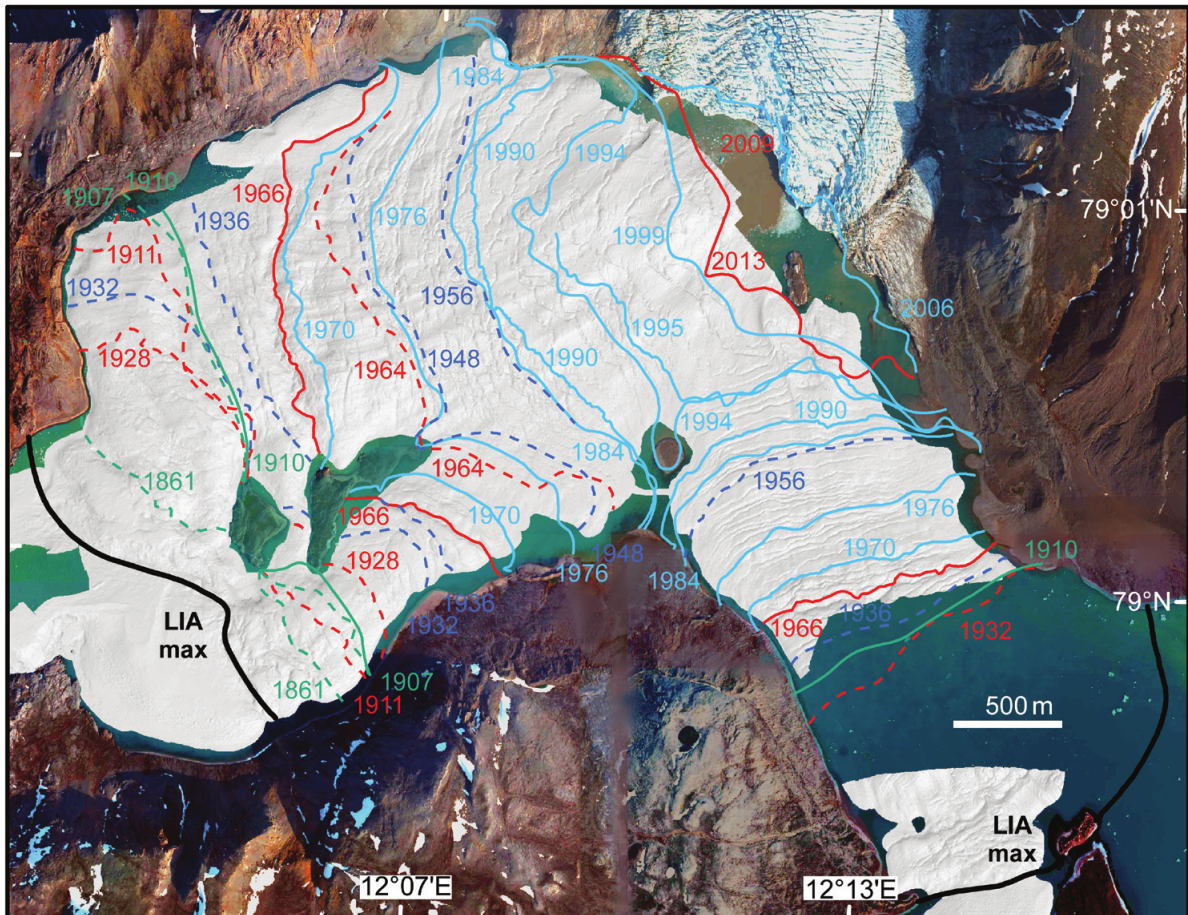


Figure 1.10 - Glacier margin fluctuations of Blomstrandbreen. Positions of the former ice-front are from a combination of evidence from Liestøl (*The glaciers in the Kongsfjorden area, Spitsbergen, 1988*), Landsat imagery, and aerial photo graphs. Dashed delineations are from Liestøl (1988). The solid lines represent margins with a higher degree of certainty. The retreat of Blomstrandbreen from its LIA maximum is separated into three retreat phases punctuated by three surges. Tj is Tjukholmen – Source: Burton et al. (2016).

The multibeam-bathymetric data from Nordvågen demonstrate an assemblage of submarine landforms that represents the style of retreat for Blomstrandbreen since the LIA. The morphology of the channels has clearly affected the pattern of glacial retreat. Shallow areas acted as pinning points that enabled a relatively gradual retreat. There are very clear and regularly spaced annual-push retreat moraines orientated transverse to flow, representing a gradual retreat of the glacier, especially across the shallow and narrow eastern channel. Regularly spaced annual-push retreat

moraines, often indicating retreat rates of $<20 \text{ m yr}^{-1}$, are visible in the shallow eastern channel. Retreat moraines in the deeper areas have more irregular morphologies and wider interridge spacings, suggesting greater instability of the former ice margin and possible decoupling of the grounding-line from the bed, promoting more rapid retreat at these locations. These submarine landforms at Blomstrandbreen record three recent surges, with a spacing of about 50 years between each of them, a relatively short quiescent phase between surges (Burton et al., 2016).

1.5 Suspended particulate matter and sedimentation processes

1.5.1 Water Column

The concentration of suspended particulate matter in Kongsfjorden is mainly a reflection of the activity of glaciers, which bring melt-water and inorganic particles into the fjord. The transport of glacier meltwater into the marine environment depends on the position of the glacier terminus and its geomorphology. Land-terminating glaciers discharge their meltwater into the sea via surface runoff from rivers, whereas meltwater from tidewater glaciers enters the fjord mainly by subglacial discharge below sea level. When subglacial low-density water enters the fjord at the base of the glacier, it rises towards the surface, entraining large volumes of ambient fjord water and can lead to a continuous upwelling of nutrients along the water column. Glacier ice and meltwater itself can also be direct sources of nutrients. The mineralogical characteristics of the particles eroded by the glacier and contained within the meltwater runoff depend on the lithology of the underlying bedrock. Chemical weathering can enrich glacier meltwater in silicic acid, phosphate and nitrate, whereas elevated ammonium concentrations can result from microbial degradation of organic matter within the snowpack and glacier ice, or particle-bound ammonium (Halbach et al., 2019).

The concentration of total suspended solids and the extent of the sedimentation processes in the different parts of the fjord have a direct influence on some key characteristics of the fjord system such as:

- the extent of the euphotic zone and its consequence for primary production;
- heat exchange with the atmosphere;
- flocculation of colloids and aggregation of particles (influence on carbon flux);
- direct impact on organisms living both in the water column and in superficial sediments;
- physical–chemical and geotechnical properties of the sea floor (Svendsen et al., 2002).

1.5.2 Sediments

Sediment supply in glaciated fjords can occur by a variety of processes. The dominant process in the fjord today is settling of fine-grained sediments from meltwater plumes and ice rafting. Tidewater glaciers can supply sediments from clay to boulders, but clay and silt are typically transported over large distances in Kongsfjorden. Rivers are also a dominant source of sediment supply to the fjord, transporting mainly fine-grained sediments (Forwick et al., 2015). Geomorphological changes along the coast also document terrestrial sediment input along the fjord

shore (Husum et al., 2019). The bottom of inner Kongsfjorden has waveform morphology interpreted as moraines, partly originating from surges (Howe et al., 2019). Three glaciers are documented as surge type glaciers: Kronebreen–Kongsvegen surged around 1869 and 1897, Kongsvegen around 1948 and Blomstrandbreen, possibly between 1911 and 1928, around 1960, and recently in 2010. Glacier surges lead to short-term reworking of sediments and deposition of sediment lobes containing massive glaciomarine muds with sedimentation accumulation rates up to 30 cm y^{-1} . Suspension settling from meltwater plumes and ice rafting are the dominant sedimentary processes, leading to the deposition of stratified glaciomarine muds with clasts from melting icebergs. The fjord topography has been smoothed by bottom currents (Lindbäck et al., 2018).

The particles exported by the glacier are mainly trapped in the inner part of the fjord, where the sediment accumulation rate is higher than in the central fjord and than in the outer shelf area (Svendsen et al., 2002). In particular the sediment accumulation rates decrease sharply by about one order of magnitude from the glacier front ($20\,000 \text{ g m}^{-2} \text{ a}^{-1}$) to the secondary sill in the central part of the fjord ($1800 - 3800 \text{ g m}^{-2} \text{ a}^{-1}$) and, again, by another order of magnitude towards the outer fjord ($200 \text{ g m}^{-2} \text{ a}^{-1}$).

1.6 Underwater radiation regime

As mentioned previously, the glaciers transport a large amount of mineral particles to Kongsfjorden, which results in a strong gradient in sediment loading from the glacier to the outer fjord. This content of sediment particles is the main factor controlling both the irradiance of UV and visible light penetrating the water column in Kongsfjorden and, therefore, the extent of the euphotic zone as well as the spectral composition of penetrating radiation. Another factor that reduces available light in the water column is the ice cover, particularly when the ice is snow-covered (Hop et al., 2002). During the ice-free season, the influence of suspended particles on the extent of the euphotic zone is substantial. As the increase in concentration of suspended inorganic matter in the surface water results from the seasonal input of turbid freshwater from melting snow and calving glaciers, water turbidity changes drastically over the year and it may limit the extension of the euphotic zone as follow (Svendsen et al., 2002).

- in the mouth of the fjord the lower limit of the euphotic zone was determined to be about 30 m depth;
- in the central part of the fjord, e.g. in the area between the islands of Lovénøyane, the concentration of suspended particles range from 15 to 50 mg/dm^3 and the observed thickness of the euphotic zone varies from 6 to 25 m;
- in the innermost part of the fjord, where the concentration of suspended mineral particles can be $> 340 \text{ mg/dm}^3$ close to fluvio-glacial outflows, the euphotic zone might be limited to only 0.3 m.

The marine communities in Kongsfjorden respond to the variability and changes in environmental conditions, as documented in seasonal and long-term studies. Long-term changes involve alterations of pelagic primary production, dependent on light as well as on stratification and mixing, and algal community composition (Hop et al., 2019).

1.7 Gaps of knowledge and research priorities

Given the high degree of complementary expertise in the international community conducting science at Kongsfjorden, greater integration of research activities would provide the opportunity to accelerate development of mechanistic understanding of adaptation processes, life-cycle control of key organisms, and ecosystem structure, function and services (Hop et al., 2019).

Oceanographic processes observed in Kongsfjorden can be closely linked to long-term time series of atmospheric data recorded in Ny-Ålesund, comprising records of temperature, precipitation, radiation transfer including UV-radiation (Maturilli et al., 2013). The coupling with physical data from atmospheric and oceanographic records also facilitates research with respect to the movement patterns of the higher vertebrate fauna (birds, seals, whales, polar bears) in the system (Hop et al., 2019; Lydersen et al., 2014). The world-class infrastructure hosted in Ny-Ålesund supports an increasing number of research projects during the winter season, which is of utmost importance to complete our understanding of marine ecosystem functionality (Hop et al., 2019). Such monitoring efforts have already allowed for deeper understanding of the functionality of the Kongsfjorden system and its adjacent environments (Svendsen et al., 2002). However, as yet research and data management have failed to achieve a high level of integration of data and there remain important gaps in knowledge, which need to be addressed with high priority in order to give robust foundation for predictions on the future trajectory of Arctic coastal ecosystems in the face of environmental change (Hop et al., 2019). A non-exhaustive list of these gaps will be discussed below.

1.7.1 The abiotic environment

In order to gain a better understanding of ecosystem functionality, improved and integrated monitoring of a number of physical drivers is of utmost importance, including ice and glacial regimes, air and water temperatures, oceanographic forcing, light and nutrient regimes (including near-shore areas), as well as the discharge dynamics and chemical characteristics of the freshwater sources (glaciers and streams).

There is a high level of uncertainty with respect to the future radiation environment in Kongsfjorden (Hanelt et al., 2001).

Sea ice cover in Kongsfjorden will be reduced and at the same time increased terrestrial run-off will increase the discharge of sediments to near-shore ecosystems: the consequences for the phenology and productivity of the phytoplankton and phytobenthos communities need to be evaluated. Intensified monitoring and, eventually, modeling of radiation and nutrient environments may allow prediction of the phenology, primary productivity and species composition of phytoplankton blooms and changes in the distribution of seaweeds with water depth (Hop et al., 2019). For these reasons, glacial influences, phytoplankton bloom events and sediment discharge rates in time and space should be evaluated further.

The inflow of Atlantic and Arctic water masses into the fjord has been identified as a key driver for water column stability and, furthermore, represents an important source of inorganic nutrients, contaminants, and seeding populations of planktonic organisms. Thus, characterizing patterns of, and changes in, advection dynamics will become the key for understanding the environmental controls of the Kongsfjorden marine ecosystem, providing valuable insight into community composition of local vs. advected organisms (Hop et al., 2019).

1.7.2 Land-Sea-Ice-Atmosphere Interactions

The coupling of atmosphere, land, ice and sea has been largely overlooked in the research conducted in the Kongsfjorden area to date, although being of primary importance to coastal processes. Glacial and terrestrial meltwater discharge will alter the in-fjord salinity regime. How the shallow-water communities present in Kongsfjorden may adapt to the changing spatial gradients in light, sediment load and desalination along the fjord axis is as yet poorly understood. Increasing run-off events also have the potential to alter the input of nutrients from the terrestrial system into Kongsfjorden, in particular with respect to different forms of inorganic N and P along with dissolved organic carbon from the soil. However, conclusive data on the effects on growth and physiological performance of primary producers are still lacking (Hop et al., 2019).

There are several tidewater glaciers in Kongsfjorden, as is also typical in many other Arctic coastal regions. The fronts of these glaciers have been identified as “ecological hot-spots” due to their importance as feeding areas for seabirds and mammals. The freshwater plumes from these glaciers transport a large load of suspended matter, contributing to the extremely high water turbidity near the glacier fronts, with direct implications for primary production and benthic deposition processes. The full extent of the contribution of these plumes to fjord biogeochemistry in terms of nutrients and organic matter is yet unknown. Tidewater glaciers in Svalbard are retreating but it is difficult to predict how long it will take for the glaciers in Kongsfjorden to retreat onto land and what consequences this will have on the fjord ecosystem (Kohler et al., 2007).

As already mentioned, recently there has been an increase in the diffusion of warm and moist air from low latitude, favored by the change in atmospheric circulation, which has caused a warming of surface temperatures, and more generally of the entire troposphere. A temperature increase of about 0.45 K per decade over the estimated 2 K for the entire Arctic is attributable to the difference in tropospheric temperature for air masses coming from south to that coming from north. The strong increase in atmospheric temperature and humidity, in particular during winter is a consequence of a change on the atmospheric circulation (Mazzola et al., 2020).

Moreover interesting scientific questions, when looking at environmental changes, address the couplings (e.g. energy fluxes) between atmosphere, sea ice and ocean, including fjords. Ultimately these processes control how much and which type of sea ice is present in a region. In some recent studies the coupling of atmospheric properties and sea ice extent is investigated, with a focus on the Svalbard region. Comparing information on surface air temperature (SAT) and sea ice extent (SIE) in Svalbard fjord systems led to the conclusion that, on time scales of a few months, changes in SAT affect SIE more than the other way around. This is an important finding for improving the understanding of the Arctic system, and how the system is changing, from local to larger scales (Gerland et al., 2020).

1.7.3 Additional remarks

In addition to the above-mentioned and more specific research topics, some overarching fields for improvement have been identified. Overall, the links between the physical environment and key ecological processes need to be strengthened, in particular with respect to the drivers of primary and

secondary production. The overriding factor of seasonality needs to be addressed by increasing research activity throughout the year (including winter observations and experiments).

More in general, the diverse monitoring activities already underway generate extensive but often independent databases, and greater integration is required. A first, but critical, step forward would be to provide a facilitated and integrated accessibility to existing knowledge, to allow available data and information to be obtained more easily through a single source, rather than being scattered in various data repositories. Future research on the links between the physical and chemical environment and key ecological processes will benefit from improved access to existing datasets (Hop et al., 2019).

Chapter 2

Metrology for marine environmental monitoring: observation requirements and essential variables

Metrology, the science of measurement, is an essential tool for scientific research and development as well as for technological innovation. Key societal challenges such as sustainability of energy, environment and health demand new and reliable measurement technologies with traceability that has to be accepted worldwide. Thus, advances in metrology and its effective use have a profound impact on our understanding of and ability to shape the world around us. These considerations become of fundamental importance when addressing the issue of the environment status as reliable climate predictions require quality models, traceable data and uncertainty budgets (EURAMET, 2016).

Metrology has recently been applied to our environment and to climate change since, basing environmental measurements on the International System of Units (SI), may help extend our current knowledge of the complex interactions between weather, sea currents and the various layers of our atmosphere. In order to do this, metrology starts to give a recognized contribution by stressing that slow or small changes must be measured in a traceable way and with respect to the unchanged reference standards offered through the SI system units (Haensch et al., 2007).

The SI is a coherent system of measurement units and the reasons for using a measurement system such as the SI as the reference for measurements are the following three criteria:

- the results of the same measurements against the same references made in a different laboratory should be the same (“comparability”).
- the same measurement made against the same references should remain the same over time (“stability”).
- the results of the same measurements against different references, usually on the basis of different measurement methods, will be the same (“coherence”).

These three properties of comparability, stability and coherence are the fundamental reasons why scientists go towards the use of a measurement system such as the SI. Thus, the understanding of many interesting environmental issues depends on the availability of stable and comparable measurement results. Calibrations and measurement uncertainties evaluations are fundamental to reach full data comparability on climate-change scales, to fundamental physical models, across generations, across borders and organizations and finally across instrument and measurement types. Additionally, since it is essential to bring together measurement data of different species from different methods, it is also essential that they are produced by reference to a measurement system

that is coherent. Moreover accurate measurements can reduce the time necessary to capture trends in the data (Milton, 2007).

In order to quantify the rate of climate change and its anthropogenic origin, changes of physical parameters of a few percent per decade need to be measured. This long time base of measurements is likely to be beyond the active lifetime of any one instrument and so it will be essential to have well calibrated and consistently calibrated instruments to allow this record to be established. In addition, slow drifts or time-variant systematic errors will be a likely source of error and there are always likely to be local geographical anomalies, particularly when making measurements over such a long time base, making it essential that truly global measurements are made at as many sites as possible. The need for this global averaging and inter-site comparison requires that each of these sites measures the same thing in the same way, and it is difficult to simply compare results between sites, even if regular inter comparisons are carried out, unless the instrumentation is fully traceable. Nowadays the use of satellite data has helped to provide real global, reliable and integrated information. However, since each individual mission has a different project team and may even be developed by a different space agency, it is essential that each sensor is calibrated in as accurate a way as possible and that the calibration is demonstrably traceable to SI units. This ensures that any measurements or conclusions drawn from the data can be substantiated and believed (Fox, 2007). Clearly, metrology has key roles to play in supporting climate change understanding, monitoring, modeling and forecasting and there are a number of key activities that need to be considered, each presenting its own challenge (EURAMET, 2016).

* Global warming, an indicator of climate change, is mainly based on surface air temperature trends, mostly obtained historically from records of surface based meteorological observations. The reference-grade ground based stations for the generation of temperature data purposely designed for climate trend records need metrological support in evaluating sensors characteristics, calibration and measurement uncertainties, and in defining data qualities and target uncertainties. These need to be correlated with observations derived from satellites which by their global nature are becoming the bedrock of future long term climate data records.

* For improved modeling of ocean currents, metrological traceability and accurate measurement of relevant parameters in the marine environment (such as sea water salinity, pH, density, speed of sound, heat capacity, dissolved oxygen content and composition including chlorophyll and other biophysical indicators) are key challenges.

* Climate trends in the arctic regions are significantly amplified: accurate measurements to quickly capture trends are there of unique importance at a global scale. As climate change melts arctic permafrost, it releases large amounts of methane into the atmosphere, creating a feedback loop that triggers additional warming. Global warming also reduces the iced surface in the arctic and anticipates the snow melting day in land areas, changing radiative equilibrium thus amplifying the feedback. The extreme ranges of variability of the key-quantities measured requiring higher accuracy than for other areas need dedicated calibration procedures and specific uncertainty evaluation. The logistical difficulties in reaching, removing, handling instruments for the calibration campaigns require self-validating in situ measurements and calibration devices operating in arctic-based research stations (EURAMET, 2016).

By combining individual measurements with simultaneous multiparametric measurements and interdisciplinary and multidisciplinary work, it will be possible to quickly obtain an increase in the amount of data available provided by a multitude of systems, locations, instruments and methods that are comparable; develop improved measurement methods, calibration standards and guidelines across a variety of technical disciplines based on coordinated and globally shared research; create multidecadal records of fundamental climatic data with sufficient uncertainty and confidence, ideally limited by the noise coming from the natural background variability and not by the accuracy of the underpinning observation; have high-quality data available for the accurate determination of trends in global temperature and atmospheric trace gas anomalies and understanding of atmospheric processes as well as the cycles of carbon, water and radiation which drive the climate forecast model (EURAMET, 2016).

The successful implementation of such a demanding plan requires a shared effort globally. To this end, several global key institutions such as the World Meteorological Organization (WMO), Global Climate Observing System (GCOS), Global Atmosphere Watch (GAW), Intergovernmental Panel on Climate Change (IPCC), and the Food and Agriculture Organization (FAO) are working to provide environmental traceable measurements with reliable uncertainty. This means better comparability as well as lower uncertainty and a larger volume of high quality stable standards and reference materials that meet the objectives of these organizations and the global demand for data quality. To reach higher effectiveness, it is essential to combine the expertise achieved in the individual, traditional fields of metrology into new interdisciplinary and multidisciplinary strategies to be developed and embraced also by National Metrology Institutes (NMI) (EURAMET, 2016).

EURAMET, the association responsible for coordinating the integrated metrology community in Europe, has recently established European Metrology Networks (EMNs) to support its aim to bring high-quality scientific research and coordinated metrological services to meet the rapidly advancing needs of different stakeholders for metrology. The EMN for Climate and Ocean Observation is one of the initial six EMNs and has been set up as a European coordination body to formalising and coordinating metrological activity (and resources) of the National Metrology Institutes (NMIs) in support of climate and ocean observation (Woolliams et al., 2019).

2.1 Essential Climate Variables - ECV

The challenge of monitoring and modeling the Earth's climate and its changes requires the measurement of a wide range of climate parameters. The Global Climate Observing System (GCOS) is a program, co-sponsored by the World Meteorological Organization, the Intergovernmental Oceanographic Commission of UNESCO, the United Nations Environment Programme and the International Council of Science (Woolliams et al., 2019) who has defined a list of 54 Essential Climate Variables (ECVs) to assess features of the atmosphere, oceans and land. An ECV is a physical, chemical or biological variable or group of linked variables that critically contributes to the characterization of Earth's climate. ECV datasets provide the empirical evidence needed to understand and predict the evolution of climate, to guide mitigation and adaptation measures, to assess risks and enable attribution of climatic events to underlying causes, and to underpin climate services. The ECVs must not be understood as a select group of stand-alone variables but they are part of a wider concept (Bojinski et al., 2014).

Measurements of these variables need to be comparable irrespective of location and time and the instrumentation or method used. This requires both improved measurement accuracy across the measurement infrastructure and the development of innovative, practical and cost-effective measurement technologies. Remote observation of the Earth from satellites for measurements of atmospheric chemistry, surface radiation budget, and ocean and land cover properties as well as surface based measurements for atmospheric monitoring and soil, snow, ice, deep water and permafrost properties generate daily amount of data requiring robust quality assurance. High-quality observations are possible only if they are based on a sustained traceability to SI and with uncertainties associated to the measured ECVs.

Metrology is fundamental in order to link to the SI the important variables and to enable rigorous assignment of uncertainty to multi-decadal climate data records which are representative of the globe but derived from local samples (EURAMET, 2016).

The ECV are divided in three principal domains: Atmosphere, Ocean and Land. In the following table the ECV for each domain are listed.

Table 2.1 - Essential Climate Variables for the three measurements domains

Measurement domain	Essential Climate Variables (ECVs)
Atmospheric	Surface: air temperature, wind speed and direction, water vapour, pressure, precipitation, surface radiation budget Upper-air: temperature, wind speed and direction, water vapour, cloud properties, Earth radiation budget, lightning Composition: carbon dioxide (CO ₂), methane (CH ₄), other long-lived greenhouse gases, ozone, aerosol, precursors for aerosol and ozone
Oceanic	Physics: temperature: sea surface and subsurface; salinity: sea surface and subsurface; currents, surface currents, sea level, sea state, sea ice, ocean surface stress, ocean surface heat flux Biogeochemistry: inorganic carbon, oxygen, nutrients, transient tracers, nitrous oxide (N ₂ O), ocean colour Biology/ecosystems: plankton, marine habitat properties
Terrestrial	Hydrology: river discharge, groundwater, lakes, soil moisture Cryosphere: snow, glaciers, Ice sheets and Ice shelves, permafrost Biosphere: albedo, land cover, fraction of absorbed photosynthetically active radiation, leaf area index, above-ground biomass, soil carbon, fire, land surface temperature Human use of natural resources: water use, greenhouse gas fluxes

2.2 Essential Ocean Variables - EOVS

Climate variability and change on timescales from seasons to millennia is closely linked to the ocean through its interactions with the atmosphere and cryosphere. The ocean therefore contributes strongly to our ability to develop climate predictions and projections on timescales from weeks to decades and centuries (GOOS-214, 2016).

In particular the ocean influences our weather and climate through its capacity to absorb, transport, and emit heat, carbon and radiation. Ocean life recycles nutrients and is the basis of the planet's largest habitat. Through fisheries, aquaculture, transport, energy, tourism and recreation, the ocean contributes directly to the economic wealth and security of a majority of nations. There is a growing need for more systematic ocean information at local, national, regional, and global scales to support efforts to manage the health of the ocean.

Because of the vastness, remoteness, and harshness of the ocean environment, and the costs involved in collecting any observations over, on or beneath the sea surface, many ocean observing systems have been, and will continue to be, designed to measure as many variables as possible. There is a need to avoid duplication across observing platforms and networks, and to adopt common standards for data collection and dissemination to maximize the utility of data. To address these concerns, the approach is based on lessons learned from the global climate observing community, which organize the effort around essential climate variables (ECVs). Applying this concept to ocean observations yields the introduction of the Essential Ocean Variables (EOV) by Global Ocean Observing System (GOOS), a program executed by the Intergovernmental Oceanographic Commission (IOC) of the UNESCO. In particular, the EOVs include all the Essential Climate Variables in the oceanic domain and additional variables that relate to ecosystem, disaster warning and commercial observational requirements (Woolliams et al., 2019). There are considerable conceptual overlaps among the Essential Climate Variables (ECVs) introduced by GCOS, the Essential Variables defined for meteorological services by WMO Resolution 40 (Cg-XII), emerging Essential Biodiversity Variables (EBVs) being defined in the global biodiversity observing system GEOBON, and the EOVs for Ocean Observations, as shown in Figure 2.1 (FOO, 2012).

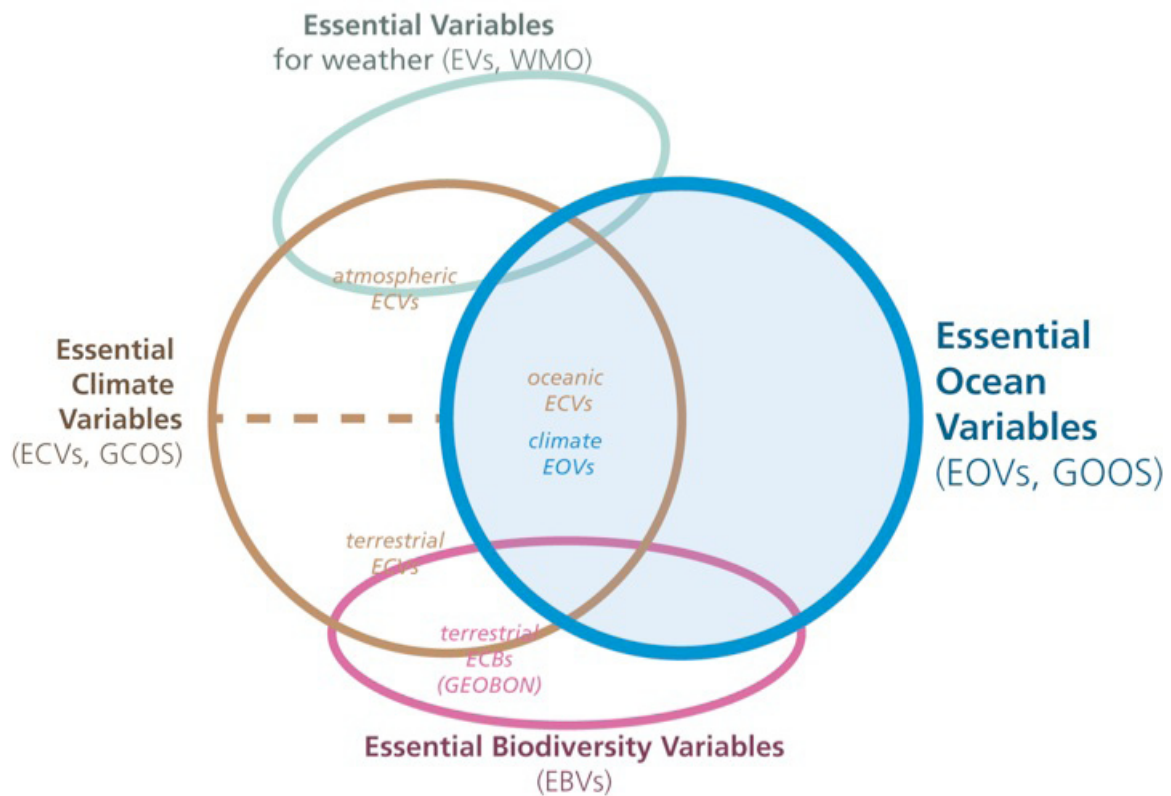


Figure 2.1 - Conceptual Overlap of Essential Ocean Variables in a Venn diagram. Essential Variables defined by the WMO for weather forecasting inspired the Essential Climate Variables later defined by GCOS. The concept has been adopted for Essential Biodiversity Variables on land by GEOBON. The Global Ocean Observing System define ocean observing EOVs. Overlap among these groups is shown, which argues for the need to adopt a consistent approach (FOO, 2012).

Ocean observations with a focus on EOVs will ensure assessments that cut across platforms and recommend the best, most cost-effective plan to provide an optimal global view for each essential ocean variable. Moreover, implementing new EOVs will be carried out according to their readiness levels, allowing timely implementation of components that are already mature, while encouraging innovation and formal efforts to improve readiness and build capacity (FOO, 2012).

The requirements of the system is described in terms of the environmental or ecosystem information needed to address a specific scientific problem or societal issue. The societal issues may include a short-timescale need such as hazard warning, or a long-timescale need for information such as knowledge of ecosystem limits required to set sustainable uses of ocean resources. The observation elements are the technology and networks used to collect the data needed to address these requirements. The outputs (data and information products) are the best syntheses of ocean observations to provide services and inform scientific problems or decisions about societal issues. (FOO, 2012). This kind of approach provides a common language and consistent handling of requirements, observing technologies, and information flow among different, largely autonomous observing elements linked in a collaborative framework (FOO, 2012). Nowadays new and lower-cost technologies have greatly enhance our capability to observe the oceans. Networks of gliders, autonomous underwater vehicles, Argo floats, moorings and research platforms, all equipped with

low-power sensors and artificial intelligence, can automatically adjust to changing needs parts of the sampling system and send real-time or near-real-time measurements to open databases, complementing satellite observations of the ocean surface (2030Strategy, 2019).

In practice, EOVs are identified according to the following criteria:

- Impact: the variable is critical for characterizing the climate system and its changes;
- Feasibility: observing or deriving the variable on a global scale is technically feasible, using proven, scientifically understood methods.

A further characteristic that identifies the EOV is the Cost-effectiveness: generating and archiving data on the variable is affordable, mainly relying on coordinated observing systems using proven technology, taking advantage where possible of historical datasets (Bojinski et al., 2014).

In the following table, a summary of EOV is shown and subsequently some EOV of interest for the data analysis reported in this work will be examined.

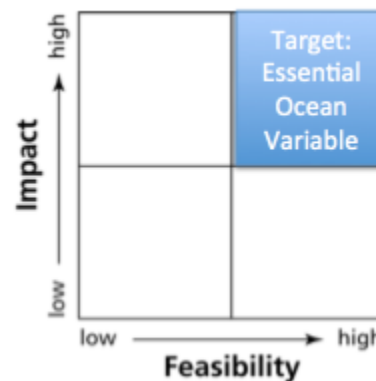


Table 2.2 - List of the Essential Ocean Variables (EOVs) by Global Ocean Observing System (GOOS)

PHYSICS	BIOGEOCHEMISTRY	BIOLOGY AND ECOSYSTEMS
Sea state	Oxygen	Phytoplankton biomass and diversity
Ocean surface stress	Nutrients	Zooplankton biomass and diversity
Sea ice	Inorganic carbon	Fish abundance and distribution
Sea surface height	Transient tracers	Marine turtles, birds, mammals abundance and distribution
Sea surface temperature	Particulate matter	Hard coral cover and composition
Subsurface temperature	Nitrous oxide	Seagrass cover and composition
Surface currents	Stable carbon isotopes	Macroalgal canopy cover and composition
Subsurface currents	Dissolved organic carbon	Mangrove cover and composition
Sea surface salinity		Microbe biomass and diversity (*emerging)
Subsurface salinity		Invertebrate abundance and distribution (*emerging)
Ocean surface heat flux		
CROSS-DISCIPLINARY		
Ocean colour	Ocean Sound	

2.2.1 EOVS - Physics

Sea Surface Salinity - Salinity is the fraction of water that comprises salt and other impurities. Sea Surface salinity observations contribute to monitoring the global water cycle (evaporation, precipitation and glacier and river runoff). On large scales, surface salinity can be used to infer long-term changes of the global hydrological cycle. Sea Surface Salinity is observed principally in situ from flow-through water intake systems on research and commercial ships, or conductivity sensors deployed on autonomous floats, drifters, and unmanned surface vehicles. More recently, the advent of satellite sea surface salinity sensors has provided less precise but global coverage including marginal seas. In situ surface observations will remain an important validation and calibration complement to satellite observing. Sea surface salinity features is important to estimate ocean circulation and marine biogeochemistry. Along with coincident SST observations, it allows surface-water density to be estimated (GOOS website).

Sea Surface Temperature - SST plays important roles in the exchanges of energy, momentum, moisture and gases between the ocean and atmosphere. The spatial patterns of SST reveal the structure of the underlying ocean dynamics, such as, ocean fronts, eddies, coastal upwelling and exchanges between the coastal shelf and open ocean. In situ SST observations are taken from a variety of platforms, including, ships, buoys, drifters and floats. In situ observations are essential for calibration and validation of satellite data. Satellite Sea Surface Temperature applies to the skin temperature down to a few mm, and is sometime adjusted down to the foundation depth (the depth at which diurnal heating is not important), but largely focuses on the upper few millimeters. The skin temperature (the temperature within a few micrometers of the surface) plays an important role in air-sea exchange of energy, moisture, and carbon (GOOS website).

Subsurface Salinity - Subsurface salinity, along with coincident subsurface temperature and velocity observations, are required to calculate in situ density and ocean freshwater transports, respectively, and coincident subsurface observations of salinity, temperature and pressure provide an estimate of the ocean geostrophic velocity. In addition, subsurface salinity, together with temperature and pressure and satellite surface observations of SST, SSS and SSH are used to derive large-scale gridded climate products including ocean velocity, mixed-layer depth, density stratification, sea level and indirect subsurface ocean mixing used in many weather and climate applications. Subsurface salinity observing systems acquire data over a large range of spatial and temporal scales. Moorings offer very high temporal resolution at specific locations, but with spatial resolution limited by density of the array. Gliders and other autonomous platforms achieve much higher spatial resolution depending on endurance and other instrument characteristics (GOOS website).

Subsurface Temperature - Subsurface temperature is a fundamental variable that is required to monitor variability and change in the physical environment of the ocean, energy flows, climate patterns and sea level, and is essential to the understanding of changes in many other variables in the realms of marine biogeochemistry and biology. Ocean heat content directly derived from subsurface temperature is of paramount importance in the monitoring of the Earth's climate system

and marine environment. Many other physical variables are derived from subsurface temperature along with subsurface salinity, including subsurface density, geostrophic circulation, heat transport and steric sea level. These variables are essential to the understanding of variability and change in ocean stratification, circulation patterns (uptake and redistribution of heat and freshwater) and sea level. Changes in subsurface temperature induce changes in mixed-layer depth, thermal/density stratification, mixing rates and currents. All of these physical changes can affect marine biology, not only directly but also indirectly through changes in marine biogeochemistry, such as nutrient and O₂ recycling, uptake of carbon emissions, ocean acidification and so on. Subsurface temperature observing systems acquire data over a large range of spatial and temporal scales. Moorings offer very high temporal resolution at specific locations, but with spatial resolution limited by density of the array. Gliders and other autonomous platforms achieve much higher spatial resolution depending on endurance and other instrument characteristics (GOOS website).

2.2.2 EOV - Biogeochemistry

Oxygen - O₂ is essential for nearly all multicellular life. Future projections indicate that oceanic O₂ levels will decrease substantially, in part because of ocean warming and increased stratification (a process often referred to as ocean deoxygenation), but also because of increased nutrient loadings in nearshore environments that lead to eutrophication. This could have dramatic consequences for marine biogeochemistry and marine life, as the ocean's O₂ minimum zones will expand substantially, and large swaths of ocean will appear that have O₂ levels that are too low for fast-swimming fish to survive, and can potentially reduce the pool of bioavailable nitrogen due to reduction of nitrate (GOOS website).

2.2.3 EOV – Cross Disciplinary

Ocean Color - Ocean color is measured as the ocean color radiance (OCR). OCR is the wavelength-dependent solar energy captured by an optical sensor looking down at the sea surface. The phenomenon of color is the result of absorption and scattering, as light interacts with the water and materials suspended or dissolved within it (i.e., the optically active 'constituents'). Ocean color encompasses a multitude of biological, biogeochemical, and ecological properties of the ocean, and is an EOV because changes in the color of the ocean can be related to changes in the presence and magnitude of living and non-living particles and of dissolved materials in the water.

These water-leaving radiances contain information on the ocean albedo and information on the constituents of the seawater, in particular, phytoplankton pigments such as chlorophyll-a.

Current methods to observe the ocean's optical properties include underwater optical sensors as well as airborne and satellite observations. Data analysis is not easy as satellite measurements also include radiation scattered by the atmosphere and the ocean surface. Products derived from OCRs include phytoplankton chlorophyll-a concentration, biogeochemical and ecological indexes including water quality measures, metrics to gauge phytoplankton physiology, and indicators of ecosystem status and health. Environmental variables such as bathymetry, dissolved organic carbon, and suspended sediment concentration can be derived from OCRs (GOOS website).

2.2.4 Support variables

It must also be kept in mind that in order to be able to study and model the environment from the point of view of the climatic changes taking place, complementary information to the EOVs, called support variables, is required. These are other EOVs or other measurements from the observing system that may be needed to deliver the sub-variables and/or derived products of the EOV, in response to specific needs. For example, the impact of bathymetry, where models are still affected by a basic lack of supporting observations, is fundamental for accurate ocean circulation and mixing and is critical for climate studies since seafloor topography steers surface currents, while the roughness controls ocean mixing rates (GOOS-214, 2016).

Other examples of complementary information are weather conditions such as wind, humidity, cloud cover, rainfall, which can locally influence some measurements of the above-mentioned parameters.

2.3 Metrological requirements for ECV and EOV observations

Assessing climate change will depend crucially on the uncertainties associated with measurements and the robustness of climate data and their compliance with the internationally agreed climate monitoring principles of the Global Climate Observing System. Measurement uncertainties can only be determined, and hence minimized, if proper consideration is given to the metrological traceability of the measurement results to stated standards (IOM-Report, 2010). These may come from in situ observations or from satellite remote sensing. At present, 14 of the 17 atmospheric ECVs, 6 of the 18 oceanic ECVs and 11 of the 16 terrestrial ECVs have a significant contribution from satellite Earth observation (EO). The others are observed primarily by in situ observational networks (Woolliams et al., 2019).

To provide robust, inter-operable and long-term data records of ECVs and EOVs, GCOS and GOOS have listed a set of observational requirements that cover the spatial and temporal resolution of the observation and the uncertainty required both for individual measurements and for trend observations (the latter called the “stability”) (Woolliams et al., 2019). The indicative requirements have been determined from a consideration of the user needs for different climate applications. Setting these requirements is sometimes difficult, due to limited knowledge of the expected variability or likely benefit of the dataset on the application (GCOS-154, 2010). The GCOS Implementation Plan (and its 2010 update) and the Satellite Supplement 4 are reviewed on a regular basis. The searchable database OSCAR holds the most recent version of GCOS requirements and is the official repository of requirements for variables in support of WMO Programmes and Co-sponsored Programmes (Guidance Note 1).

The metrological requirements for ECV and EOV observations regard horizontal, vertical and temporal resolution, accuracy and stability.

- Horizontal resolution: in most cases this means the sampling distance of analysed products (in some form of gridded or otherwise standardized representation). In some cases, the horizontal resolution refers directly to retrievals, and in the case of images, horizontal resolution means the

image resolution. It should be recognized however that the grid on which a product is supplied or the distance between successive retrieved values may be less than the horizontal scale of the information a product provides, for example due to horizontal correlation of error in retrievals.

- Vertical resolution: this means vertical sampling distance or average spacing of independent pieces of information.

- Temporal resolution: this is the required interval between two successive instances of a product. Where the stated products are averaged over long periods (such as months), the measurements themselves may need to be sub-daily samples, for example to eliminate aliasing errors due to diurnal effects, or to eliminate effects due to weather conditions.

- Accuracy: the user requirement for accuracy is a requirement for closeness of agreement between product values and true values. As true values are unknown, users are provided in practice with product values that are estimates of true values, and producers may also provide estimates of the uncertainties of their product values. The requirements tabulated numerically as “accuracy” are indicative of acceptable overall levels for the uncertainties of product values. Uncertainty can be influenced by factors such as spatial/temporal sampling, biases introduced by the retrieval method, biases introduced by interpolation methods, calibration errors, geo-location errors, and instrument noise. It may be quantified by the root mean square (or other measure) of the estimated distribution of errors in product values over a spatial domain, a time interval or a set of similar synoptic situations. Uncertainty may accordingly vary in space and time. The errors in product values, the differences between product values and true values, can be sampled if there are independent, well-characterized, “reference” measurements with relatively low uncertainties that can be compared with a subset of product values.

- Stability: the user requirement for stability is in general a requirement on the extent to which the error of a product remains constant over a long period, typically a decade or more. The relevant component of error of a product for climate application is often the systematic component defined by the mean error over a period such as a month or year. Values quoted as “stability” refer to the maximum acceptable change in systematic error per decade, except for variables for which trends are usually expressed in terms of an annual rate of change, in which case the stability is expressed in terms of this rate of change (GCOS-154, 2010).

Many of these requirements are difficult to achieve and moreover robust metrological methods are not routinely applied to many observations of ECVs and EOVs (with a few notable exceptions), but there is a growing recognition by the observation communities in the value that metrology can provide (Woolliams et al., 2019). This is due to the recognition that many of the challenges faced by climate science are measurement challenges and that assessing climate change will depend crucially on the uncertainties associated with measurements and the robustness of the climate data (IOM-Report, 2010; Woolliams et al., 2019).

Collaborations between communities are needed to develop improved measurement standards, to perform comparisons, to establish metrological guidelines and operating procedures for observational networks (Woolliams et al., 2019).

For what concern ocean observations, they are lacking a multidisciplinary and coordinated approach to provide metrological traceability, comparison and uncertainty analysis to the EOVS observations. At present, such metrological referencing is limited for some EOVS. To ensure data quality, oceanographic institutes are increasingly implementing metrological principles in their quality assurance systems, meaning that they would have to give evidence that their measurements are performed in compliance with international (written) standards, e.g. ISO/IEC 17025 or ISO 22013, which include metrological requirements like traceability and adequate uncertainty calculations explicitly. Besides some typical physical measurement quantities also measured in other areas, accreditation bodies are rarely prepared to cover EOVS that are based on measurement procedures specific to oceanography (Woolliams et al., 2019).

2.4 Essential Arctic Variables – EAV

Arctic regional climate and ecosystems are unique and require specific motivate development of an Arctic Region Component of the Global Ocean Observing System (ARCGOOS) capable of collecting the broad, sustained observations needed to understand and predict Arctic environmental change. ARCGOOS design and implementation needs to leverage from a range of existing observing efforts operating at different scales with different objectives and missions (Lee et al., 2019). An example is the Sustaining Arctic Observing Networks (SAON), a joint initiative of the Arctic Council and the International Arctic Science Committee (IASC), who has the purpose to identify the need for a Roadmap for Arctic Observing and Data Systems (ROADS). ROADS will be organized around Essential Arctic Variables (EAVs) (Larsen et al., 2020).

These EAV, analogous to Essential Ocean Variables of the Global Ocean Observing System, are selected for relevance to climate, operational services and ocean health, modulated by feasibility and cost effectiveness. While the ultimate selection and definition of EAVs, and the scales at which they must be measured, should flow from the identification of Societal Benefit Areas (SBAs) and the science questions they engender, the GOOS EOVS provide a starting point for considering some of the EAV baseline variables and how they might be shaped by challenges and concerns particular to the Arctic (Lee et al., 2019).

Potential high-impact EAVs can include sea ice, sea surface height, sea state, phytoplankton, surface and subsurface temperature, salinity and ocean velocity. Although this subset is clearly incomplete, the example serves to illustrate how a requirements-driven framework might be used to trace and understand the impact of observations across multiple scientific and operational endeavors (Lee et al., 2019).

EAV's are defined by their observing system requirements (e.g. spatial resolution, frequency, coverage, accuracy), which are technology-neutral and should transcend specific observing strategies, programs or regions. They are implemented through specific recommendations based on best available technology and practices in order to satisfy the speed at which data and products must be delivered (Guidelines ROADS, 2019). It must be underlined that the definition of EAVs is a process still in progress. They could be an extension of existing Essential Ocean Variables in term of temporal requirements or spatial resolution or a creation of New Regional Variables, to integrate region-specific knowledge.

2.5 Positioning and range measurements in the context of metrology

The variables described above, in order to be effectively used in practice, must be placed in space with precision and reliability. As it will be analysed in next chapters, some of these variables will be more sensitive to spatial precision while others will be less affected. In both cases, however, the question of positioning is crucial.

From a strictly metrological point of view, there are currently no reference standards that can be traced back to the SI when considering positioning both on the ground and in navigation. These are in fact topics in a field that can be defined as restricted, involving a smaller community of researchers compared to other field of measurements, like for example the Earth observation from satellite. However, it is essential for this thesis to address this type of topic by introducing what are the principles of positioning in air and underwater, with particular attention to the case of navigation of autonomous vehicles, and the measurement of the range, whether it is intended as a reconstruction of the bathymetry of seabed or as a means of studying the morphology of the submerged part of ice.

The discussion will then be focused on the case of critical environments in order to describe how critical issues and limitations may arise due to the particular working conditions.

2.5.1 Positioning for autonomous vehicles in air

The determination of the coordinates of a point on land, at sea, or in space with respect to an implied coordinate system is called point positioning (Vaníček et Krakiwsky, 2015).

Determination of position for points on the earth's surface requires the establishment of appropriate coordinates in the selected geodetic reference system (DATUM). Calculation of position with repeatable accuracy is the central problem for the geographical reference of terrestrial information and the principal function of geodesy. A three-dimensional position is defined by two horizontal coordinates and a vertical component which is the height above the reference surface. The ellipsoid surface is regular and derived mathematically; it is for these reasons that, as a reference surface, it is the widely used for horizontal co-ordinate systems. However it is of limited use as a reference for heighting as it is such a coarse approximation of the earth's shape. The Geoid, defined as the equipotential surface of gravity strength field, is used as a reference surface for heights; Mean Sea Level (MSL) is the best approximation of such a surface (IHO-C13, Chapter2).

Positioning is the fundamental framework and starting point for every survey operation. The position of any point (e.g. sounding, feature, etc.) can be referenced using either geodetic coordinates defined by latitude (φ), longitude (λ) and ellipsoid height (h) or Cartesian coordinates (x, y, z) (IHO S44, 2019).

Several satellite positioning systems are available for positioning, such as GPS, GLONASS, GALILEO, BEIDOU etc. The performance standards for the position/time domain are dependent on the availability of "good geometry" of the in-view satellites relative to the assumed user. Without "good geometry", it can sometimes be impossible for users to even determine a Position-Velocity-Time solution. The relative goodness of the satellites-to-user geometry is quantified by a set of metrics collectively known as the "dilutions of precision" (DOPs) (TR-SGL-20-02, 2020).

As an example, with current (2018) Signal-in-Space (SIS) accuracy, well-designed GPS receivers can achieve horizontal accuracy of 3 meters or better and vertical accuracy of 5 meters or better 95% of the time (TR-SGL-20-02, 2020).

Improved degrees of accuracy can be reached using different positioning principles: with Differential with code phase measurements (DGPS) an accuracy of few meters can be obtained; the Relative with measurements of phase (RTK) allows to reach the decimeter and with Differential with carrier phase measurements (RTK DGPS) few centimeters can be obtained (IHO-C13, Chapter2).

2.5.2 Underwater positioning for autonomous vehicles

Acoustic Positioning Systems play an important role in providing accurate positioning in all the situations where there is no GNSS position available like, for example, for towed bodies, AUVs (Autonomous Underwater Vehicles), ROVs (Remotely Operated Vehicles) as well as manned submersibles vehicles. The acoustic systems are designed with the purpose of tracking the evolution of an underwater platform from a surface ship or from the shoreline (Alcocer et al., 2006).

The acoustic positioning is able to provide very high positional repeatability over a limited area, even at a great distance. In many situations, repeatability is more important than absolute accuracy, and so the possibility to use integrated GPS/INS technology, together with the acoustic systems, makes it possible to achieve both high precision and accuracy.

Acoustic Positioning Systems measure ranges and directions to beacons that are deployed on the seabed or fitted to autonomous vehicles and towed bodies. There are three primary techniques used in acoustic positioning systems, Long Baseline, Short Baseline and Super or Ultra Short Baseline with some modern hybrid systems using a combination of these techniques. The accuracy achieved will depend on numerous factor such as technique used, frequency, range and environmental conditions. It can vary from a few meters to a few centimeters. Accuracy increases with increasing frequency but at the expense of range and the power required. The accurate determination of sound velocity and velocity gradients will influence the accuracy in the position: seawater is not a uniform, isotropic medium and therefore the velocity of sound in water is affected by changes in temperature (the dominant factor), salinity and depth so a precise knowledge of the average sound velocity and preferably knowledge of the sound velocity profile is required. Moreover, multipath effects (reflections), geometry and seabed topography i.e. whether or not there is a 'line of sight' between transponders, and noise in the received signals could affect the effectiveness of acoustic positioning (IHO-C13, Chapter2).

2.5.3 Range measurements: seabed bathymetry and ice morphology

The navigation of surface vessels and underwater platform requires accurate knowledge of depth and features in order to exploit safely the maximum available water (IHO S44, 2019). Bathymetry, the depth of the seafloor, besides having vital importance to navigation, at the largest scale, provides the fundamental information from which the tectonic setting can be determined. At finer scales, it provides a long-term record of the interactions of bottom currents, ice, geochemical processes, and

biological activity with the seafloor. Observations of ocean currents, temperature, biological production and diversity, and chemical and physical properties invariably require a description of the seafloor's shape in order to be fully understood (Jakobsson et al., 2015).

Bathymetric data can be collected with, or derived from, various technologies such as single or multibeam sonar, sidescan, lidar, other optical techniques (such as satellite derived bathymetry, photogrammetric point clouds or structure from motion). Given the variety of instruments, specific standards have been defined by the International Hydrographic Organization (IHO) in order to make the final bathymetric data uniform and independent of the instrument with which it was acquired (IHO S44, 2019). By the way, recent developments in multibeam sonar mapping have so dramatically increased the resolution with which the seafloor can be portrayed that it has become the preferred tool for making bathymetry. Moreover, the newest generation of multibeam sonars allows also for mapping and visualization of features in the water column, like for example the presence of gas bubbles emanating from the seabed (Jakobsson et al., 2015).

The method of using sound waves to derive the depth and morphology of the seabed can also be used on board autonomous robotic platforms (ROV, AUV) to obtain the thickness and morphology of floating ice. For example, a single-beam sonar can be positioned looking directly upward at a depth safe from moving ice (>35 to 50 m); the depth of the sonar is determined from the difference between measured total pressure at depth and local sea level atmospheric pressure, with knowledge of the ocean density profile enabling conversion from pressure to depth. The distance to the bottom of the ice is determined from the echo travel time, with knowledge of the ocean sound speed profile allowing conversion from travel time to distance. The ice draft (roughly 90% of its thickness) is calculated as depth minus distance to the ice, and ice thickness is estimated from knowledge of the ratio of sea ice to seawater density, assuming local isostasy (Rice et al., 2013). Single-beam sonars on underwater platforms provide valuable data on under-ice features, but they provide a linear, two-dimensional view. In 2004, a multibeam sonar, commonly used for bathymetric surveys, was mounted upward looking on the Autosub AUV to survey the underside of the ice canopy. This effectively expands the field of view several tens of meters wide, capturing a 3D elevation (depth) swath of the underwater surface of the ice. With these observations, first-year ice features are easily distinguished by their sharp, rough character, while older multi-year ice becomes apparent due to its smoother, weathered appearance. This cross-track view also gives a better estimate of the overall volume of submerged ice features and highlights the highly irregular shape of ridge features (Wadhams et al., 2006).

The two cases described above are examples of range measurement (distance between instrument and seabed or between instrument and ice) based on the propagation of acoustic waves, whether they are structured in a single beam or in multiple beams. In both cases, there are range-dependent and -independent error sources that affect the measurements of the range and that should be considered to compute measurement uncertainties and acceptance interval (IHO S44, 2019). Accuracy in the range measurement is a function of several factors both from the echosounder itself and the medium, including beam angle and frequency, incident angle on the seafloor, transmit and receive beam widths, attitude and heave accuracy, bottom detection algorithms and sound speed profile variation (due to temperature, salinity and pressure), positioning system (GNSS) and heading sensor (IHO-C13, Chapter2).

2.6 Limitation due to critical environments

The uncertainties and errors on the measures can further increase when operation take place in environments with critical and particular characteristics that can lead to limitations in the quality and quantity of data acquired. Instruments that in normal conditions allow to reach remarkable accuracy, if operated in critical conditions can experience a reduction in their performance or, in the most extreme cases, stop working. This is the case, for example, of observations made in an Arctic environment.

It is a fact that the inaccuracy for the position received from the GNSS systems will increase at higher latitudes. This is mainly due to the lack of satellites over the polar areas, which will lead to a poor satellite-geometry that will result in inaccuracy for the position. Another problem that can occur is the freeze of GNSS position (position will not change even though the vehicle is moving) mainly induced by two types of failures, being internal failure for the GNSS receiver or problems with the antenna. The main antenna-related problem in polar areas is icing (Røds, 2018). Furthermore, in areas where sunspot activity (most pronounced around the magnetic equator and the Polar Regions) can cause interference to GNSS signal, acoustic positioning system can provide a useful backup for GPS.

Still about navigation and positioning at high latitudes, also gyro and magnetic compasses experience problems in operation and provide measurements affected by high uncertainty. The gyrocompass uses a gyroscope, a wheel that is spinning at high speed and installed in such a way that that it can rotate in every direction, for the determination of true course of navigating vehicles. Tilt and drift are depending on the latitude and, in particular, the drift increases with latitude. The development of optical gyro compasses, special types of gyro compasses based on the technique of measurement of angular acceleration through the use of laser-light, permits to have a latitude-dependent error significantly reduced compared to the classic gyrocompass. This is very important as failure and/or inaccuracy in gyro-course will lead to wrong input to essential navigational systems and/or autopilot (Røds, 2018).

Magnetic compasses as well are subject to possible malfunctioning at high latitude as they depend on the horizontal component of the earth's magnetic field to determine directions. At the equator the magnetic field is largely in the horizontal plane and a magnetic compass works well. At higher latitudes, the earth's magnetic field dips downward, until at the magnetic north pole the horizontal component is negligible. As a result, the directional accuracy of these instruments is degraded in Arctic regions, especially in the western Arctic where the magnetic north pole is presently located. Compass accuracy can be improved in Arctic Regions by calibrating locally rather than at facilities where they are manufactured or maintained (ECO Magazine, March/April 2019).

Even the acoustic positioning systems, which in some situations can help to remedy the malfunction of the GNSS and gyro positioning systems, are not however immune to problems deriving from use in critical environments. This is the case of operations carried out in areas where there is a strong stratification of the water masses or, more generally, in areas where there are sudden variations in the chemical-physical characteristics of water. Examples of this type of situation can be plume due to the introduction of freshwater near the fronts of glaciers, events of leakage of substances due to accidents and/or pollution, gas emissions from the seabed. In these cases, the acoustic positioning systems may lose effectiveness as the transmission of acoustic waves is strongly influenced by the characteristics of the medium in which they propagate and therefore strong variations, for example

in the temperature or density of the water, can lead to loss of accuracy and, in the worst cases, also to the loss of the positioning ability.

The limitations of the typically used measurement methods, which create problems during campaigns in hostile environments, bring to the attention of scientists the need to mitigate and overcome them, developing new approaches for environmental observation.

It is precisely in this context that the work described in this thesis was born, with the aim of providing observation methodologies for the accurate measurement of variables to characterize peculiar aspects of hostile environment, in a safe and cost-effective way.

In the next chapters, examples of measurements carried out in two different critical conditions will be described together with the procedures followed to mitigate the possible negative effects of the malfunction of the instruments, due to environmental problems, in order to obtain useful data for the identification of transient phenomena occurring there.

Chapter 3

Methods and technologies for observation and monitoring in harsh Arctic environment

Ocean observations are a key source of information on natural hazards (e.g., harmful algae and bacteria blooms, tsunamis, storm surges, marine heat-waves, and storms and other extreme weather events), ecosystem health and biodiversity (including shifting distributions of organisms and the increased risk of extinctions), ocean pollution (including acidification, de-oxygenation, and plastics), and sea level change. They highlight the need for observations to support ecosystem-based management, marine and weather forecasting, climate predictions and projection, marine safety and navigation, decision support for climate adaptation, deep-ocean exploration, and seafloor mapping, among many other areas. To cope with all these needs, observing systems of various scales, from the global ocean (e.g., Argo, GO-SHIP, Volunteer Observing Ships, and an active constellation of satellites), basin-scale (e.g., AtlantOS, Tropical Pacific Observing System 2020, Indian Ocean Observing System, Tropical Atlantic Observing System, Arctic Ocean and Southern Ocean observing systems, and a developing Deep Ocean Observing Strategy), regional scale (e.g., for boundary currents and inter-ocean exchanges), to various coastal observing systems have been developed and released (Speich et al., 2019).

Operational forecasting, climate monitoring, process understanding and model development are some practical examples that demonstrate that observation requirements are different depending on the applications. For weather prediction applications, the most important requirement is that the observations are in real time. For climate monitoring, the absolute accuracy and location is more important than frequency of observations. High quality observations in long time series at specific locations are more important than a high frequency of observations. For process understanding and model development representatively is important as well as degree of detail; observations must include parameters that tells something about the underlying processes for a specific phenomenon (Buch et al., 2017). For all these reasons, improved understanding and quantification of the state of the ocean is needed at multiple spatial and temporal scales, in particular with regard to:

- mesoscale and sub-mesoscale processes and dynamics and their interactive role and impact on energy transport, marine ecosystems and biogeochemical cycles;
- physical and biogeochemical air/sea interaction processes and the subsequent transfer of heat, gases and nutrients within the oceans by turbulence, mixing, convective motion and biological pumping;
- regional and global sea level;
- forecasting oceanic and interacting Earth-system conditions over all time scales.

The Essential Ocean Variables (EOVs), introduced in Chapter 2.2, are physical, biogeochemical and

biological measurements fundamental to understand ocean phenomena and to assess ocean state and change of a global nature. Derived products and other relevant information, in response to user requirements, are calculated from the EOVS (Buch et al., 2017). For example, Oceanic circulations are largely driven by fluxes of heat, momentum and fresh water at the ocean surface. Modeling and data assimilation for the ocean thus have a predominant need for good-quality atmospheric data and data on the input of fresh water from rivers. Linked to these inputs is the need for data on ocean-surface variables such as sea-surface temperature (SST), sea-surface salinity (SSS), surface current and sea state (ocean-surface-wave conditions). This has to be complemented by data on the sub-surface state of the ocean from both in situ and remote-sensed observations, in particular to constrain models used in estimating the ocean state (Simmons et al., 2016).

Satellites provide the global or near-global coverage that is needed to describe the Earth system, but are limited in what they can sense. For the atmosphere this includes limits to the extent to which fine-scale vertical structure can be resolved and to which information can be provided on wind and below clouds. For ocean and land, the information provided from space is largely restricted to the near-surface layer, although important inferences can be drawn on bulk properties from altimetry and gravimetry. In situ data are crucial both as validation/calibration data for satellite data products and also as observations that cannot be obtained from satellites. Yet, in situ data generally have far from uniform geographical coverage (Simmons et al., 2016). This is particularly true if we focus on the Polar region, where a significant gap exists in the ocean observing system, compared to most areas of the global ocean, hindering the reliability of ocean and sea ice forecasts (Smith et al., 2019).

The Arctic is a region very sensitive to environmental changes. There is a very close interrelation and delicate balance between atmosphere, terrestrial, cryosphere, sea ice and ocean areas, especially in relation to solar energy, radiation budget and hydrological cycle. This has a great impact on physical, chemical and biological processes in the area. For what concerns the cryosphere, for example, basic data such as fjord bathymetry and glacier trough depths are challenging to obtain, yet essential in order to model the ice-ocean interaction. As novel methods and large-scale airborne, satellite and in-situ campaigns slowly start to fill this gap: ice velocity and ice elevation are useful for the understanding of ice-dynamics; other highly valuable observations conducted at the surface of the ice sheets or glaciers relate to surface mass balance and the connection to the atmosphere and climate system, such as surface albedo, longwave radiation, surface and sub-surface temperature, 2m air temperature, barometric pressure, wind speed and direction, relative humidity and precipitation, serve the purpose of monitoring key processes at the ice/atmosphere boundary and establish a benchmark for regional climate models attempting to estimate the past, present and future surface mass balance (Buch et al., 2017).

However, polar regions present a number of unique observing challenges: process understanding is hampered by the sparsity of observations from the marine Arctic, related to the high cost of observations, difficult accessibility to the measurement sites, and the harsh environment for instruments.

Possibilities to observe the spatial distribution and temporal evolution of sea ice, snow, and melt ponds in the Arctic Ocean have recently improved due to better satellite remote sensing methods (Sprenn et al., 2017), airborne electromagnetic mapping methods (Haas et al., 2009), sea ice mass-balance buoys (Perovich et al., 2007), and community-based observations (Vihma et al., 2019). Arctic observation systems rely heavily on satellite observations supplemented by in-situ platforms.

Especially for the marine environment, several other platforms such as ships, profiling floats, gliders, moorings, AUV's etc. are used to monitor the interior of the Arctic Ocean (Buch et al., 2017). Even if there is a need for more in situ observations on the marine atmosphere, sea ice, and ocean, increasing the amount of such observations include several technical and environmental challenges, such as riming of instruments, darkness of the polar night, instability of sea ice as a measurement field (leads may open within the field, causing danger for instruments and people), tilting of weather masts due to sea ice motions, low clouds and fog hampering airborne (research aircraft, unmanned aerial vehicles, UAVs and tethered balloon) operations, polar bears' interest towards the measurement devices, and disturbance of the airflow caused by ships and other constructions on ice stations (largest in conditions of stably stratified boundary layer typical of the Arctic). The Svalbard Integrated Observing System (SIOS) is an example of international observing system for long-term measurements in and around the Norwegian archipelago of Svalbard addressing Earth System Science questions, trying to contribute in reducing the gap in the data available for the Arctic Polar region. SIOS integrates the existing distributed observational infrastructures into a coherent observational program over a long period (Hübner et al., 2019). Extending the established in situ sea ice monitoring at Svalbard with autonomous technology and remote sensing tools would provide a robust suite of complementary monitoring methods. This integrated observation system and enhancement of monitoring activities with additional biogeochemical and molecular sensors would give a more comprehensive overview of the biological and chemical changes in oceans and fjords (Van den Heuvel et al., 2020).

3.1 The need for autonomous platforms to observe the marine Arctic areas

Over recent years, improvements in observing technology and capabilities have been made to create new possibilities to construct and maintain reliable observing systems in Polar ocean.

The traditional approach to obtaining ocean measurements is costly, labor intensive and provides limited data; ocean going research vessels, with complements of marine staff and research scientists, sail to a single point in the ocean and take a series of measurements over a very short timescale (generally a week to a month). Not only is this expensive and technically challenging for some measurements, but there are regions of the ocean that are inaccessible for large periods of the year such as the Arctic and Antarctic oceans (Connelly, 2017) . Moreover a deep understanding of the numerous processes connected to changes in the Arctic climate, sea ice and ocean is needed for better forecasting models and improved risk assessment and is thus a key to improved safety and sustainability of all the Arctic operations (ARICE, 2019).

For all these reasons the trend in marine observations, both globally and in the Arctic, has been towards increasing application of autonomous buoys, moorings, autonomous underwater vehicles (AUVs), and unmanned aerial vehicles (UAVs) (Vihma et al., 2019). Robotic systems are increasingly being utilized as fundamental data-gathering tools by scientists, allowing new perspectives and a greater understanding of the planet and its environmental processes. What robots promise for the ocean sciences is a great reduction in the threshold for access, allowing a much more pervasive presence in the ocean. At high latitudes, AUVs have been used to make measurements under ice, measuring heat flux and distributions of biological populations, both key

observations for understanding the current rapid rate of change of Arctic climate and ecosystems. Autonomous mobile robots used in exploration activities are highly dependent on their ability to sense and respond to their environment. In contrast to a robot in structured settings, such as a factory floor, an exploration robot must accomplish its goals in a previously unmapped environment with unpredictable disturbances and threats. The more sophisticated their perception of their surroundings, the greater their ability to respond constructively.

The success of autonomous platforms has encouraged the development of sensors that capitalize on and complement the availability of lower-cost methods of observing the ocean. Although sensors to measure physical properties such as temperature, salinity, and current have been available for many years, many research laboratories are creating sensors for the chemistry and biology of the ocean. For example, the introduction of instrumentation for determining nitrate concentrations allows AUVs to characterize nutrient availability in situ, where it previously could be determined only by laboratory analysis of samples taken from ships. Moreover the need to observe and understand the internal weather of the ocean and the changing composition of ocean ecosystems at ever-higher spatial and temporal resolutions has motivated the creation of observing systems using fleets of AUVs (Bellingham et al., 2007).

However, the AUVs are not the only types of autonomous vehicles used as observing and monitoring systems. Wide varieties of marine robotic platforms are now available for both industry and research, both in the air, on the surface and underwater. While most in-situ oceanographic data traditionally has been gathered from crewed vessels, Autonomous Surface Vehicles (ASVs) are becoming an increasingly valid alternative or complement to a crewed vessel. An ASV relies on a computer controlled system and positioning from global navigation satellite system (GNSS), rather than a human operator that is susceptible to fatigue and needs to be kept safe. This means the ASV can operate in areas and conditions that would be deemed too dangerous for a manned platform, while maintaining consistent performance over extended periods of time. Being restricted to the surface does limit the types of measurements that can be made in contrast to underwater platforms, but in return allows for constant access to both GNSS and long range communication with relatively high bandwidth. Unmanned Underwater Vehicles (UUVs) consist of both tethered Remotely Operated Vehicles (ROVs) that are piloted manually from the surface and untethered Autonomous Underwater Vehicles (AUVs) that can operate independent of human intervention. If the AUV is within an acoustic network or surfacing for e.g. position fix from GNSS, the AUV may also communicate high level mission commands with a supervisor. Additionally, some hybrid vehicles combine strategies from both ROVs and AUVs for increased flexibility. AUVs have become a highly reliable platform for seafloor mapping over the past decades. While ROVs have lower capability in spatial coverage compared to AUVs, the ROV umbilical allows real-time transfer of video data to the pilot, and the traditional video and sampling surveys using a manually operated ROV are often preferred for seafloor mapping in both research and industry (Nornes, 2018).

As illustrated in Figure 3.1, the temporal and spatial resolution and coverage capabilities varies between the different platforms. Based on the data request, selections of platforms, sensors and parameters are made within appropriate temporal and spatial ranges, coverage and resolutions. Selection of parameters to measure should fit the environment in question and the aim of mission. Dependent on the environment, there will be a minimum set of parameters that always should be measured, either as an essential or supporting parameter for interpretation of other data gathered. In

addition to measurements of essential parameters, the quality of the data interpretation is dependent on the spatial and temporal resolution and coverage of the data. Hence, the dynamics in both space and time have to be considered in the mission planning process (Nilssen et al., 2015).

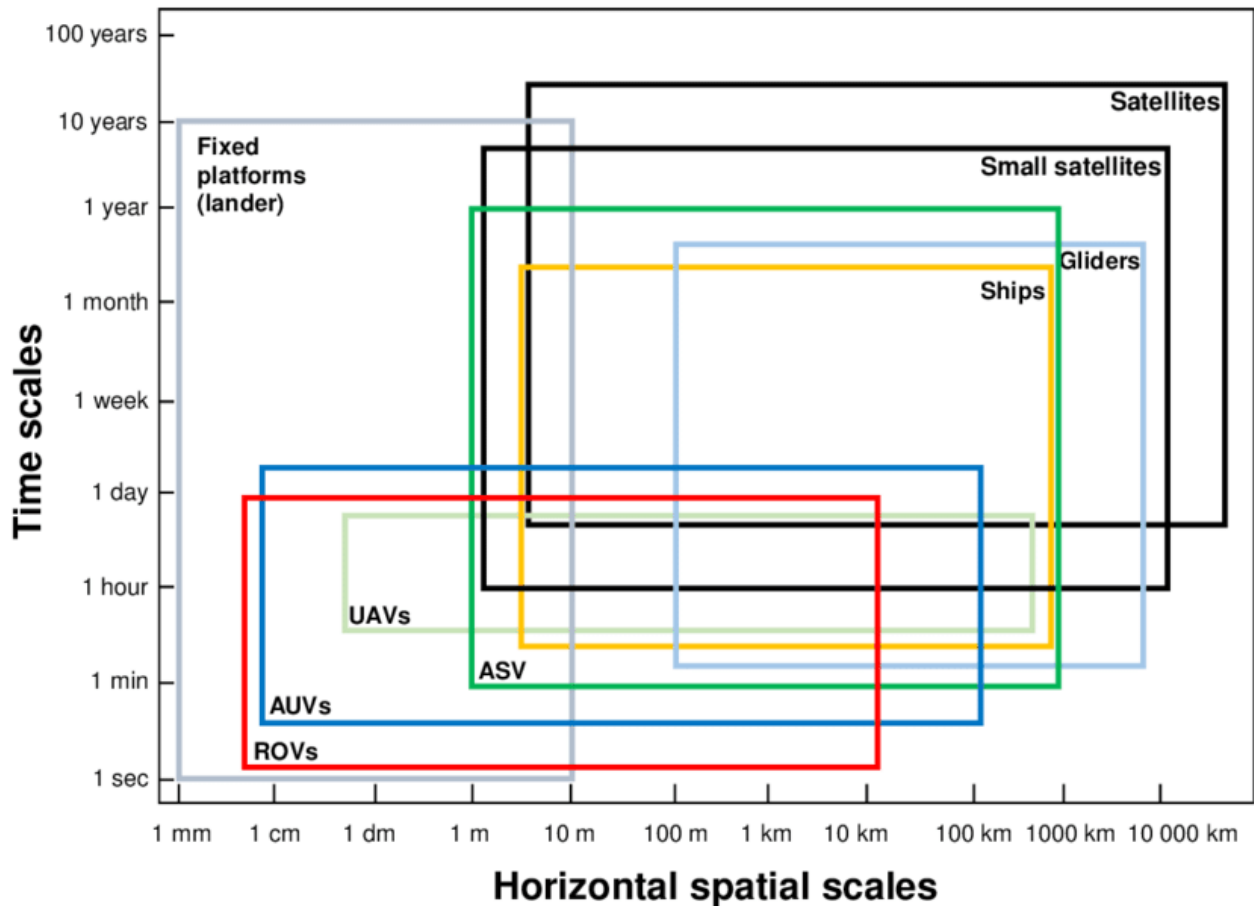


Figure 3.1 - Spatial and temporal platform capabilities. The lower end of the axis represents resolution, while the upper end represents maximum coverage. ROV=Remotely Operated Vehicle, AUV=Autonomous Underwater Vehicle, ASV=Autonomous Surface Vehicle, UAV=Unmanned Aerial Vehicle (Source: Nilssen et al., 2015).

In recent years, numerous research teams have been working to contribute in filling data gaps in the Arctic environment through robotic applications. Below are some examples of these robotic applications in the Arctic area, known in recent literature. For example, in 2010 an Unmanned Surface Vehicle (USV) based on an dinghy hull was designed as a remote controlled glacier-surveying robot with the primary goal of reducing the risk to workers in the field and being able to carefully take measurements of the calving glacier fronts above and below the water, using swath bathymetry and laser scanning hardware (Neal et al., 2012). In 2014, the JETYAK, a gasoline-based vehicle, highlighted the possibility of using autonomous surface vehicles (ASV) close to calving glaciers' fronts. The investigation with a multibeam sonar on the calving front allowed to obtain the shape profiles of the Sarqardleq glacier in Greenland with a surface vehicle, operating in an area prohibited for Autonomous Underwater Vehicles (AUV) due to the shallow depths (Kimball et al., 2014). In 2016, overcoming the difficulties of navigating in the acoustically noisy, iceberg-filled

fjord, the same research team used an AUV REMUS-100 which covered a large portion of the near-ice waters along the terminus of the Sarqardleq Fjord for the collection of useful observations to study the characteristics and distribution of near-ice area (Stevens et al., 2016). Another example of how robotics can provide effective solutions to collect high quality data in hazardous environments, mitigating risks, is the use of a Teledyne Gavia Offshore Surveyor 'Freya' operated by the Norwegian Polar Institute ship MV Teisten, which has allowed in 2016 and 2017, a high resolution mapping of bathymetry and CTD profiles in front of Fjortende Julibreen, Conwaybreen, Kongsbreen and Kronebreen glaciers of Svalbard (Howe et al., 2019).

New solutions have recently been developed to increase the number of data collected, not only limited to the marine area but also extended to the atmosphere. For example an Unmanned Aerial Vehicle (UAV) with IceDrone demonstrated the potential of unmanned aerial drone systems to facilitate ice sampling operations (Carlson et al., 2019).

In the wake of the activities listed above, there are also the field experimental campaigns carried out from 2015 to 2018 by Italian CNR-INM researchers in Arctic regions (Bruzzone et al., 2018).

3.2 The environment as driver of technological innovation and new observation methods

Monitoring the processes occurring in the Arctic region is crucial to identify the damages caused by the climate changes and to put in place appropriate strategies to counteract the process. To identify such changes it is appropriate to choose the most vulnerable sites, consolidate the state of our knowledge for the sites and develop a plan for sampling of time series of selected parameters. Particularly interesting is the case of the Kongsfjorden where, in the inner part of the fjord, many glaciers reach the sea with marine fronts that form a high vertical wall of ice protruding above seawater. In this area, as well as in similar cases, direct measurements in the proximity of glacier fronts are often lacking because the possibility of sudden falls of massive ice blocks makes data acquisition in these areas extremely dangerous. The navigation is even forbidden in this area due to safety reasons. In this context, robotics can provide effective solutions to collect high quality data in risky environment to catch the changes occurring near the front of the glaciers (snow-melt and transfer of water from land to the fjord) which result in physical and biogeochemical properties variations (like temperature, salinity, turbidity) of the nearby water masses that can affect the marine ecosystem and possibly reduce the biodiversity of the area. Thus risk mitigation and the necessity of collecting data not otherwise available consequently leads to the development of new technological solutions both in terms of autonomous vehicles and on-board instrumentation.

This is a first and fundamental aspect but this is not the only to consider. The other major issue linked to the limitations and constraints given by the particular environment where the measuring operations take place is the methodologies in which these observations are executed. The innovative procedures of observing the Arctic environment can be defined "data driven" as the choice on how to operate during the acquisition campaigns is dictated by the final data required, in turn linked to the information that is extracted from the data. The focus is therefore on the measurements in particular on the type of measure that is made, on the phenomenon that is observed and also on the temporal and spatial scale required.

Framework for Ocean Observing Process Diagram

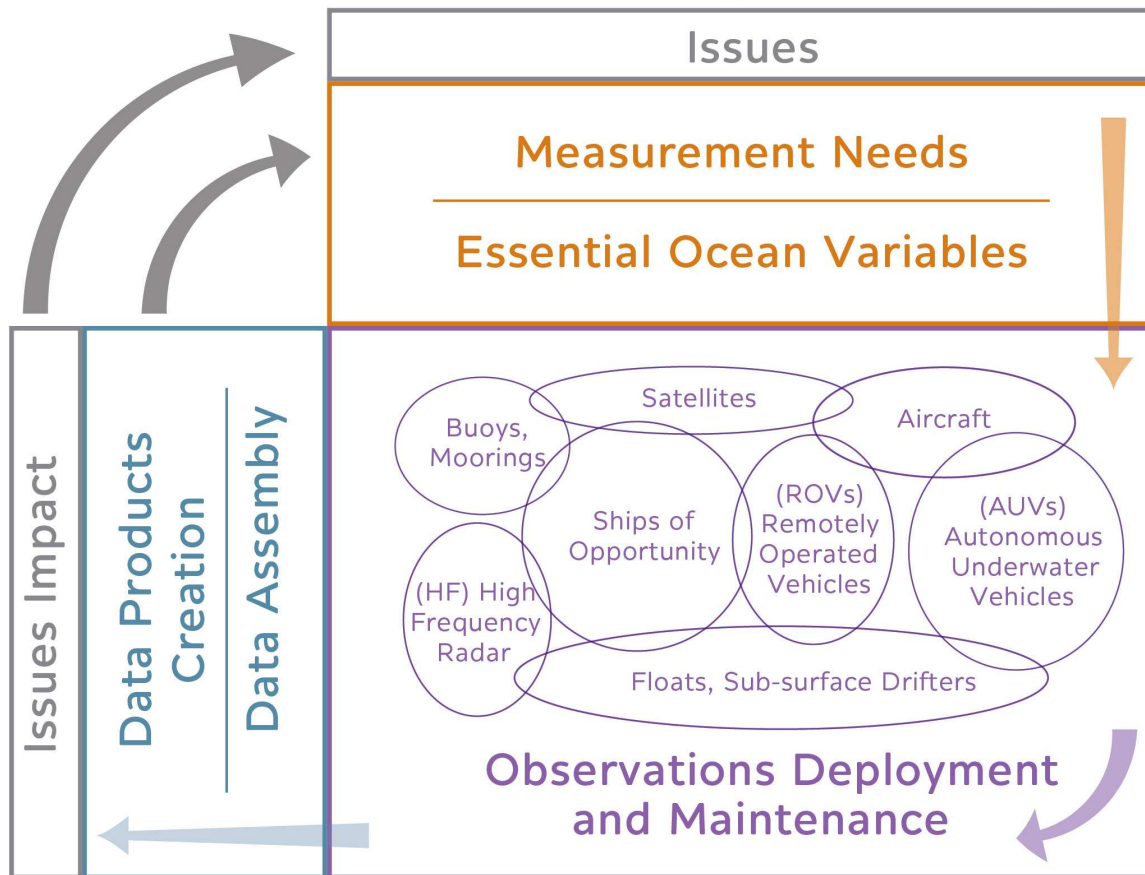


Figure 3.2 - Overview of the key elements in the Framework of Ocean Observing (FOO). Source: Tanhua, 2019.

These aspects are of fundamental importance for the Arctic area but can generally be used to develop an integrated system for observing the marine environment which, starting from the Inputs (e.g., essential ocean variables) and the measurement needs, determines which tools and procedures to implement (observations and maintenance) in order to obtain the desired outputs (data and products). The process obviously provides feedback on what were the initial targets inputs and therefore an iterative process is generated that gradually leads to improving the quality of the procedures and results. An example of this concept is shown in the Figure 3.2, borrowed from the Framework for Ocean Observing which introduces the following system design principles (Tanhua, 2019):

- Essential Ocean Variables (EOVs);
- Requirements;
- Observing system elements;
- Data management and information products;
- Readiness levels (for requirements, observations, and data and information).

The close link between the specific application, characterized by certain environmental constraints and specific outputs to be obtained, and the development of technological tools and operating procedures to be implemented, is clear. Autonomous operations in hardly accessible areas such as Polar Regions require specific designs and ad-hoc studied solutions. Usually different requirements have to be met, like for example provide an accurate assessment of condition in a relatively short time period, ensure repeatability, high positioning precision and a high degree in the control of the system. To satisfy all the numerous requests, sometimes in conflict with each other, it is necessary to mediate and find solutions that constitute the best compromise. To do this, it is necessary to develop research work that naturally leads to technological innovation and which in turn can improve the application from which the process originated. This approach, based on the **application** that drives **research** and leads to **innovation**, is shown in the Figure 3.3 and was used to develop the PROTEUS autonomous vehicle, described in the following paragraph.

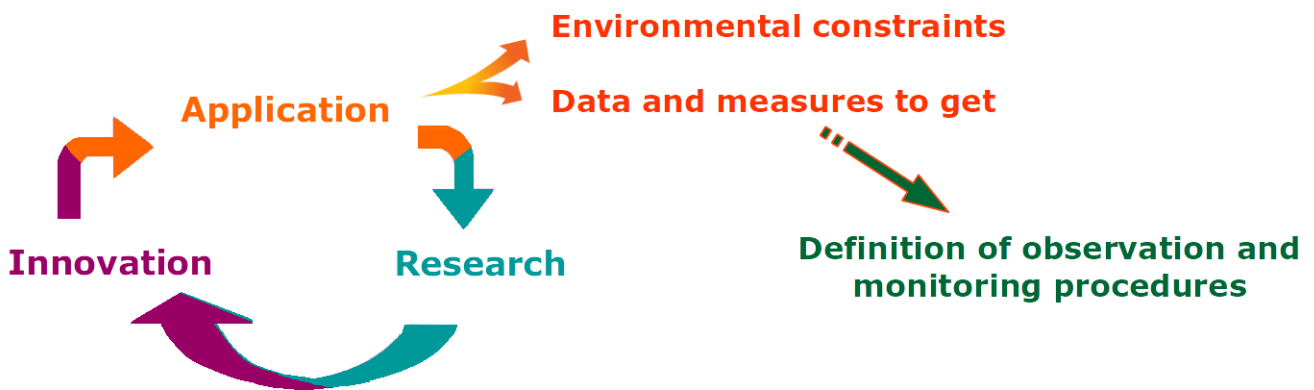


Figure 3.3 – Schematic representation of the approach based on the application that drives research and leads to innovation. At the same time, the specific application, characterised by environmental constraints and by data and measures to get, is the leading factor towards the definition of observation and monitoring procedures.

3.2.1 The PROTEUS USSV example

As discussed above, robotics can provide effective solutions to collect high quality data in hazardous environment, mitigating risks as the use of autonomous vehicles in these dangerous areas allows overcoming some of the limitations typical of traditional surveys. The ability to work autonomously of a host vessel makes this kind of vehicles suitable for the explorations in extreme conditions, as the Arctic environments, where there is limitation in the navigation of traditional boats due to safety reasons. These vehicles can execute fully autonomous and very precise motion in the area of interest, thus increasing the quality and accuracy of the collected data and can navigate also very close to the glacier front, collecting data that could not be collected in other ways.

The main concept behind the design and development of a robots expressly addressed for a peculiar ambient should be its adaptability to the specific environment constraints. Particular care is brought on the most suitable platform for the required operation, involving a continuous trade-off between

conflicting requirements: if on one side the problem is designing small, portable and highly controllable targeted solutions on the other side the aim is the seeking of long range and extended duration of autonomous operations with the problem of motion efficiency, low energy consumption and sea keeping ability (Odetti, PhD Thesis 2020). An additional consideration in using such autonomous platforms is they are limited in terms of space, power, data handling and servicing. Therefore, the sensor technology deployed on these platforms must be small, energy efficient, require minimal servicing and be able to store/transfer data. Moreover, to satisfy the need for measurement at an increased temporal and spatial resolution, the sensors should be low cost and ideally, mass producible (Connelly, 2017).

An example of autonomous robotic platform, integrating the requirements listed above, is PROTEUS (Portable RObotic TEchnology for Unmanned Surveys), designed by the CNR-INM (National Research Council – INstitute of Marine engineering) group based in Genoa. PROTEUS is a fully electric vehicle, that physically implements the concept of portable modular reconfigurable Unmanned Marine Vehicles: 45 kg of weight, 1.5 m long, 0.35 m wide and 0.35 m high, it is a highly modular and reconfigurable vehicle that has the possibility to act as either a ROV, an AUV or a USSV. PROTEUS is the evolution and adaptation of another vehicle, called P2-ROV (Portable-Polar Remotely Operated Vehicle), which was a pioneer implementation of the ecorobotics paradigm, that is the integration of ecological approaches and robotics to develop technological tools for environmental monitoring. P2-ROV was designed with a special eye on functionality and usability in harsh and remote areas. In particular P2-ROV dimensions (which are the same as PROTEUS) are studied to access under the thick layers of the ice sheet of Antarctica by exploiting the holes drilled in the ice by means of a special hand-auger which diameter is 350 mm. For this reason a torpedo-shape is chosen, due to its perfect matching with this operational requirement. See Figure 3.4 (Odetti et al., 2017).

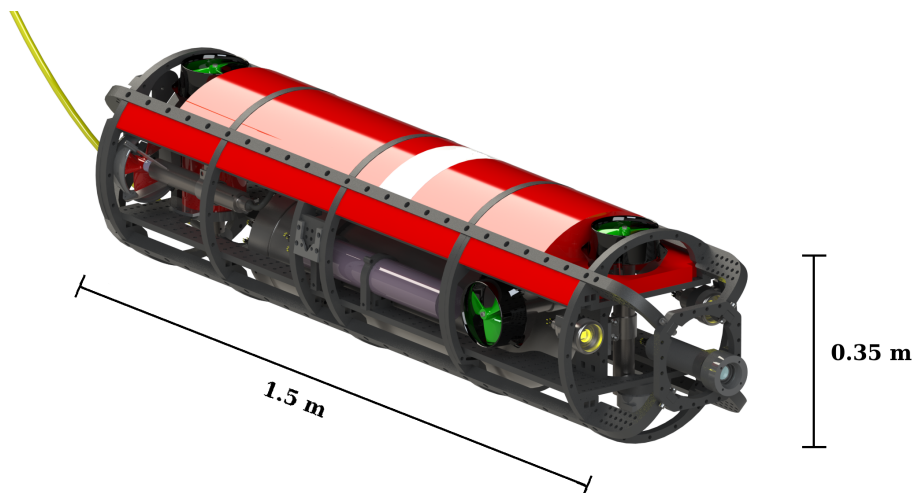


Figure 3.4 – Rendering of P2-ROV / PROTEUS in ROV configuration.

P2-ROV, and PROTEUS (Figure 3.4) accordingly, is a perfect example of the approach based on the application that drives the research and produces innovation (see Figure 3.3) as it was developed to meet a specific operational request but, thanks to the open hardware and software architectures, it can easily be fitted on board with a number of different sensors and actuators which allow it to operate also in other harsh environment situations.

The basic PROTEUS components, necessary for navigation, guidance and control are shown and listed in Figure 3.5 The additional payloads mounted on-board PROTEUS during the campaigns were selected based on the specific purpose of the mission and will be discussed in detail below.

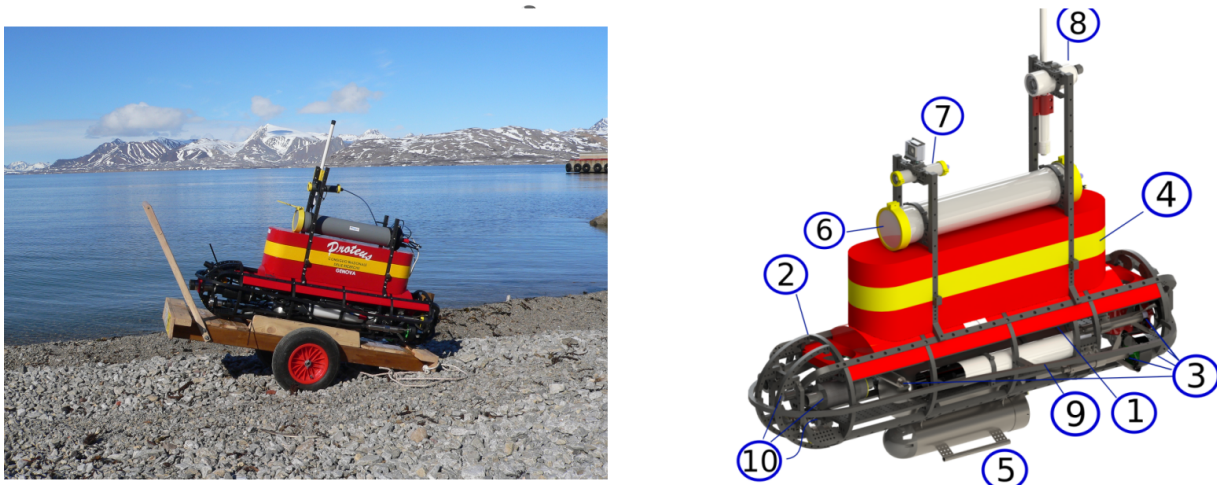


Figure 3.5 – Left: Picture of PROTEUS (Portable ROBotic TEchnology for Unmanned Surveys) in Ny Alesund. Right: PROTEUS components: 1- Control system in a pressure-tight canister; 2- Shockproof frame of Polyethylene; 3- Thrusters; 4- Removable foam; 5- Battery pack for USSV operations; 6- Surface control unit, GPS and inertial sensors; 7- Cameras; 8- Communications, Wi-Fi antenna and auxiliary Ethernet cameras; 9- Multi-probe CTD; 10- Front sensors: Turbidimeter, fluorimeter, altimeter.

3.3 The “data-driven” acquisition campaigns of the CNR-INM Group

Different scientific campaigns were carried out by CNR-INM in Ny-Ålesund, Svalbard Islands, to collect data necessary to study the important processes that are controlled by the mutual interactions between the atmosphere, the ice, the sea water and the fresh water originated by the melting of ice near the front of tidewater glaciers.

In the framework of the ARCA project (ARctic: present Climatic change and pAst extreme events), a preliminary scientific data collection campaign was carried out by CNR-INM in 2015 in Kongsfjorden. For the first time a marine unmanned semi-submersible vehicle (Shark) was specifically adapted and used to perform the discrete sampling of waters and the sensing of CTD Multi-parameter probe data in the area close to the Kronebreen glacier (Zappalà et al., 2016). A subsequent, more complex data acquisition campaign, involving simultaneous operation of three

unmanned vehicles was, performed during summer 2017 (from June 13th to June 26th) by CNR-INM in cooperation with researchers from other institutes of the National Research Council (IAMC, ISMAR, ISAC, IBIMET) and Tuscia University in the framework of the UVASS (Unmanned Vehicles for Autonomous Sensing and Sampling) project. During Spring 2018 (May 17th to June 4th), a third scientific campaign was carried out in the Svalbard Islands together with a field training period for researchers as part of the H2020 project "EXCELLABUST – Excelling LABUST in marine robotics" (Caccia et al., 2019).

Each campaign was conceived and implemented to achieve a specific purpose in terms of acquired data. This has led to the definition of methodologies and procedures, that can be defined as “data-driven”, for observing the environment in the Arctic area, adapted to the exceptional nature of the environment in which they are performed. The purpose of these field campaigns was:

- i) to demonstrate the capability of an Unmanned Semi-Submersible Vehicle (USSV) to approach a glacier front and collecting water samples just below it in order to study the microbiological status in this specific area;
- ii) to collect data for sea surface and air column characterization in the proximity of fronts of tidewater glaciers using a USSV working in cooperation with UAVs;
- iii) to perform repetitive sampling of water in the surface as well as characterise the bio-chemical-physical parameters of the water and air column close to the front of glaciers using a single USSV, equipped with suitable tools and instruments (Bruzzone et al., 2020).

In the following paragraphs the second and third campaigns (2017-2018) will be described in detail as they are more interesting from the point of view of the operating procedures and the data collected.

3.3.1 Sea surface and air column characterization – 2017 UVASS campaign

During the 2017 campaign PROTEUS was mainly used as USSV (Unmanned Semi-Submersible Vehicle) and remotely controlled by means of a guidance camera mounted on-top of the vehicle.

The choice of the USSV configuration is advantageous since the vehicle can move well between icebergs and growlers by pushing them from the submerged part without the risk of remaining stuck or trapped as it can happen to other kind of vehicles, for example the ROV connected to an umbilical cable.

The acquisition campaign took place in the stretch of sea facing the Kronebreen and Blomstrandbreen glaciers, in the Kongsfjorden. The changes occurring near the front of these glacier (snowmelt and transfer of water from land to the fjord) result in variations in temperature, salinity, turbidity of the nearby water masses that can affect the marine ecosystem and possibly reduce the biodiversity of the area. The purpose of the campaign was to capture bio-chemical-physical parameter variations with respect to the distance of the glacier front.

To achieve this goal, it was necessary to select the instruments to be mounted on board PROTEUS and define the operating procedures.

In particular, PROTEUS was equipped with the following sensors/samplers:

- an underwater video-camera, led lights and GoPro camera for the navigation;
- one Tritech Micron echosounder for acquiring bathymetric data;
- one Idronaut Ocean Seven 305 CTD multi-probe sensor for performing water data sensing (conductivity, temperature, depth, pH, Eh, oxygen);

- one small and low-cost sensor for measuring pressure, temperature and fluorescence of chlorophyll named ArLoC (Arctic Low-Cost probe) and developed by Tuscia University (Piermattei et al., 2018a);
- one Turner Cyclops-7 turbidity sensor.

All the data collected by these sensors were integrated in real-time with PROTEUS telemetry (for having all data synchronized and geolocalized), obtained with the GPS+AHRS integrated in the Microstrain 3DM-GX3-35 for position and attitude measurements. During the surveys, the communication system allowed the collected data to be accessible in real-time to the scientists so that they could modify the sampling area according to the previously acquired data and the position. Moreover, due to the necessity of acquiring data for the study of microbial biomass and bacteria respiratory activity, a small trimaran vessel was towed by PROTEUS during its surveys. This trailer was used to host particularly heavy and bulky sensors i.e. an automatic water multi-sampler provided by IAMC-CNR, a plankton multi-sampler and a Seabird SBE19plus v2 multiprobe sensor, provided by ISMAR-CNR (see Figure 3.6).

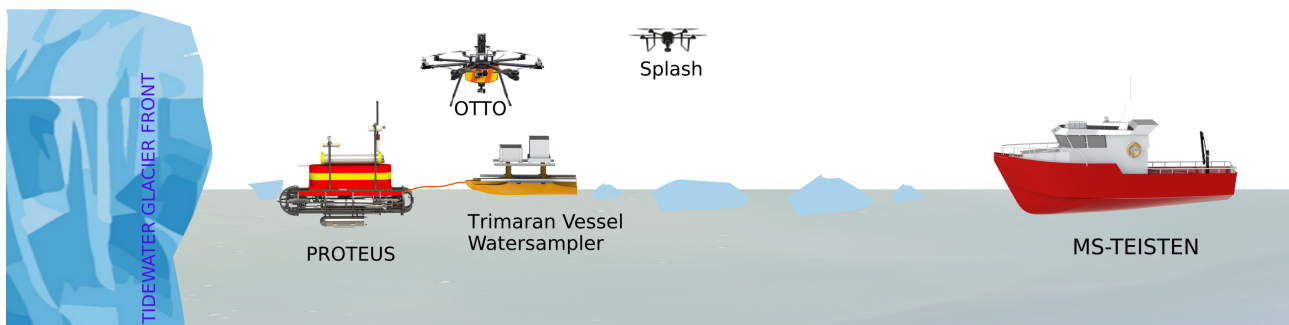


Figure 3.6 - Scheme showing the typical procedure used for data acquisition: PROTEUS vehicle towing the trimaran vessel and flew over by the aerial drones

Besides PROTEUS, two drones were also used during the surveys for different purposes: OTTO and Splash (Figure 3.7). OTTO is an octocopter drone originally developed by Italdron and later modified by CNR-INM, characterised by a high payload capacity.

During the campaign it was equipped with the following devices:

- thermal camera (FLIR A35) for sea surface temperature measurements;
- AirQino, an air quality characterisation system provided by IBIMET-CNR (temperature, humidity, CO₂, O₃, CO, NO₂, VOC, PM2.5, PM10 and barometric pressure, Sim28 GPS) (Cavaliere et al., 2018; Zaldei et al., 2017);
- video cameras (First Person View and GoPro) for video record.

The acquired data allow to study the features of the air column overlying the area inspected by PROTEUS and also to estimate the sea surface temperature values.

The Splash drone was used to record videos and images of the coordinated operations performed by PROTEUS and OTTO for documentary and dissemination purposes.

In Figure 3.6 a scheme of the typical operation configuration used for the data acquisition is shown.



Figure 3.7. On the left there is OTTO UAV with the AirQino (red box) and the Thermal Camera (orange box) mounted on-board. On the right the Splash UAV is shown.

From a logistic point of view, PROTEUS USSV, as well as OTTO and Splash UAVs, were remotely operated by personnel on-board a small support boat (MS Teisten), which remained at safety distance, about 500 m, from the glacier front. To capture parameter variations with respect to the distance from the glacier, the robot moved along paths almost perpendicular to the glacier fronts, as shown in Figure 3.8, where examples of the vehicle motion in two different missions is reported. The fact of starting the acquisition near the front of the glacier and then moving away from it, is linked to the conditions in which the operations took place, characterised by interference in the navigation of the vehicle due to the presence of icebergs and also by sudden waves generated by calving events, very frequent in these glaciers during the season in which the tests took place (mid-end of June). The operations were therefore planned and carried out taking into account all these practical constraints due to the environment.

The acquisitions were performed in the stretch of sea facing two distinct glaciers in the Kongsfjorden, i.e. Kronebreen and Blomstrandbreen. Sampling and monitoring in front of the Kronebreen glacier, located at the head of the fjord, were carried out using only PROTEUS USSV and its towed trimaran. The Blomstrandbreen glacier, located in the north-east area of the Kongsfjorden, is affected not only by the introduction of fresh water from the melting glacier but also by the Atlantic currents that come from the North, making it particularly interesting from the climatic changes point of view. For this reason, both the autonomous marine vehicle PROTEUS (for the characterization of the water surface) and the aerial drone OTTO (for the characterization of the air column) were used in a combined manner. In Figure 3.9 the fleet of heterogeneous autonomous vehicles operating in front of the Blomstrandbreen glacier is shown.

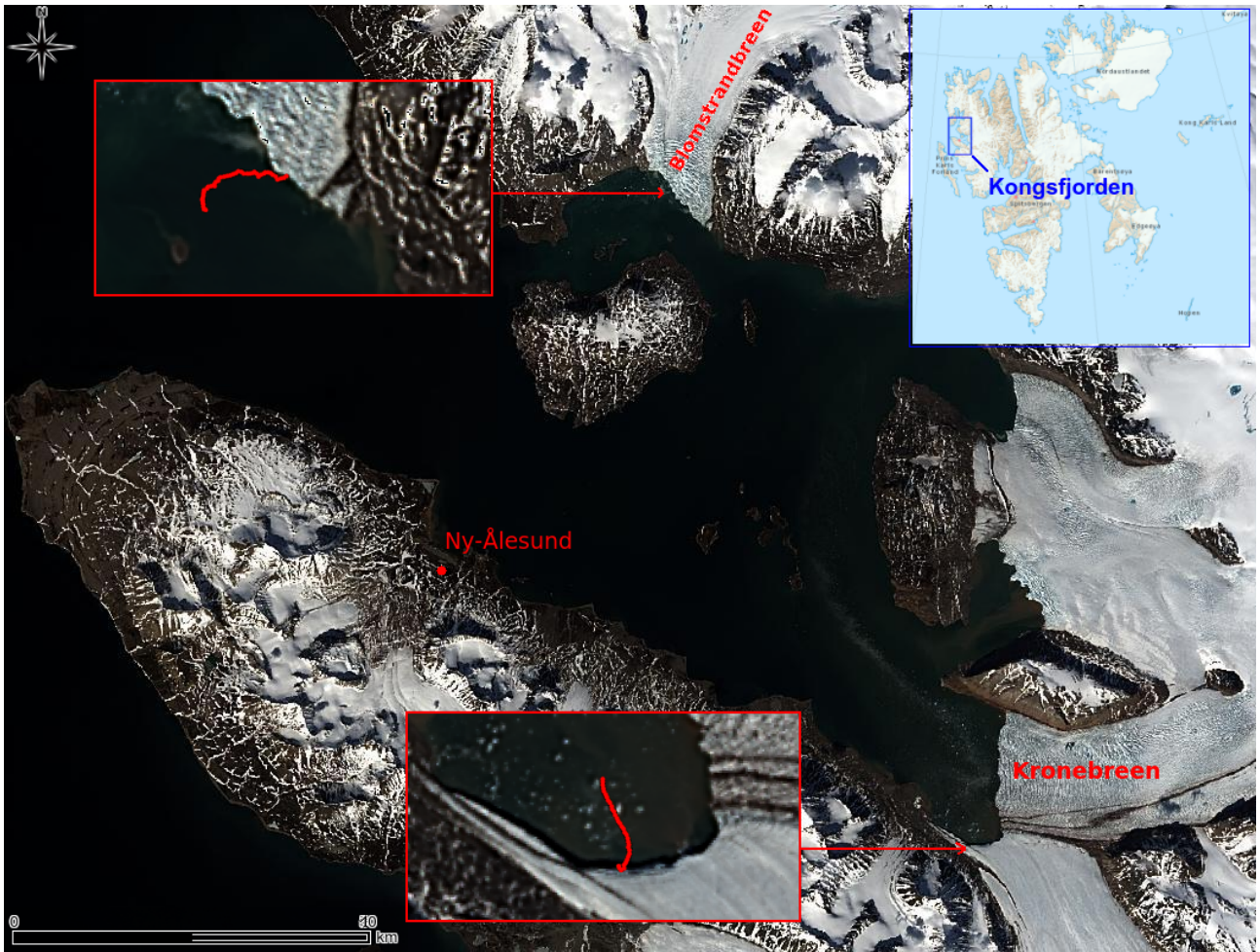


Figure 3.8 - Map of the Kongsfjorden area where data acquisitions took place during the 2017 campaign, obtained from Landsat 8 data images. In the boxes examples of GPS trajectories followed by PROTEUS during two missions are shown.



Figure 3.9 - PROTEUS, the trimaran vessel, OTTO and Splash unmanned vehicles operating near the Blomstrandbreen glacier.

From this data acquisition campaign, valuable scientific measures have been obtained, as described for example in Piermattei et al. (2018b), but also important operative indications on the procedures to be followed to carry out the observation of the environment to obtain the desired results, were learned. For example, whereas the campaign was successfully completed and the device itself always worked in the proper manner, it has been observed that the towing of the trimaran resulted to be an obstacle for the sampling. When the ice calving happens, the area in front of the tidewater glacier is often covered by floating ice debris (icebergs and growlers) that obstruct the passage for the vehicle. In these conditions, the towing cable is an obstacle to movement and the trimaran towed by PROTEUS can get trapped in the ice. Another example of indications obtained from the practice is related to the coordinated use of the aerial drone and PROTEUS: it was observed that the logistic was difficult to manage on board the small support vessel used, in particular as regards the take-off and landing operations of the OTTO drone from the plywood platform installed on the stern structure of the MS Teisten.

The experience gained with this “data-driven” acquisition campaign, together with the availability of low size commercial components, pushed research towards the design and development of new miniaturized data acquisition and sampling tools to be integrated on-board a single portable vehicle.

Considering all the requirements from the scientific as well as logistic/operational point of view, work has been done on important technological innovations that have been used in the following campaign.

3.3.2 Water column, sea surface and air column characterization - 2018 Campaign

The goal of the 2018 campaign was to perform repetitive sampling of water in the surface as well as characterise the bio-chemical-physical parameters of the water and air column close to the front of tidewater glaciers in the Kongsfjorden.

Taking into consideration the lesson learned during the campaign of the previous year and implementing the subsequent technological innovation developed, the marine and atmospheric data acquisitions along the entire vertical column, starting from the seabed up to the first layers of the atmosphere, was carried out using a single marine surface robotic vehicle, PROTEUS USSV, equipped with suitable instrumentation (see Figure 3.10).

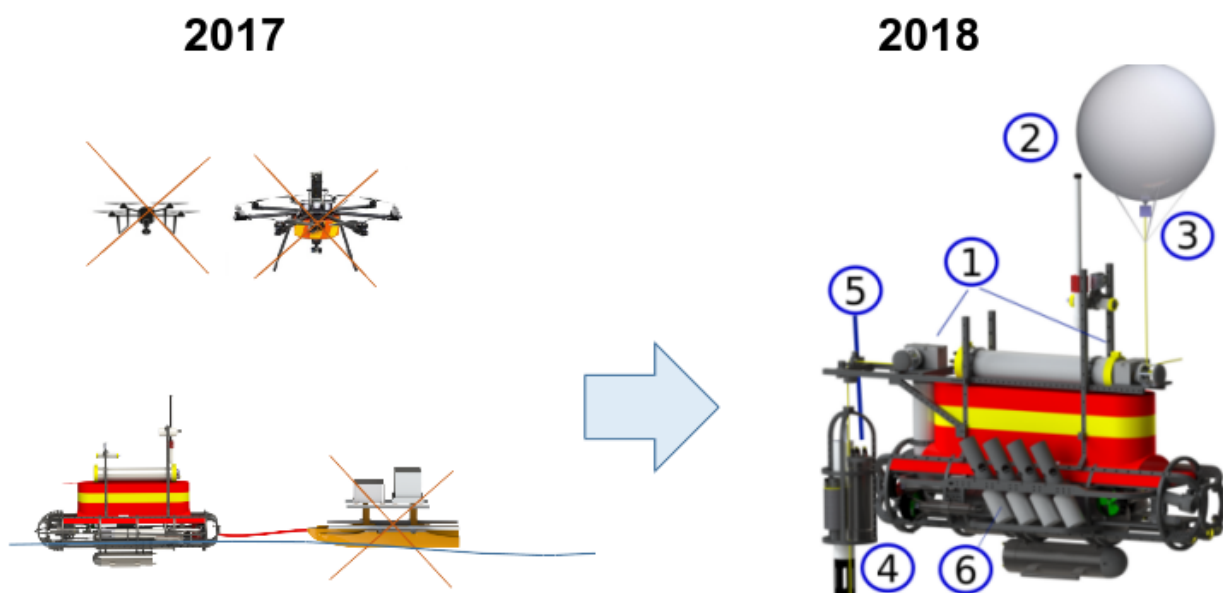


Figure 3.10 - Scheme showing the technological improvements based on the lesson learned from the 2017 campaign and in anticipation of the 2018 campaign. On the right side PROTEUS components: 1- Automatic winches for marine and atmospheric sensors; 2- Helium filled aerostat; 3- AirQino system; 4- Water sensors: CTD, ArLoC, fluorimeter, turbidimeter; 5- MPDACS Multi Purpose Data Acquisition Control System; 6- MAWS Mini Automatic Water Sampler.

In particular, the heavy water sampler mounted on the trimaran vessel was replaced by a new Mini Automatic Water Sampler (MAWS) integrated on PROTEUS and used for the collection of water samples for microbiological studies. It was built by using commercial off-the-shelf laboratory bottles on which an automatic stopper, based on magnetic fields, was applied (Odetti et al., 2019).

This improvement made it possible to eliminate the problem of the towing cable connecting PROTEUS to the trimaran that was a possible source of trapping in the ice.

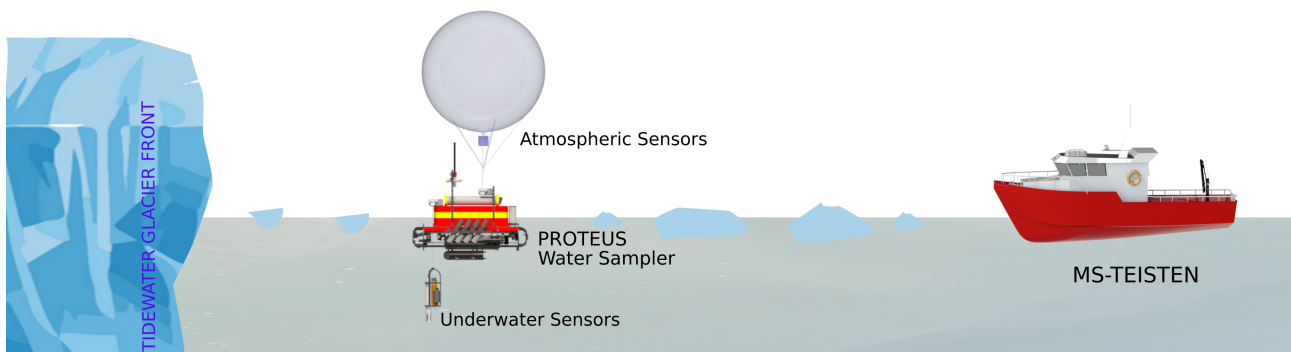


Figure 3.11 - Scheme showing the PROTEUS vehicle with all the instruments and sensors integrated on-board.

Moreover, for carrying out an integrated characterisation of the water column – water surface - air column, two release systems based on automatic winches were installed on PROTEUS. The fore winch was used for launching and recovering a helium-filled aerostat and carrying the AirQino system for air quality monitoring (humidity, temperature, CO, CO₂, O₃, NO₂, PM10, PM2.5). The use of the aerostat in place of the UAV not only simplified the logistic and the operations but also increased the duration of atmospheric data acquisitions.

The astern winch was used for releasing and recovering a set of instruments for the bio-chemical-physical characterization of the water column: an Idronaut Ocean Seven 305 CTD (conductivity, temperature, depth, pH, Eh, oxygen), a Turner Cyclops-7 fluorometer/turbidimeter and the multi-probe sensor ArLoC (depth, temperature, chlorophyll a1-a2). In Figure 3.11 a scheme showing PROTEUS and all the instruments and sensors is shown.

Also in this campaign, the operating procedures were “data driven” that means planned and performed on the basis of the type of measure to be acquired in order to obtain a complete characterization of the air column, of the air-water interface and of the water column using a single autonomous vehicle (PROTEUS USSV), equipped with instruments and sensors listed above. PROTEUS executed various missions in the proximity of the fronts of Blomstrandbreen, Kongsbreen, Kronebreen, and Conwaybreen glacier (some examples of the paths executed are shown in Figure 3.12). The data collected, the analysis carried out and the results obtained will be described in the next chapter. Attention was particularly focused on the Blomstrandbreen, known for being positioned in an area influenced both by the introduction of water due to the melting of the ice, and by the incoming Atlantic current, and on the Kongsbreen, characterised by abundant water inlet due to ice melting which colored the water with a particular brownish color due to suspended material. Particularly complex data acquisition procedures have therefore been implemented in these areas.

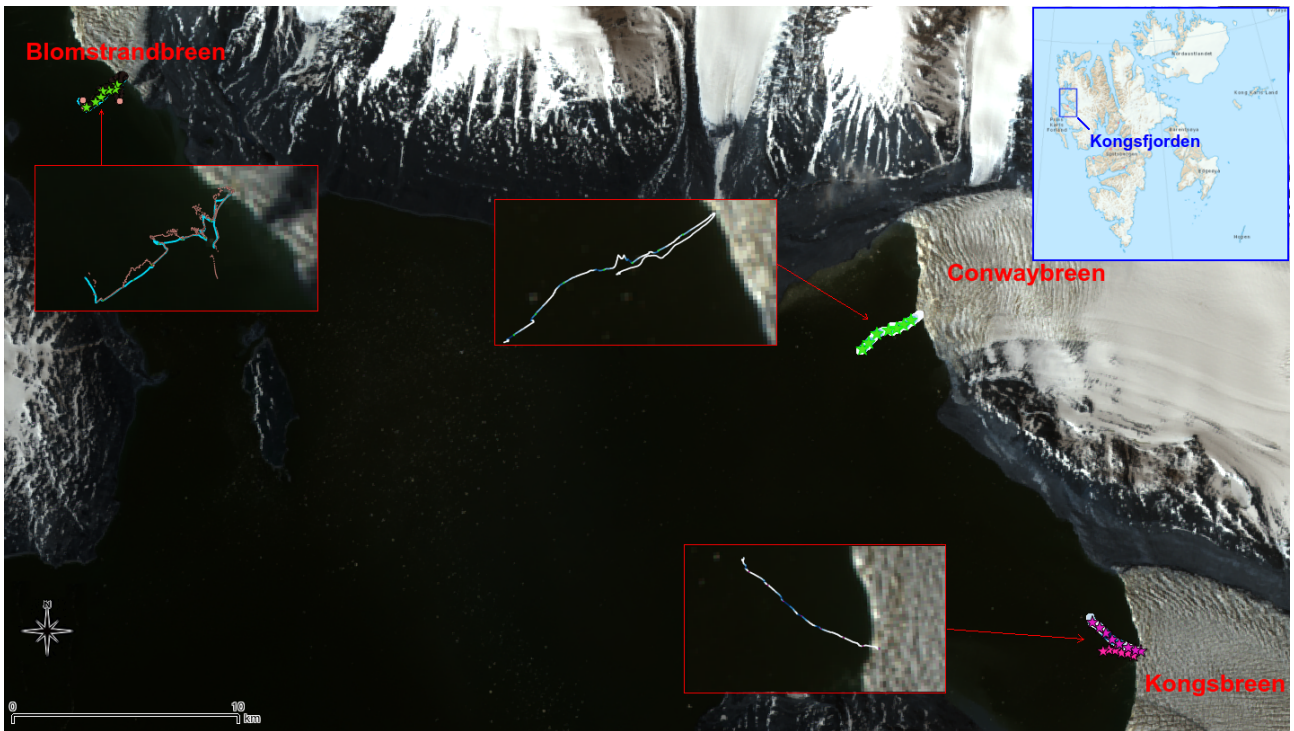


Figure 3.12 - Map of the testing sites in Kongsfjorden during the 2018 campaign, obtained from Landsat8 data images. The boxes show examples of GPS trajectories followed by PROTEUS USSV during data acquisition.

The first phase involved approaching PROTEUS to the front of the glacier, until it touched it. At this point the vehicle was stopped and made sure that it maintained its position. While the vehicle was in position, water samples were acquired with the MAWS sampler, to study the microbiological characteristics near the glacier fronts and for the research of the presence of possible heavy metals (Azzaro et al., 2018).

Simultaneously measurements of physical and bio-geo-chemical parameters along the water column were performed releasing the set of instruments by means of the winch, down to depth of 40-50 m. This operation was used to record the variation of the parameters as a function of the depth, in a fixed point, and therefore to study effects due to currents, to the introduction of substances by the water coming from the glacial ice melting and to characterize the area near the front of the glacier from a physical point of view.

At the same time, the second winch released vertically the helium filled aerostat with the air characterization system, in order to record the variation of the atmospheric parameters as a function of the height with respect to the sea level, up to about 70 meters. Pictures showing PROTEUS and the aerostat acquiring data near the front of the glacier are shown in Figure 3.13.

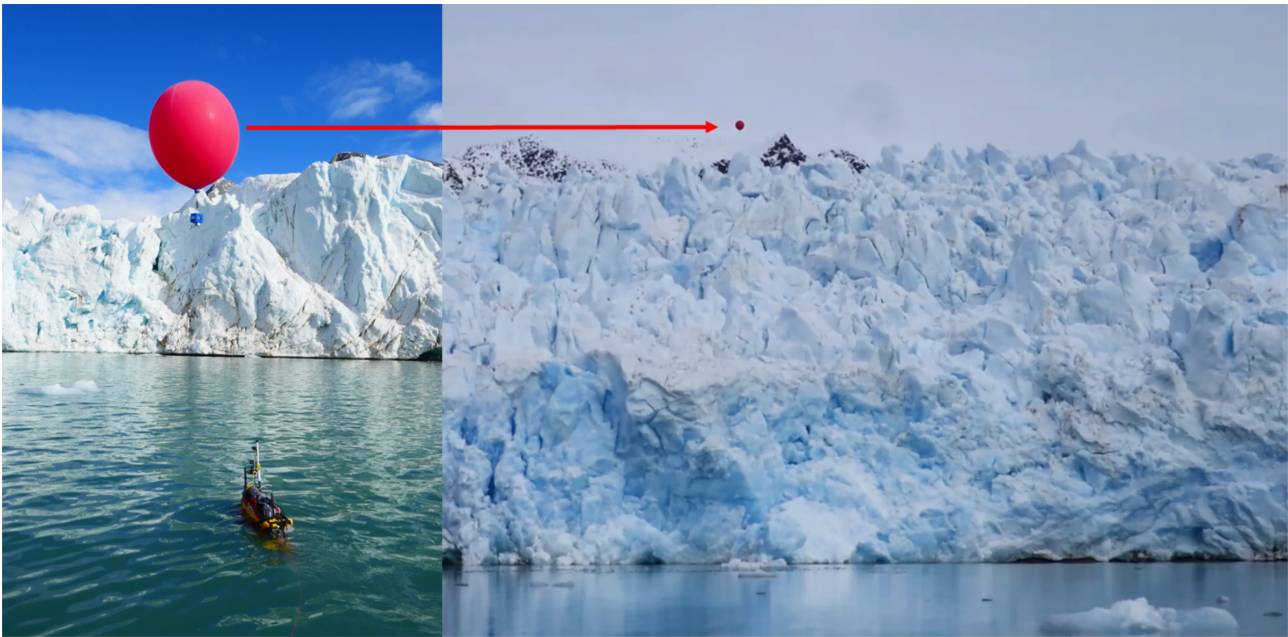


Figure 3.13 - PROTEUS with the aerostat and the AirQino system (blue box under the red balloon) measuring near the front of the glacier.

Once these operations were carried out, the winches were rewound and the vehicle was moved towards the next sampling point, located at a greater distance from the glacier front and in a direction approximately perpendicular to it. During this navigation phase, the data acquisition with the water sensors continued to have a wider representation of the variability of the parameters while moving away from the front of the glacier.

When the new sampling point was reached, the operations for collecting the water samples with MAWS and for releasing the sensors using the two winches were repeated. The whole sequence described is repeated several times in numerous points, with increasing distance from the front of the glacier, as shown in Figure 3.12.

The execution of the measures following these “data-driven” procedures allowed to collect useful data for the characterization of the environment from physical, chemical, biological point of view, coping with the hostile working conditions typical of the areas close to the fronts of tidewater glaciers.

Based on the lesson learned during the campaign and on the results from the data analysis, new technological developments are required. The next step will consist in adapt PROTEUS to work as an AUV below the floating ice tongue in order to catch the fresh water flows coming from the inner glacier (Piermattei et al., 2018a).

Chapter 4

Svalbard Field Data

Different scientific campaigns were carried out by CNR-INM in Ny-Ålesund, Svalbard Islands, to collect data necessary to study the important processes that derive from the mutual interactions between atmosphere, ice, sea water and fresh water originated by the ice melting near the front of tidewater glaciers.

Tidewater glaciers terminate in the sea where they discharge icebergs into the ocean through the process of calving and are, in general, behaving far more dynamically than land-terminating glaciers. These ocean-terminating glaciers are further characterized by fast flow at their terminus with flow speeds in the order of a few hundred meters to several kilometers per year (Joughin et al., 2010; Meier et al., 1987). The flow typically accelerates toward the terminus, causing high along-flow extension and consequently intense crevassing (Vieli et al., 2000). Sudden dynamic changes consisting of rapid retreat, flow acceleration, and surface thinning are common for tidewater glaciers with retreat rates reaching kilometers per year, manifold increases in flow speed and thinning rates of several tens of meters per year. Such rapid dynamic changes have, in the last decade, been widely observed for tidewater glaciers (Carr et al., 2013; Howat et al., 2007; Joughin et al., 2004; Moon et al., 2012). In particular, it has been observed a strong dependency of calving rates and tidewater glacier dynamics on basal topography near the glacier front. For this reason, accurate knowledge of fjord and channel geometry is a key element for predictions of tidewater glacier behavior. Moreover, the freshwater delivery from these glaciers, in the form of icebergs or as a plume of water, may potentially have an impact on thermohaline circulation in the fjord and thereby affect the climate system.

In order to understand these processes so important for the fjord and its ecosystems, it is necessary to go exactly where the processes originate, that is, as close as possible to the front of the glaciers.

The use of robotic platforms allows to reach these normally inaccessible places and to record the bio-chemical-physical parameters at spatial (from hundreds of meters down to centimetric dimensions) and temporal (from hours to minutes) resolutions that cannot be obtained with traditional methods like, for example, satellite.

The data acquisition campaigns, carried out at Svalbard in 2017 and 2018 by the CNR-INM research group and described in Chapter 3, made it possible to acquire data relating both to the surface and water-air column near the front of several tidewater glaciers of the Kongsfjorden. The following tables summarise the types of data acquired, specifying the place of acquisition (name of the glacier), the instrumentation used (type of sensor) and also the method of acquisition (surface water, water column, air column). These acquisitions can be classified under the "Raw Observations" typology and have associated the related metadata necessary for the processing, in order to obtain indicators of the state of the environment.

The execution of these measures following “data-driven” procedures allowed to collect useful data for the characterization of the environment from physical, chemical, biological point of view, coping with the hostile working conditions typical of the areas close to the fronts of tidewater glaciers.

Table 4.1 – CNR-INM Svalbard 2017 campaign description. CTD = Conductivity, Temperature and Depth; TFLAP (ArLoC) = Arctic Low-Cost probe, measuring depth, temperature, chlorophyll a1-a2; AirQino = air quality characterisation system, measuring atmospheric parameters.

Date	Time	Where	Water Sensors (Surface)					Air Sensor
			Idronaut CTD (105)	TFLAP (ArLoC)	Seabird CTD	Turner Turbidimeter	Water Sampler	Airqino
18/06/2017	16:44	Ny Alesund Harbour (78.92913, 11.94199)	V				V	
18/06/2017	18:02	Ny Alesund Harbour	V	V			V	
20/06/2017	10:20	Ny Alesund Harbour	V	V			V	
20/06/2017	17:11	Ny Alesund Harbour	V	V			V	
22/06/2017	18:04	Ny Alesund Harbour	V	V			V	
19/06/2017	11:01	Kronebreen (Area 1 - 78.87053,12.55349)	V					
19/06/2017	11:40	Kronebreen (Area 1)	V				V	
19/06/2017	11:42	Kronebreen (Area 1)	V	V			V	
19/06/2017	14:55	Kronebreen (Area 2 - 78.86237,12.56734)	V				V	
19/06/2017	14:56	Kronebreen (Area 2)	V	V			V	
19/06/2017	15:07	Kronebreen (Area 2)	V	V			V	
19/06/2017	15:12	Kronebreen (Area 2)	V	V			V	
21/06/2017	11:05	Bloomstrandbreen (79.01761,12.16775)	V				V	V
21/06/2017	11:11	Bloomstrandbreen	V	V			V	V
21/06/2017	13:29	Bloomstrandbreen	V	V			V	V
23/06/2017	10:44	Bloomstrandbreen	V	V			V	V
23/06/2017	11:10	Bloomstrandbreen	V	V	V		V	V
23/06/2017	12:23	Bloomstrandbreen	V		V		V	V
23/06/2017	13:18	Bloomstrandbreen	V				V	V
23/06/2017	13:30	Bloomstrandbreen	V	V			V	V
23/06/2017	13:33	Bloomstrandbreen	V	V	V		V	V
23/06/2017	15:17	Bloomstrandbreen	V	V	V		V	V
23/06/2017	15:35	Bloomstrandbreen	V	V	V		V	V

Table 4.2 - CNR-INM Svalbard 2018 campaign description. CTD = Conductivity, Temperature and Depth; ArLoC = Arctic Low-Cost probe, measuring depth, temperature, chlorophyll a1-a2; MAWS = Mini Automatic Water Sampler for microbiological studies; AirQino = air quality characterisation system, measuring atmospheric parameters.

Date	Time	Where	Water Column Sensors				Water Sensor/Sampler (Surface)		Air Sensor
			Idronaut CTD (105)	ArLoC	Fluorimeter	Turner Turbidimeter	Idronaut CTD (104)	MAWS	Airqino
25/05/2018	10:47	Bloomstrandbreen (Area 1 - 79.02196,12.15215)						V	
26/05/2018	13:30	Bloomstrandbreen (Area 1)	V		V	V	V	V	
28/05/2018	10:31	Bloomstrandbreen (Area 2 - 79.00915,12.21286)	V		V	V	V	V	V
28/05/2018	13:17	Bloomstrandbreen (Area 2)	V	V	V	V	V	V	V
29/05/2018	14:55	Bloomstrandbreen (Area 2)						V	
30/05/2018	18:12	Bloomstrandbreen (Area 2)					V	V	
30/05/2018	14:32	Kongsbreen (78.96574,12.61896)					V	V	
01/06/2018	11:05	Kongsbreen	V	V	V	V	V	V	V
30/05/2018	09:58	Kronebreen (78.88061,12.59886)					V	V	
01/06/2018	14:01	Conwaybreen (78.99109,12.53055)	V	V	V	V	V	V	V

Given that during the 2018 campaign the data were collected not only on the surface but also along the water column, it was decided to focus the analysis on these data that allow to detect efficiently the complex transient phenomena that occur near the front of the glaciers.

As reported in Table 4.2, in the period from May 25th to June 1st, 2018, PROTEUS USSV executed various missions in the proximity of the fronts of Blomstrandbreen, Kongsbreen, Kronebreen, and Conwaybreen glacier. Complete water and air column profiles, and surface water sampling, were performed nearby Blomstrandbreen, and Kongsbreen glaciers.

From an operational point of view, the first phase involved the approach of PROTEUS to the front of the glacier, until it touched it. Reached this point the vehicle was stopped and made sure that it maintained its position. While the vehicle was in position, measurements of physical and bio-geo-chemical parameters along the water column were performed releasing the set of instruments by means of a winch, down to depth of 40-50 m. This operation was used to record the variation of the parameters as a function of the depth, in a fixed point, and therefore to study possible effects due to currents, to the introduction of substances by the water coming from the glacial ice melting and to characterize the area near the front of the glacier from a physical point of view.

At the same time a second winch released vertically the helium filled aerostat with the air characterization system AirQino, in order to record the variation of the atmospheric parameters (e.g. temperature, humidity, CO₂, O₃, CO, NO₂, PM2.5, PM10) as a function of the height with respect to the sea level, up to about 70 meters.

Once the measurements along the air and water columns were completed, the two winches were rewound and PROTEUS was directed to the next sampling point, at a distance gradually greater from the front of the glacier. Even during the transfer phases from one sampling point to the next, the physical-chemical-biological parameters were recorded in the surface layer of the water.

More details on the operating procedures and on the sensors and samplers employed are described in Chapter 3.

4.1 Kongsbreen Glacier

The Kongsfjorden is characterized by five tidewater glaciers which, together with the Atlantic current, influence the physical-chemical and biological characteristics of the waters of the fjord and therefore of the entire system connected to them. The Kongsbreen glacier is located in the innermost part of the Kongsfjorden. The figure shows a transept executed by PROTEUS starting from a position close to the front of the glacier (bottom right in the graph) and gradually increasing its distance, in a direction approximately perpendicular to the front. The graph shows the positions recorded by the PROTEUS positioning system (latitude and longitude in WGS84, EPSG 4326 reference system) and the color is proportional to the depth (m) with respect to the surface of the water recorded by the Depth sensor mounted on the CTD: going from light blue to dark blue, the depth goes from about zero (surface) to below -25 m, as also shown in the Figure 4.1.

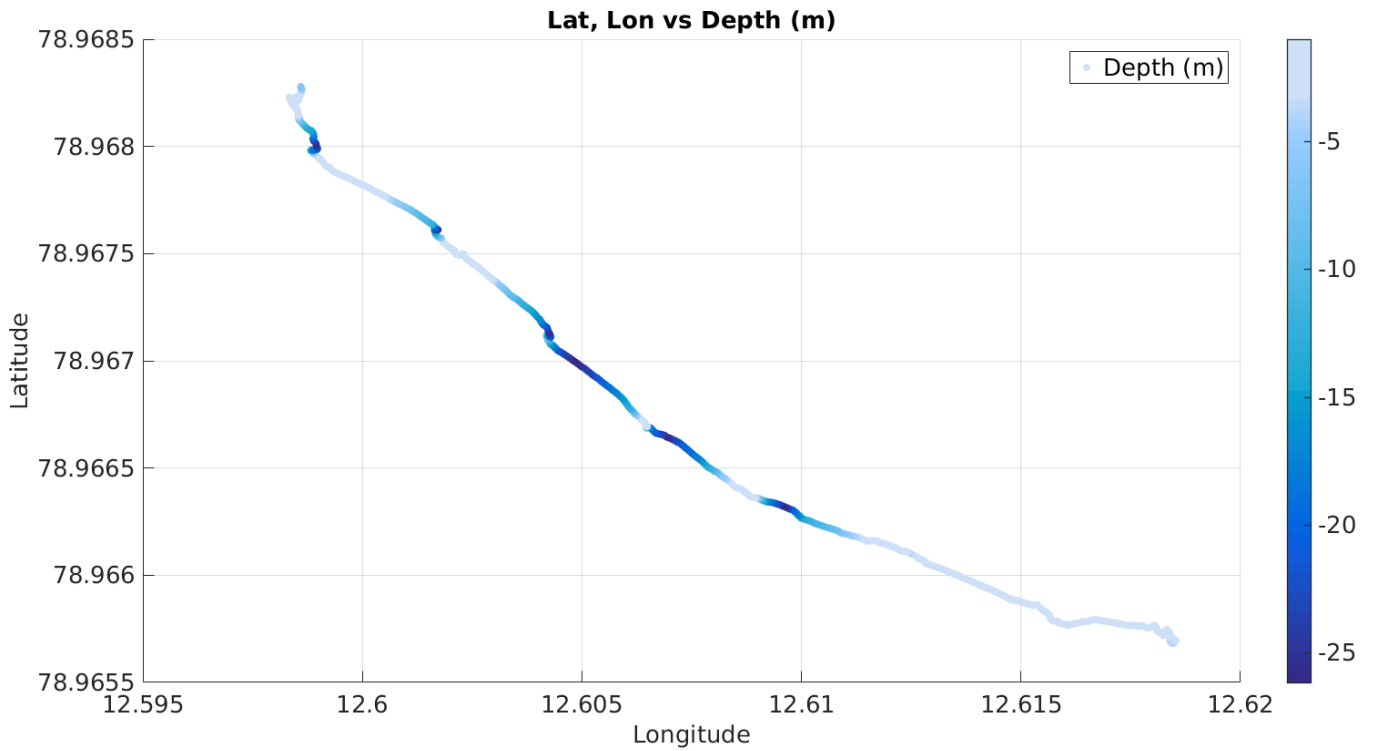


Figure 4.1 - Latitude and longitude (WGS84, EPSG 4326 reference system) positions of PROTEUS. The color is proportional to the depth (m) with respect to the surface of the water. The front of Kongsbreen glacier is in the bottom-right part of the graph.

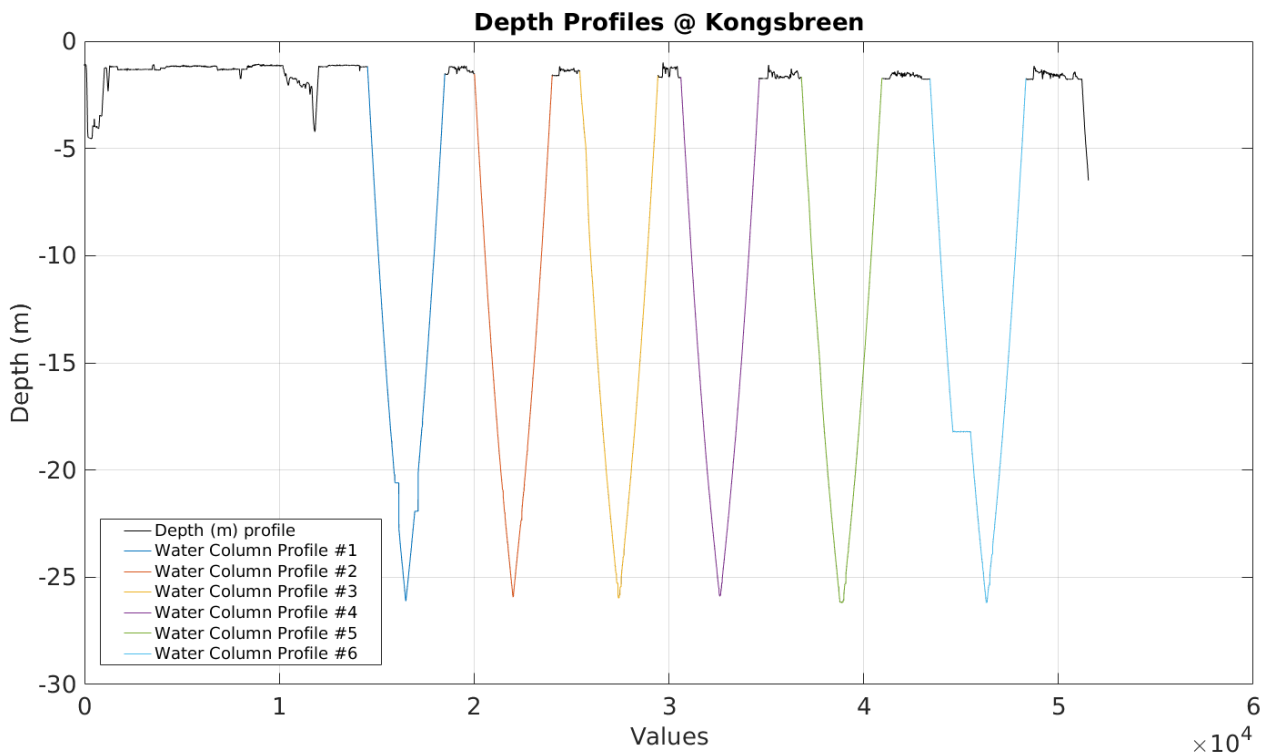


Figure 4.2 - Sequence of recorded values on the x-axis and depth (m) values on the y-axis. The different colors highlight the different water column profiles made.

The graph in Figure 4.2 shows the sequence of recorded values on the x-axis and the depth (m) values on the y-axis. The different colors highlight the different water column profiles made.

The purpose is to study how the water masses vary according to the distance from the front of the glacier. To do this, the distance from the glacier was calculated using as a reference the position of the front obtained from satellite images collected on the days the tests were carried out. Having fixed the position of the front of the glacier, the distances were calculated starting from the latitude and longitude data and using the haversine formula that returns the distance along the surface of the earth between a couple of points.

The following graph, therefore, represents the variation of the depth (m, y-axis) as a function of the distance from the front of the glacier (m, x-axis). The average distance from the front of the glacier for each profile is calculated and indicated in the legend: the vertical profiles range from a distance of about 220 m up to about 450 m from the front.

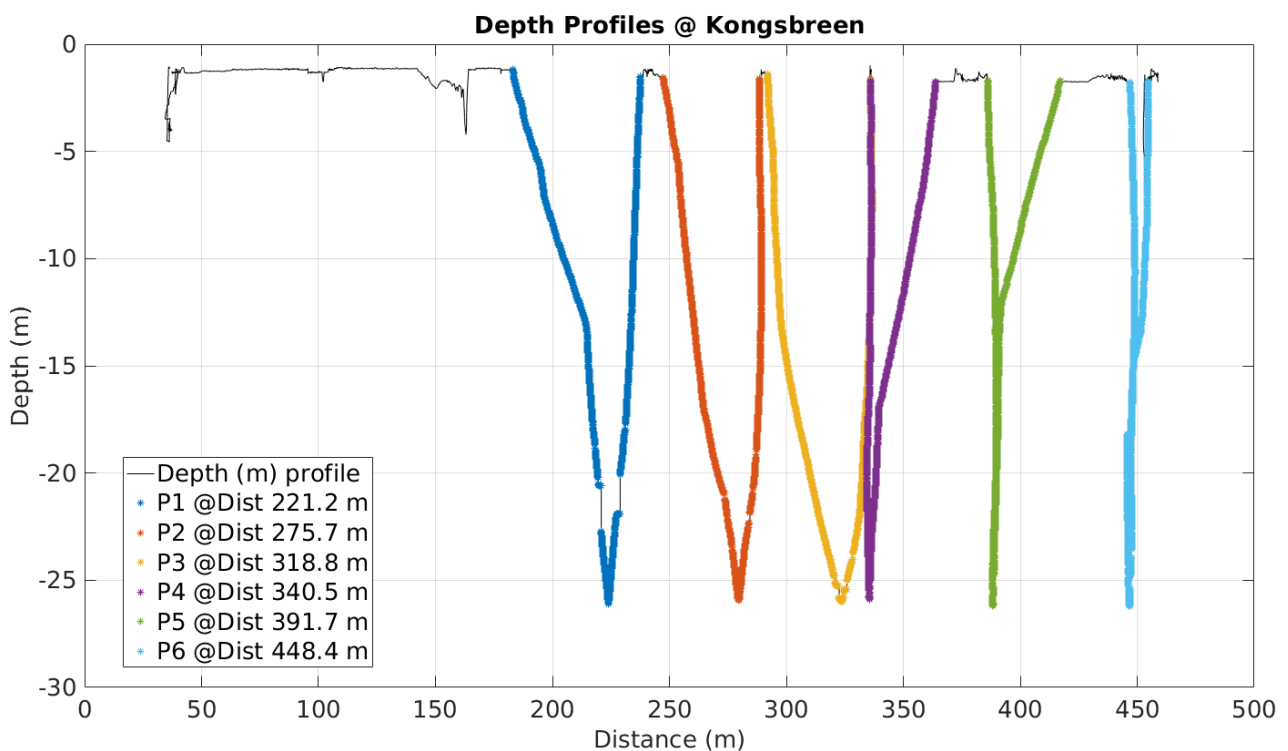


Figure 4.3 - Variation of the depth (m, y-axis) as a function of the distance from the front of the glacier (m, x-axis). The average distance from the front of the glacier for each profile is calculated and indicated in the legend.

Now the analysis of the parameters recorded along each vertical profile is performed. As a first step the focus is on two fundamental parameters: temperature and salinity.

The temperature at the sea surface varies with the geographic position on the earth, with the season of the year and the time of the day; through the water column the behavior of the temperature is also very complex. The salinity is a measure of the quantity of dissolved salts and other minerals in sea water and is measured with a CTD sensor (Conductivity, Temperature and Depth) using the observable electrical conductivity of the sea water. CTD is also constituted by thermistors, elements whose electrical resistance depends on their temperature, used to measure the water temperature at

several depths through the water column. The parameters of Temperature ($^{\circ}\text{C}$) and Salinity (PSU - Practical Salinity Unit) were acquired by means of an OCEAN SEVEN 305Plus CTD, which guarantees 0.005°C of accuracy and 0.001°C of resolution on the Temperature measure. Salinity data are obtained using the algorithms described in the UNESCO technical papers in marine science no. 44 "Algorithms for computation of fundamental properties of sea water" starting from Conductivity measures (accuracy 0.007 mS/cm and resolution 0.001 mS/cm in salt water, as tabulated in the datasheet).

The study of the variation of these two parameters as a function of both the distance from the front of the glacier and the depth allows to identify the structure of the water masses present near the tidewater glaciers, before they undergo mixing with the water of the fjord, and also to identify possible currents responsible of the circulation inside the fjord.

The following graph shows the variation in temperature ($^{\circ}\text{C}$; yellow = warm; blue = cold) as a function of depth (m, y-axis) and distance from the front of the glacier (m, x-axis).

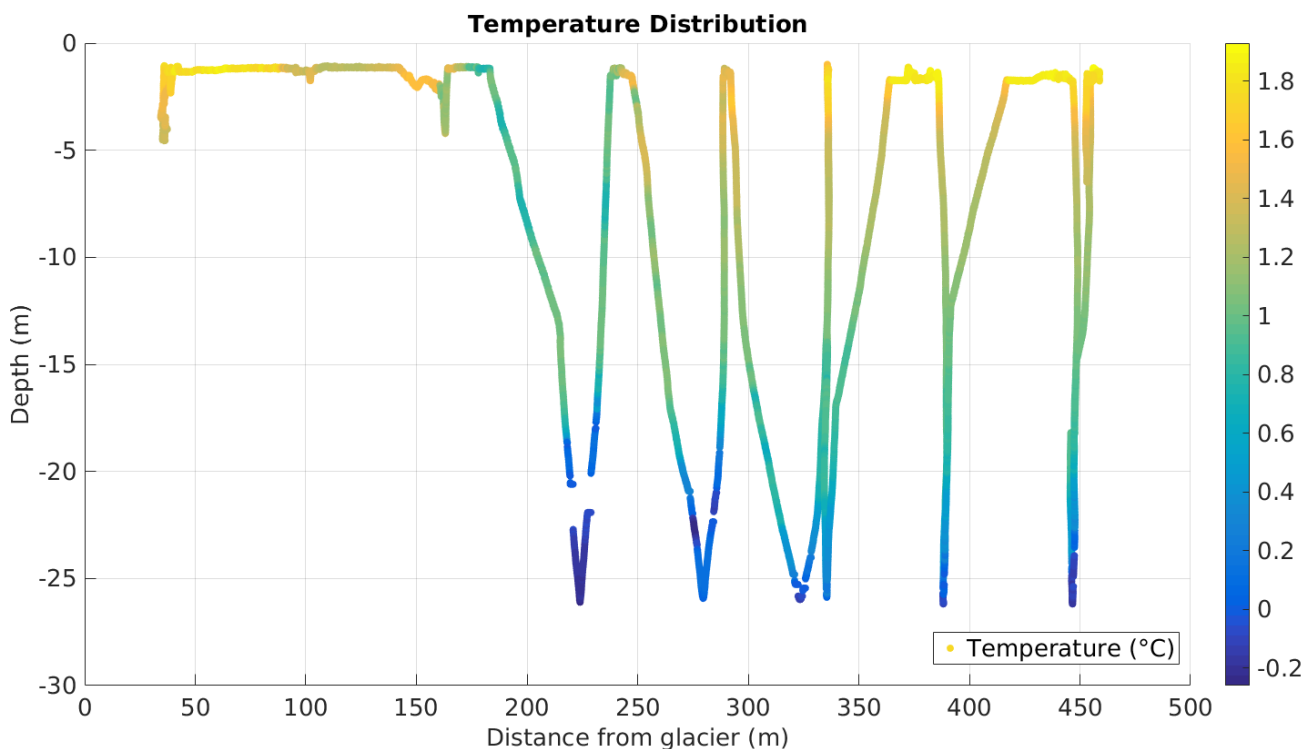


Figure 4.4 - Variation in temperature ($^{\circ}\text{C}$; yellow = warm; blue = cold) as a function of depth (m, y-axis) and distance from the front of the glacier (m, x-axis).

The graph shows mass of colder water about 200-300 m from the front of the glacier. To better understand the temperature distribution in this area, the temperature trend ($^{\circ}\text{C}$, x-axis) is analysed as a function of the depth (m, y-axis), indicating with red color the data corresponding to the surface water masses and with the scale of the colors (blue = near; yellow = far) the distance from the front of the glacier.

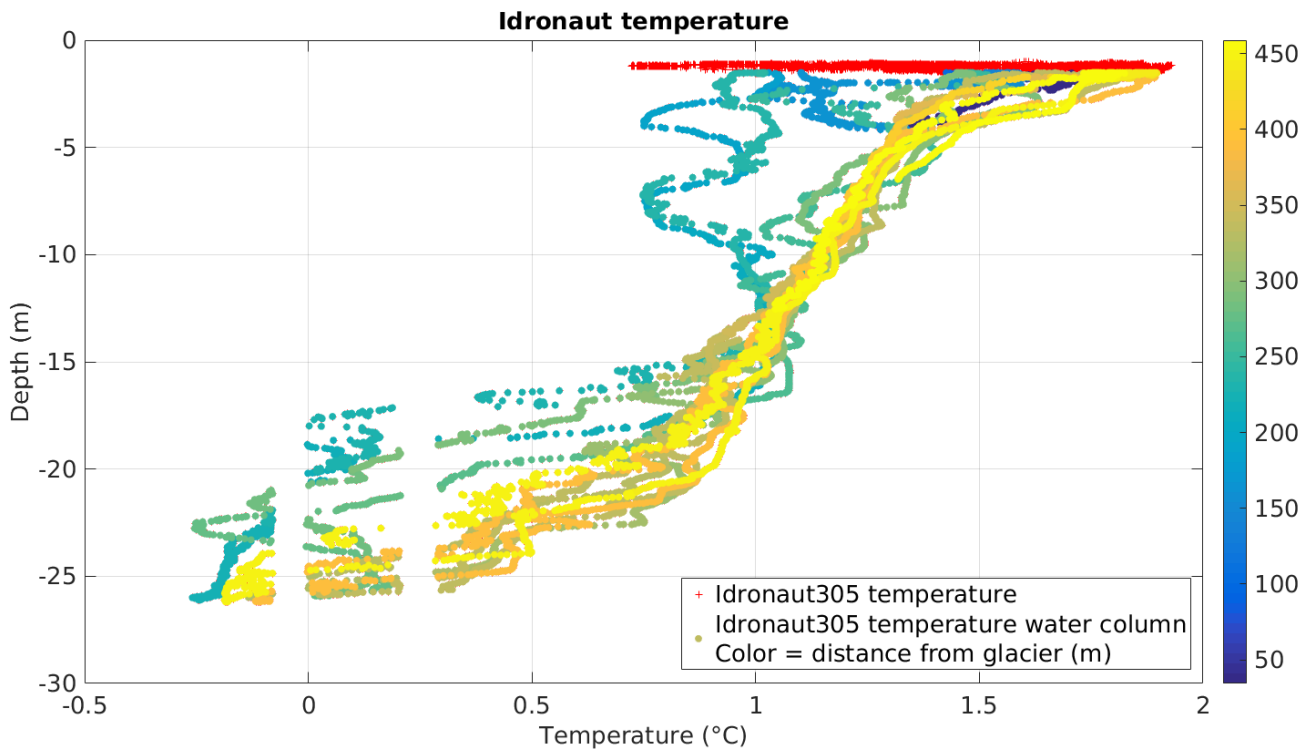


Figure 4.5 - Temperature trend ($^{\circ}\text{C}$, x-axis) as a function of the depth (m, y-axis); red cross represent data corresponding to the surface water masses; the scale of the colors (blue = near; yellow = far) indicates the distance from the front of the glacier.

It is possible to observe from the graph that at a greater distance from the front of the glacier (orange-yellow color) there is a trend in temperature in line with expectations. On the contrary, as already noted in the previous graph, it can be observed that around a distance between 200-300 m (blue - green) there is a trend that differs from the expected one, with lower temperature values. This can be explained by assuming a stream of freshwater from the glacier that breaks into the body of fjord water.

To confirm this hypothesis, the other available parameter is analysed: salinity. Graphs similar to those described above are shown: variation of salinity (PSU; yellow = high salinity; blue = low salinity) as a function of the depth (m, y-axis) and the distance from the front of the glacier (m, x-axis); salinity trend (PSU, x-axis) as a function of the depth (m, y-axis), indicating with red color the data corresponding to the surface water masses and with the color scale (blue = near; yellow = far) the distance from the front of the glacier.

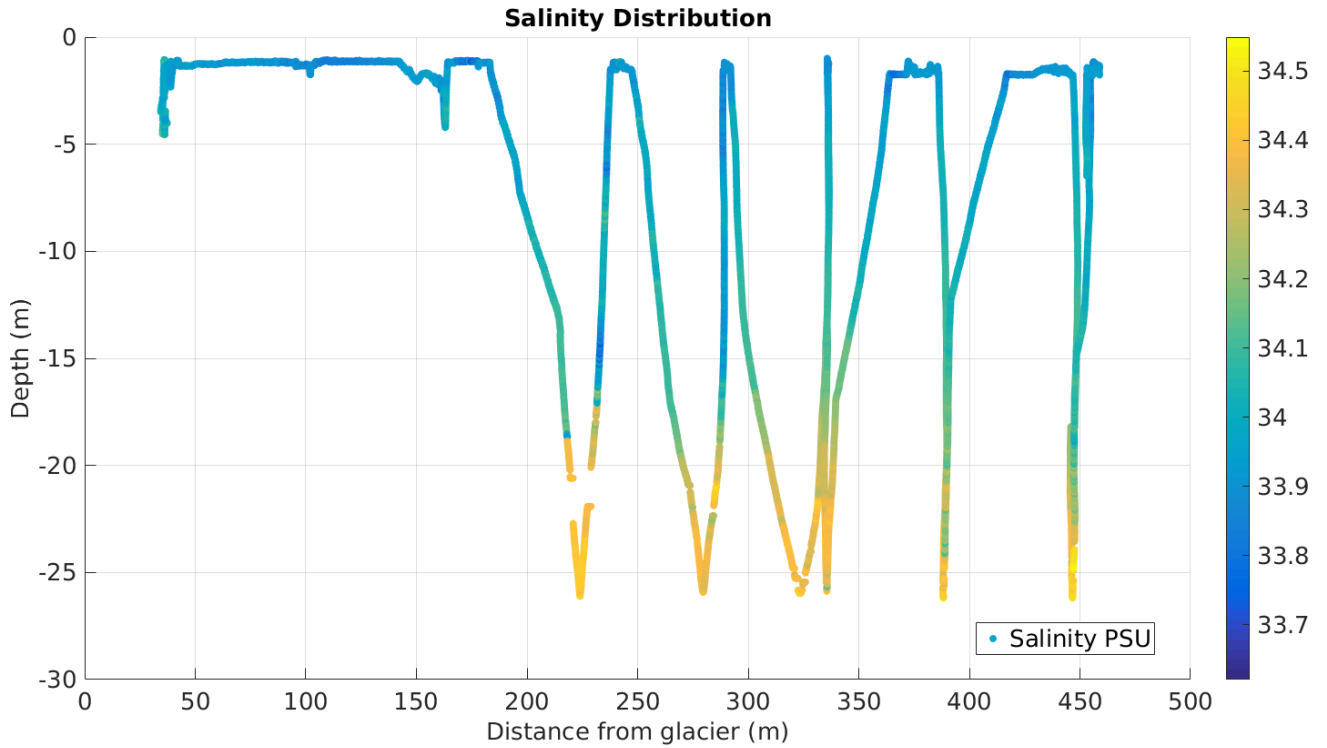


Figure 4.6 - Variation in Salinity (PSU; yellow = high salinity; blue = low salinity) as a function of depth (m, y-axis) and distance from the front of the glacier (m, x-axis).

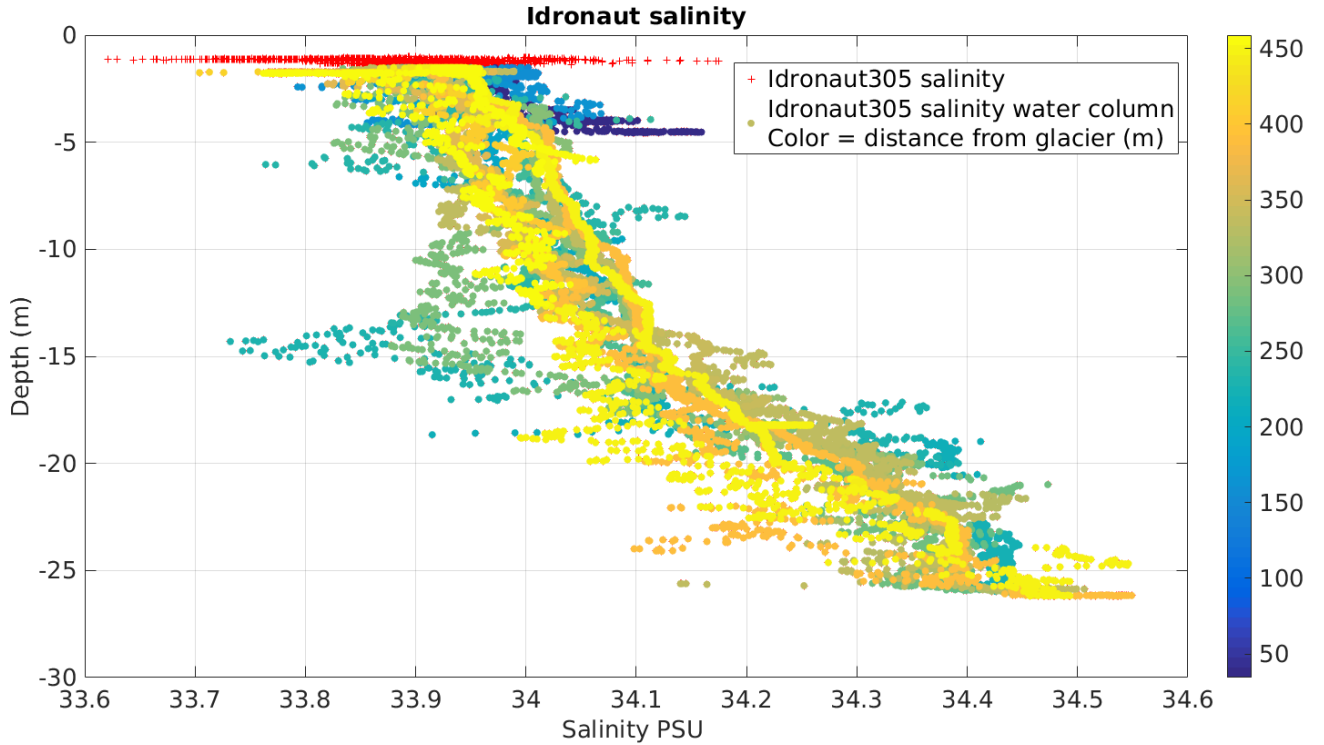


Figure 4.7 - Salinity trend (PSU, x-axis) as a function of the depth (m, y-axis); red cross represent data corresponding to the surface water masses; the scale of the colors (blue = near; yellow = far) indicates the distance from the front of the glacier.

The salinity graphs show oddities with respect to the expected trend at a depth of about 15-20 m and at a distance between 200-300 m from the glacier front: a mass of water characterised by lower salinity values breaks into the environment. These observations seems to confirm the hypothesis made on the basis of temperature data which hinted the presence of a possible mass of freshwater coming from the glacier (lower temperature and salinity).

Temperature and salinity are two of the most important characteristics of seawater since together they control its density, which is the major factor governing the vertical movement of ocean waters. It is known that ocean water circulates in currents: surface currents are driven by wind and affect the uppermost 10% of the ocean while circulation of the other 90% of the ocean is driven by gravity, as dense water sinks and less dense water rises. Upwelling and downwelling describe the vertical movement of water masses. Temperature-salinity diagrams, called T-S diagrams, are used to identify these water masses. In a T-S diagram, rather than plotting each water property as a separate "profile" as in Figure 4.4 and 4.6, temperature (on the vertical axis) is plotted versus salinity (on the horizontal axis).

The two following graphs show T-S diagrams: the first correlates the T-S water properties as a function of the depth while in the second the relation with the distance from the glacier front is highlighted.

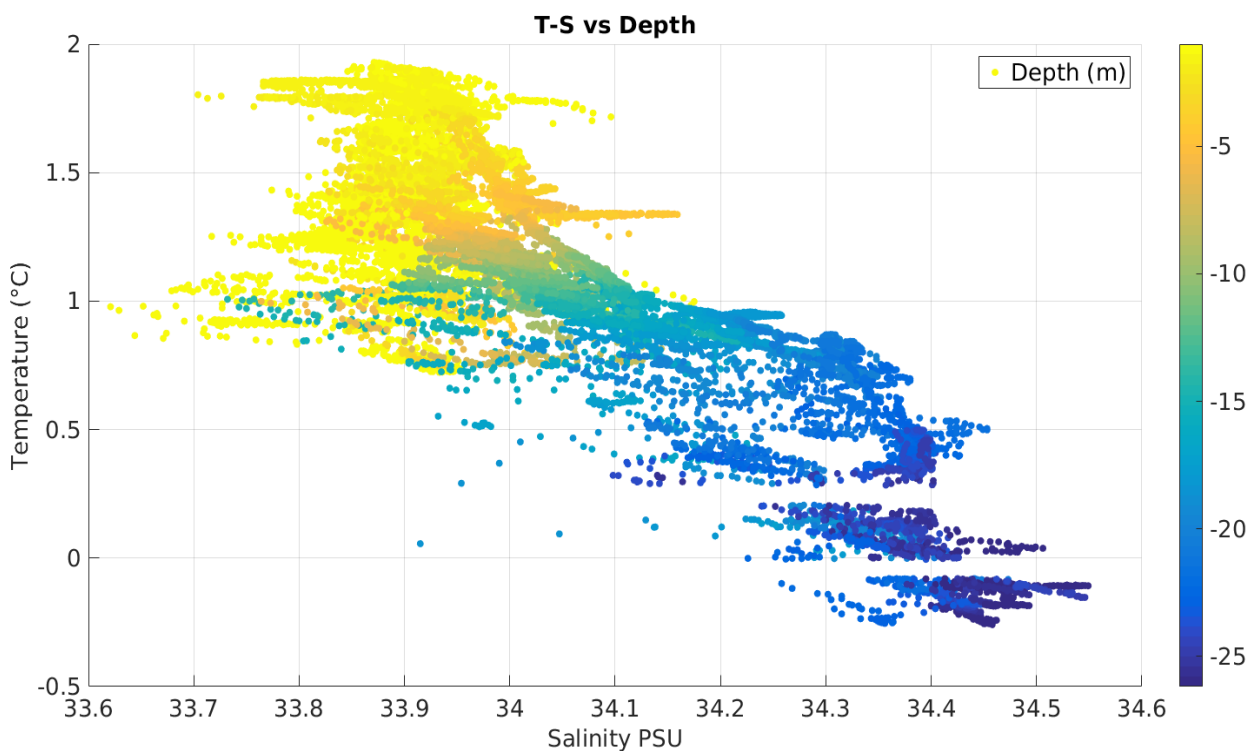


Figure 4.8 - T-S diagram: temperature (°C, y-axis) is plotted versus salinity (PSU, x-axis). The color scale is proportional to depth values (m): yellow = surface; blue = high depth.

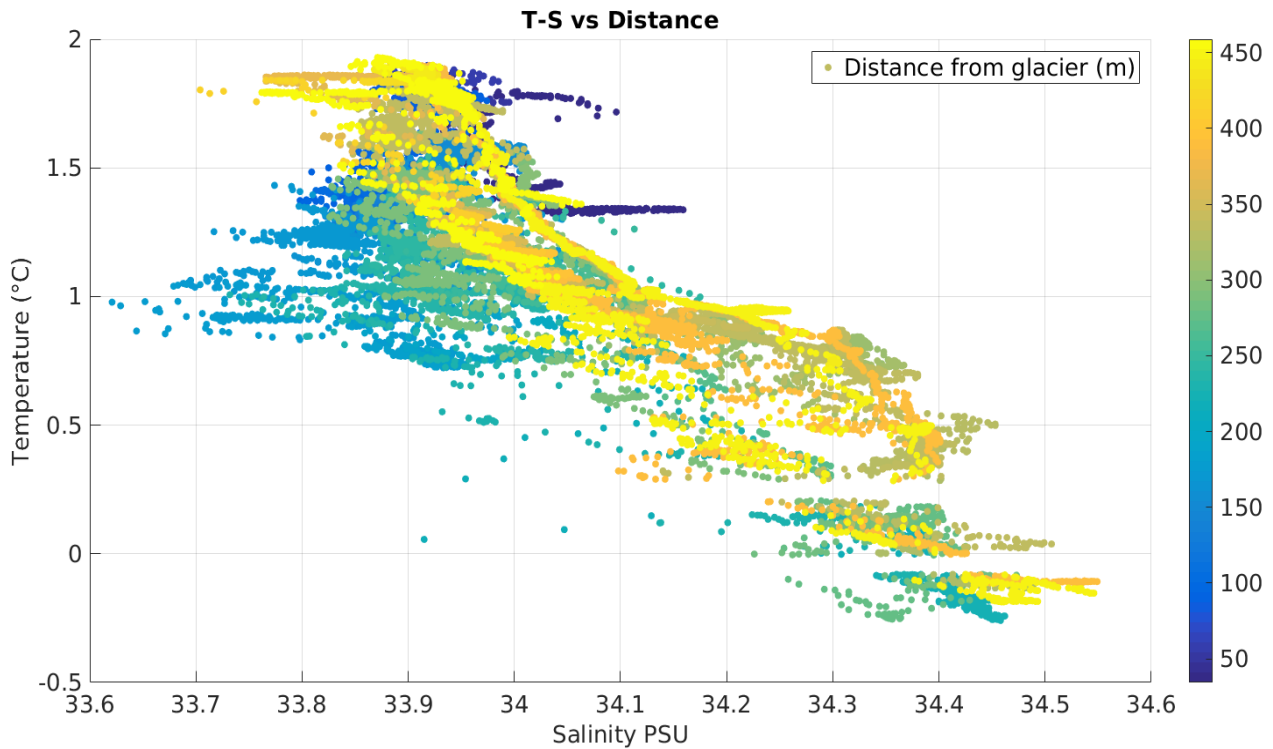


Figure 4.9 - T-S diagram: temperature (°C, y-axis) is plotted versus salinity (PSU, x-axis). The color scale is proportional to distance from the glacier front (m): yellow = far; blue = near.

The first graph (Figure 4.8) shows a descending trend for the temperature along the water column, with higher values at the surface. At the same time, salinity shows an increasing trend along the water column, with lower values on the surface and greater values in depth. The anomaly around the depth of about 15-20 m can also be seen in this graph (green dots), where salinity values are slightly lower than the average trend.

Looking at the second graph (Figure 4.9), the presence of a water mass characterised by lower values of temperature and salinity at about 200-300 meters from the front of the glacier is even more evident (green/light blue dots). This can be an indicator of the presence of a plume of meltwater coming from the glacier which has physical characteristics different from the surrounding water mass and which, thanks to the lower density, is going up the water column towards the surface to then disperse and mix with the water of the fjord.

The variations in water mass stratification, highlighted by temperature and salinity gradients, are only some of the effects produced by glacier melting; increase in turbidity and chlorophyll-a concentration, which directly affects primary productivity and the trophic chain, are other examples of consequences generated by the introduction of meltwater and sediments from the glacier in the form of plume.

Turbidity is an optical characteristic of water and is a measurement of the amount of light that is scattered by material in the water when a light is shined through the water sample. The higher the intensity of scattered light, the higher the turbidity. Material that causes water to be turbid include clay, silt, very tiny inorganic and organic matter, algae, dissolved colored organic compounds, and plankton and other microscopic organisms. It is an important indicator of suspended sediment: high

turbidity will contribute in raising water temperature, lowering dissolved oxygen and preventing light from reaching aquatic plants which reduces their ability to photosynthesize.

Chlorophyll-a is a green pigment found in plants. It absorbs sunlight and converts it to sugar during photosynthesis. Chlorophyll-a concentrations are an indicator of phytoplankton abundance and biomass in coastal and estuarine waters.

The following two graphs (Figures 4.10 and 4.11) show turbidity and chlorophyll-a distribution near the Kongsbreen glacier front, as a function of depth (m, y-axis) and distance (m, x-axis). The graph in figure 4.12 represents chlorophyll-a trend (x-axis) as a function of the depth (m, y-axis), indicating with red color the data corresponding to the surface water masses and with the color scale (blue = near; yellow = far) the distance from the front of the glacier.

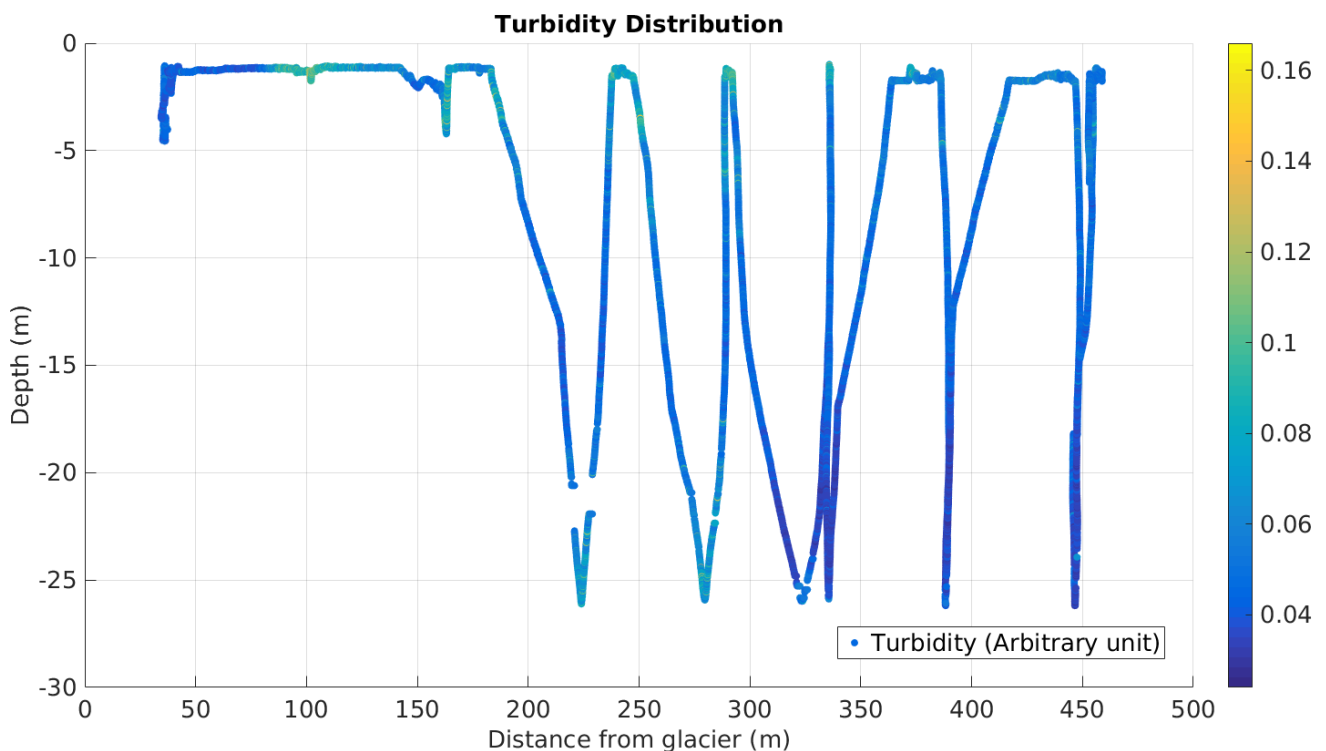


Figure 4.10 - Variation in Turbidity (arbitrary unit; yellow = high turbidity; blue = low turbidity) as a function of depth (m, y-axis) and distance from the front of the glacier (m, x-axis).

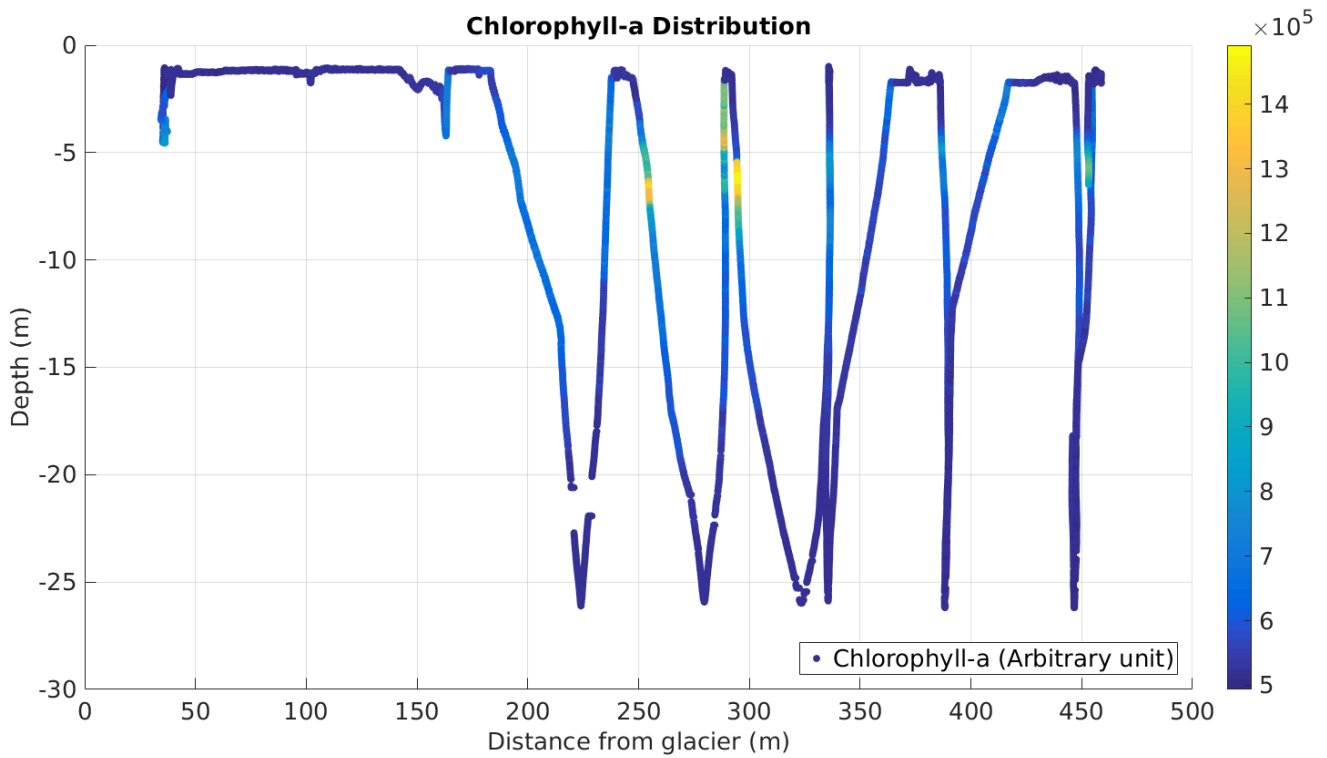


Figure 4.11 - Variation in Chlorophyll-a (arbitrary unit; yellow = high Chl-a; blue = low Chl-a) as a function of depth (m, y-axis) and distance from the front of the glacier (m, x-axis).

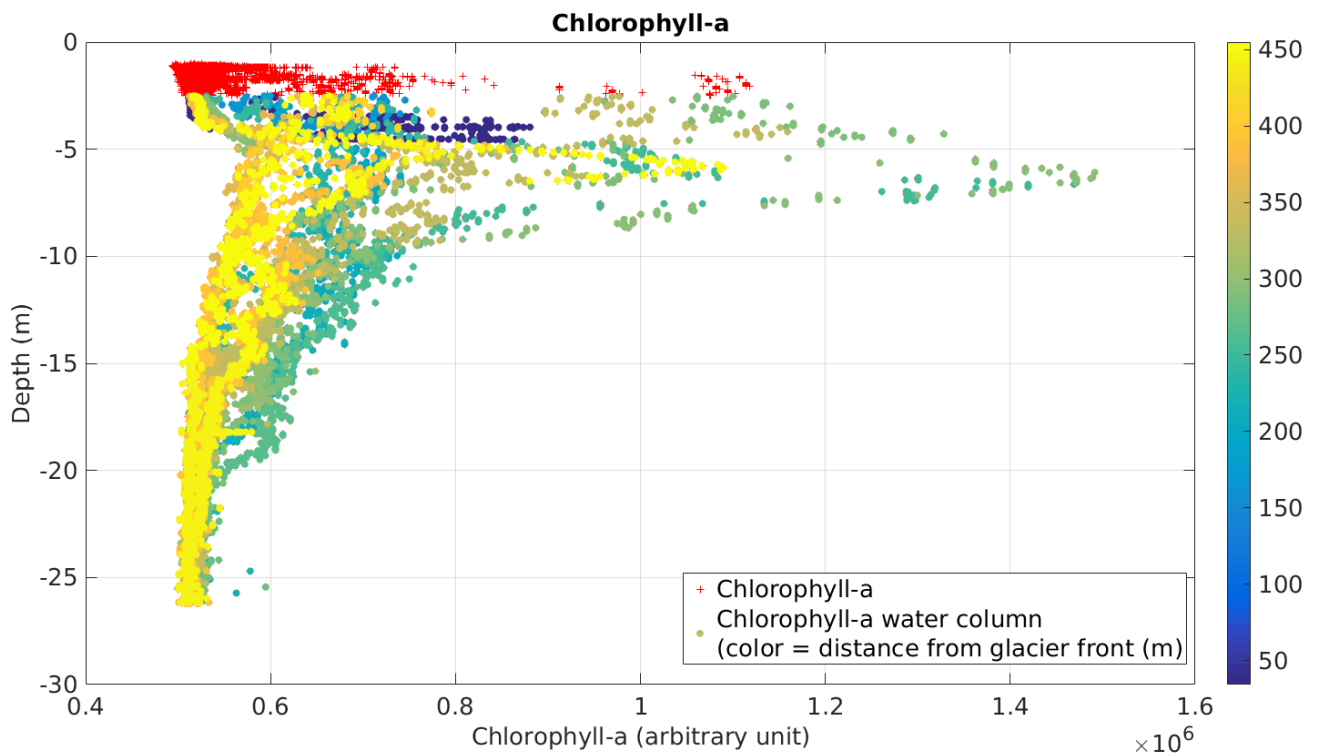


Figure 4.12 – Chlorophyll-a trend (arbitrary unit, x-axis) as a function of the depth (m, y-axis); red cross represent data corresponding to the surface water masses; the scale of the colors (blue = near; yellow = far) indicates the distance from the front of the glacier.

The two variables (turbidity and chlorophyll-a) are expressed in arbitrary units since they are raw data, which means data read directly from the serial port of the sensors, not yet converted to values with a SI measurement unit. The fact that these variables are expressed in arbitrary units is neither a problem nor a limit from a metrological point of view. This data analysis, in fact, has as its focus the study of the trend, the gradients and the variations in the space of the variables to estimate their rates of change, quantities which are therefore independent from the absolute value of the variable and from the measurement unit.

Turbidity data acquired during our surveys (Figure 4.10) show an upwelling of suspended matter at about 220 m from the glacier front, corresponding to a cold-water rising zone in the temperature section (Figure 4.4). Moreover, in Figure 4.10 turbidity values show a concentration of suspended matter below the plume, at a depth of about 25 m, and also in the rest of the water column values. This process could be due to the re-precipitation of the sediments brought to the surface by the plume. Higher turbidity values are also visible in correspondence with the upper layer near the water surface. This fact could be explained with the dispersion of the suspended matter of the plume once it has reached the surface.

Concerning the analysis of phytoplankton bloom, chlorophyll-a data show that the highest peak is found at a depth of about 6 m at a distance from the glacier front ranging between 250 m and 300 m. Other small patches of phytoplankton were recorded at a depth of about 5 m and at 450 m from the glacier front. Chlorophyll-a shows the lowest values between 20 m and 25 m in depth (Figure 4.11).

Phytoplankton bloom is also visible in the graph of Figure 4.12 where green dots and yellow dots (corresponding to distances from the glacier of about 250-300 m and 450 m respectively) create peaks of chlorophyll-a values in the depth range between 5 and 10 m.

In general, high turbidity values, might have a negative impact on phytoplankton growth due to the light absorption. In the area facing Kongsbreen glacier, chlorophyll-a is not concentrated mainly within the observed plume (first vertical profile, at about 220 m from the glacier front), but rather on its sides (second and third vertical profiles, at greater distances): this is probably due to strong turbidity, which limits light penetration, the main limiting factor for phytoplankton growth in these areas.

The complex environmental situation described above is a typical example in which measurements must be made near the front of the glacier, systematically and with elevated spatial and temporal resolutions otherwise there is a risk of missing to record the event (the plume of freshwater from the glacier) before it ends due to the effect of mixing with the water of the fjord. To be able to operate in these conditions and with procedures that ensure the safety of the operators on the one hand and the integrity of the data collected on the other, the use of robotic platforms is necessary.

4.2 Conwaybreen Glacier

As already said, Kongsfjorden is an interesting test-site due to the presence of numerous tidewater glaciers. During the campaign conducted by the CNR-INM in 2018, samples were taken near the front of the glacier called Conwaybreen. This glacier has a Northern position than the Kongsbreen previously analysed but always remains in the internal part of the fjord.

Also in this case, from the point of view of the operating procedures followed for sampling, PROTEUS performed a transept starting from a position close to the front of the glacier (up right in Figure 4.13) and gradually increasing its distance, in a direction approximately perpendicular to the front. The Figure 4.13 shows the track recorded by the PROTEUS positioning system (latitude and longitude in WGS84, EPSG 4326 reference system) and the color, from light to dark blue, is proportional to the depth (m) with respect to the water surface.

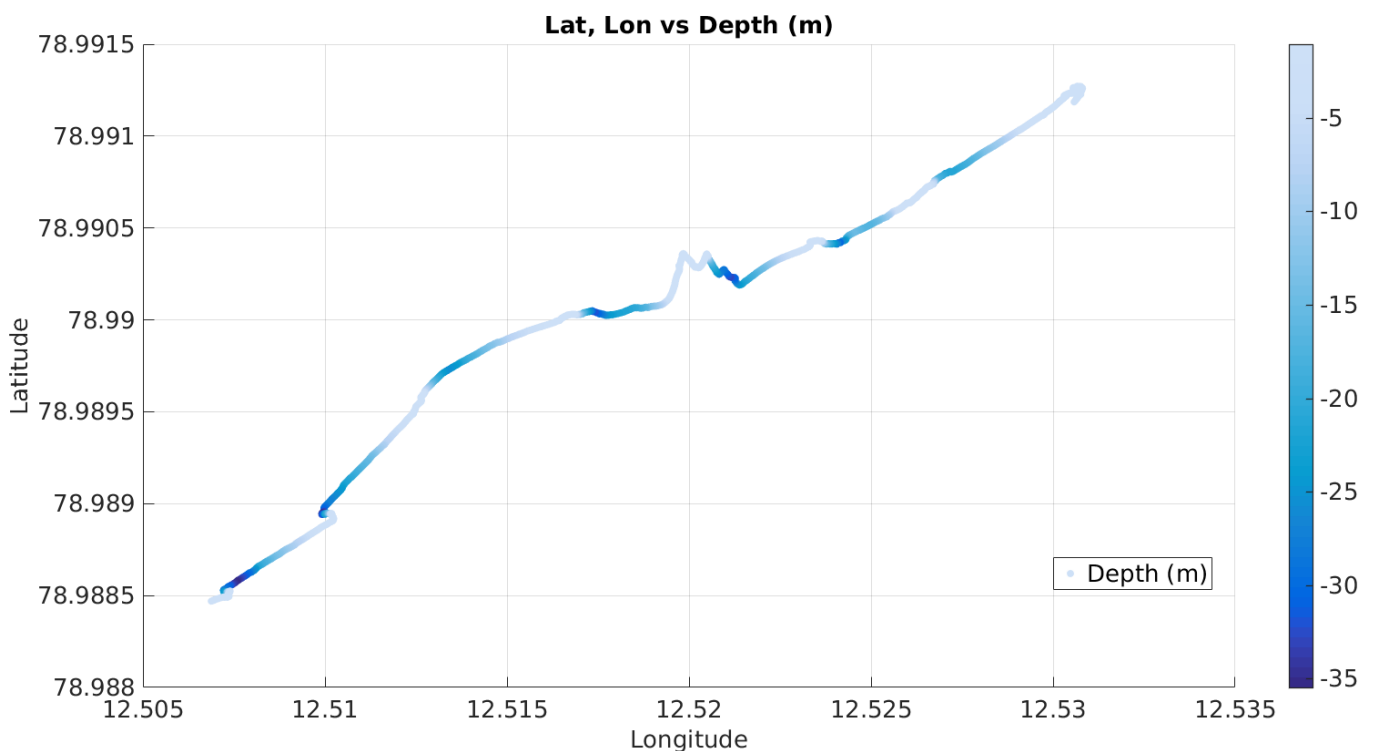


Figure 4.13 - Latitude and longitude (WGS84, EPSG 4326 reference system) positions of PROTEUS. The color is proportional to the depth (m) with respect to the surface of the water. The front of Conwaybreen glacier is in the up-right part of the graph.

As can be seen from the previous graph, also in this case vertical profiles have been made with the sensors at a distance gradually increasing from the front of the glacier. These operating procedures are even more evident in the following figures (4.14 and 4.15), where the depth data are shown also as a function of the distance from the glacier (Figure 4.15). The distances are calculated applying the haversine formula between each position of PROTEUS and the position of the front of the glacier obtained from satellite images.

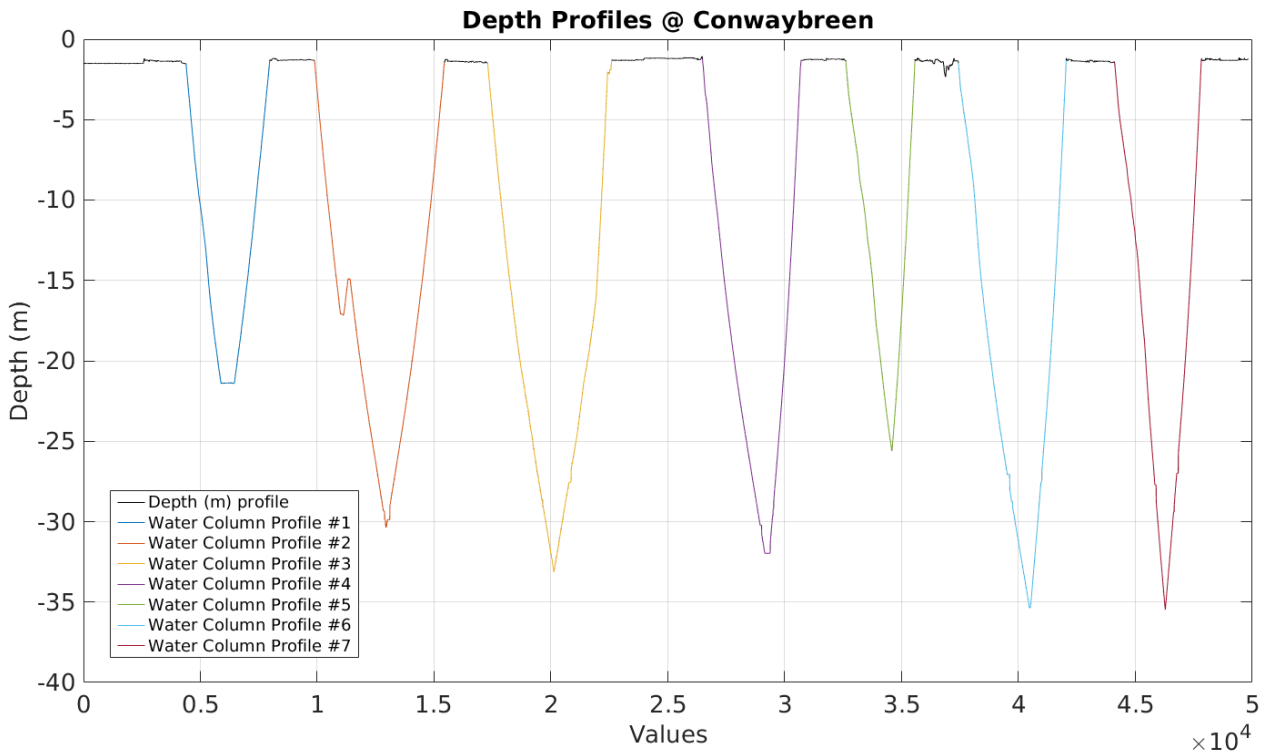


Figure 4.14 - Sequence of recorded values on the x-axis and depth (m) values on the y-axis. The different colors highlight the different water column profiles made.

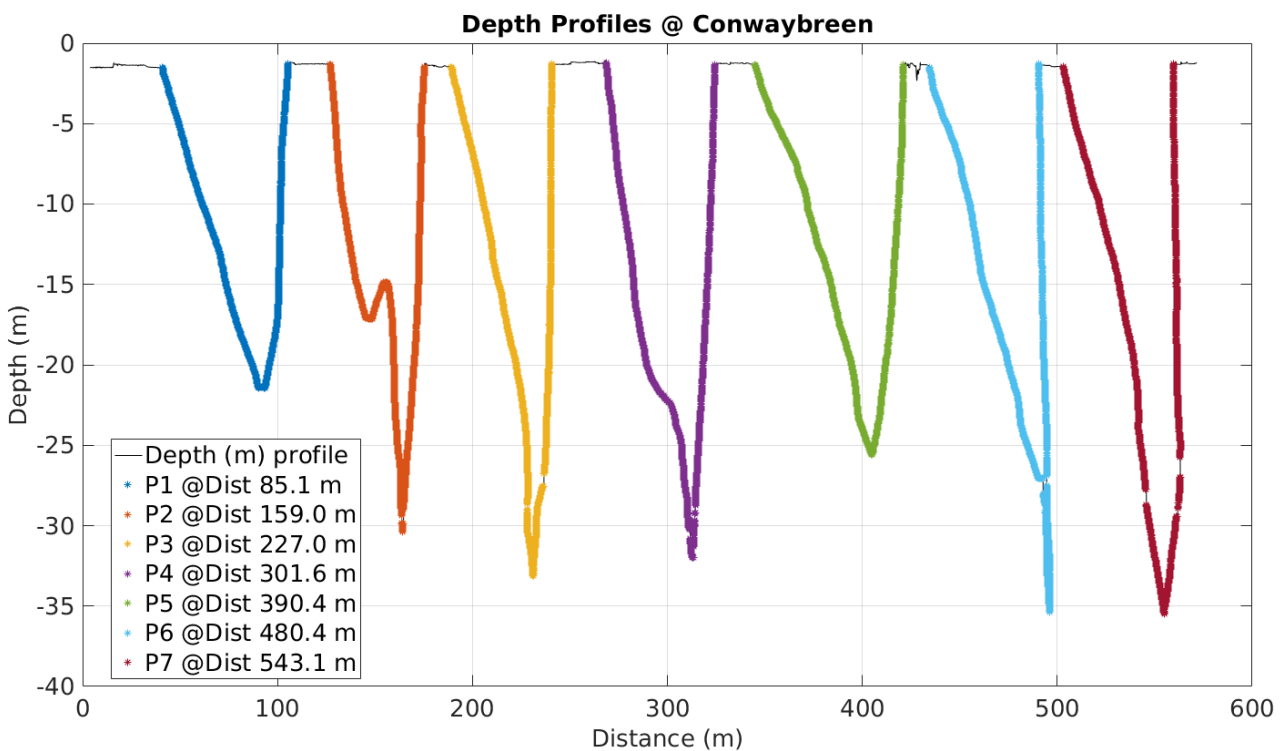


Figure 4.15 - Variation of the depth (m, y-axis) as a function of the distance from the front of the glacier (m, x-axis). The average distance from the front of the glacier for each profile is calculated and indicated in the legend.

The graph in Figure 4.15 shows that the samplings concerned an area that extends in depth from the surface of the water to a depth of about 35 m and that the positions of the vertical profiles range from about 85 m to 550 m with respect to the front of the glacier.

To identify the distribution of the water masses in this area, the temperature and salinity parameters were analysed according to both depth and distance from the glacier. This operation is used to identify any oddities in the data that may indicate the presence of water masses of a different nature than the water of the fjord.

The following graph (Figure 4.16) shows the variation in temperature ($^{\circ}\text{C}$; yellow = warm; blue = cold) as a function of depth (m, y-axis) and distance from the front of the glacier (m, x-axis).

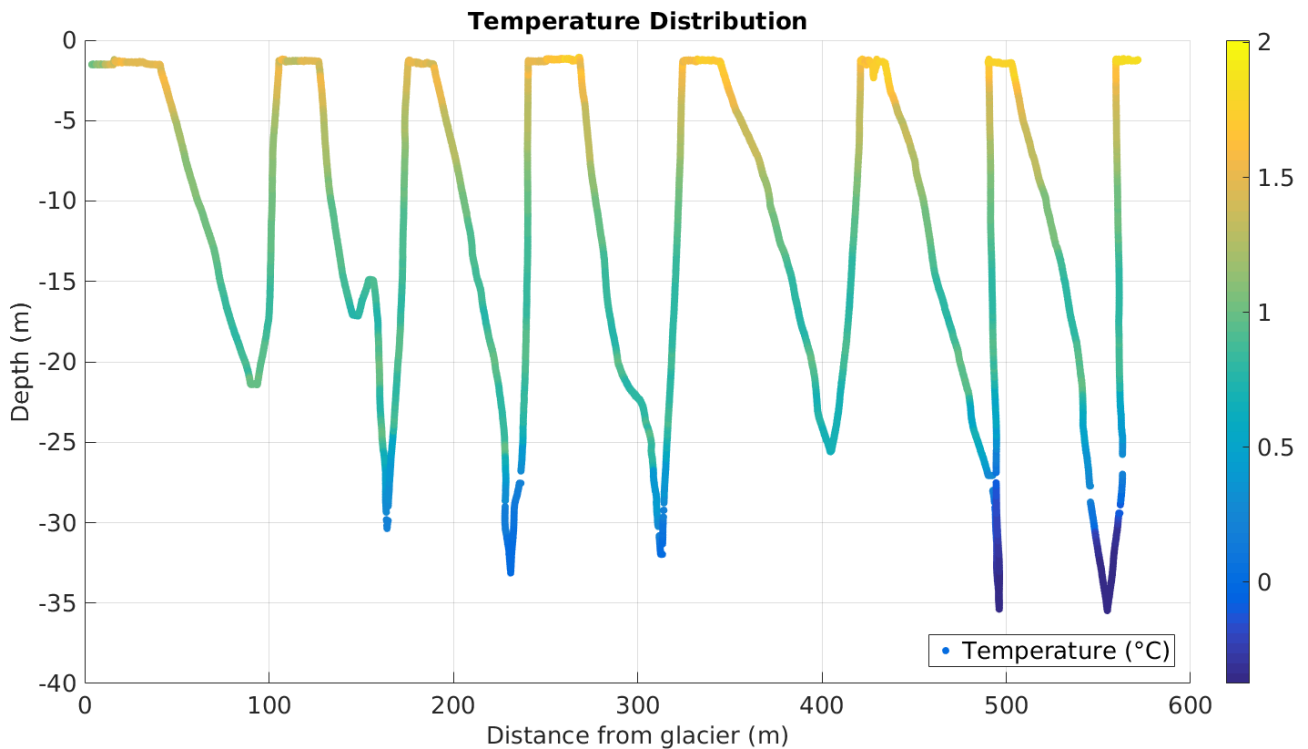


Figure 4.16 - Variation in temperature ($^{\circ}\text{C}$; yellow = warm; blue = cold) as a function of depth (m, y-axis) and distance from the front of the glacier (m, x-axis).

In this case, the temperature varies gradually along the water columns, with higher values near the surface and lower values at higher depth. This observation is also confirmed by the distribution of the temperature trend ($^{\circ}\text{C}$, x-axis) as a function of the depth (m, y-axis), indicating with red color the data corresponding to the surface water masses and with the scale of the colors (blue = near; yellow = far) the distance from the front of the glacier, as shown in Figure 4.17.

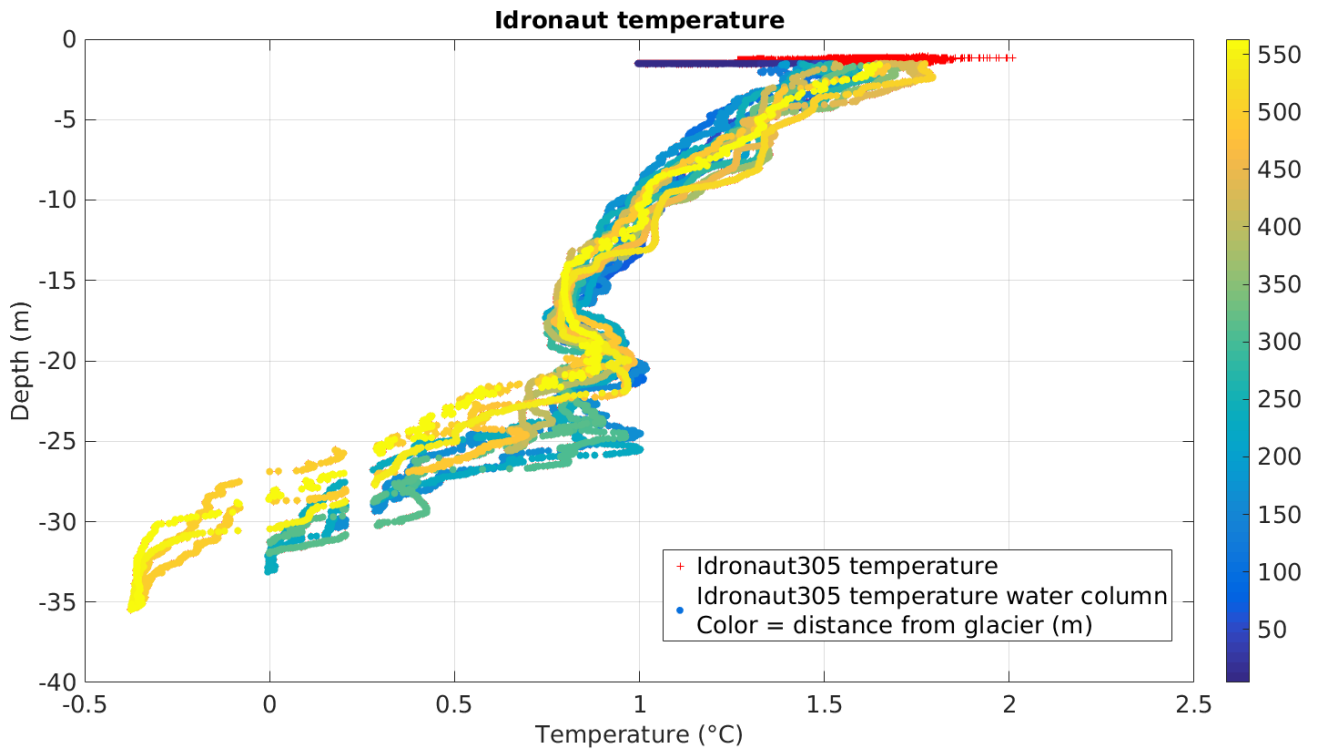


Figure 4.17 - Temperature trend ($^{\circ}\text{C}$, x-axis) as a function of the depth (m, y-axis); red cross represent data corresponding to the surface water masses; the scale of the colors (blue = near; yellow = far) indicates the distance from the front of the glacier.

What can be observed in this case are colder value of the temperature at greater distances from the front of the glacier: to better understand the origin of these observations, also the salinity data are analysed.

The two following graphs show the variation of salinity (PSU; yellow = high salinity; blue = low salinity) as a function of the depth (m, y-axis) and the distance from the front of the glacier (m, x-axis) in Figure 4.18 and the salinity trend (PSU, x-axis) as a function of the depth (m, y-axis), indicating with red color the data corresponding to the surface water masses and with the color scale (blue = near; yellow = far) the distance from the front of the glacier in Figure 4.19.

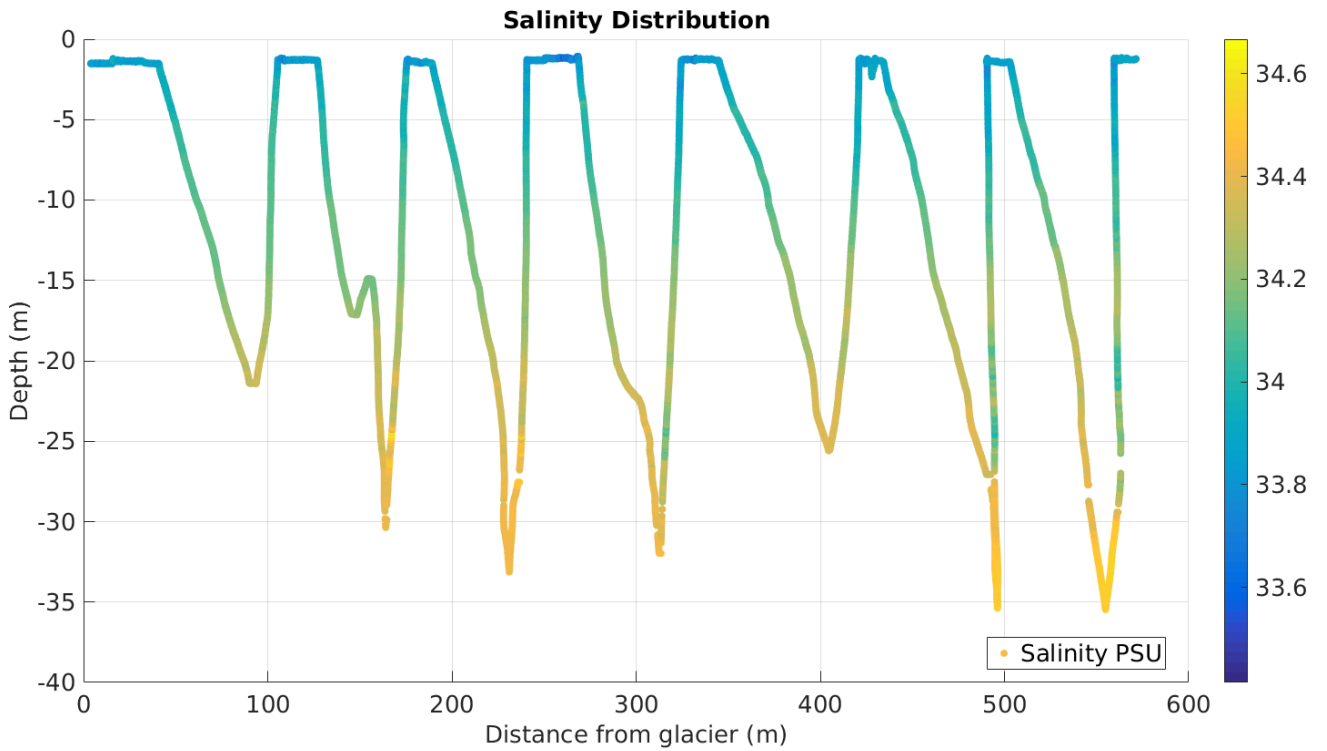


Figure 4.18 - Variation in Salinity (PSU; yellow = high salinity; blue = low salinity) as a function of depth (m, y-axis) and distance from the front of the glacier (m, x-axis).

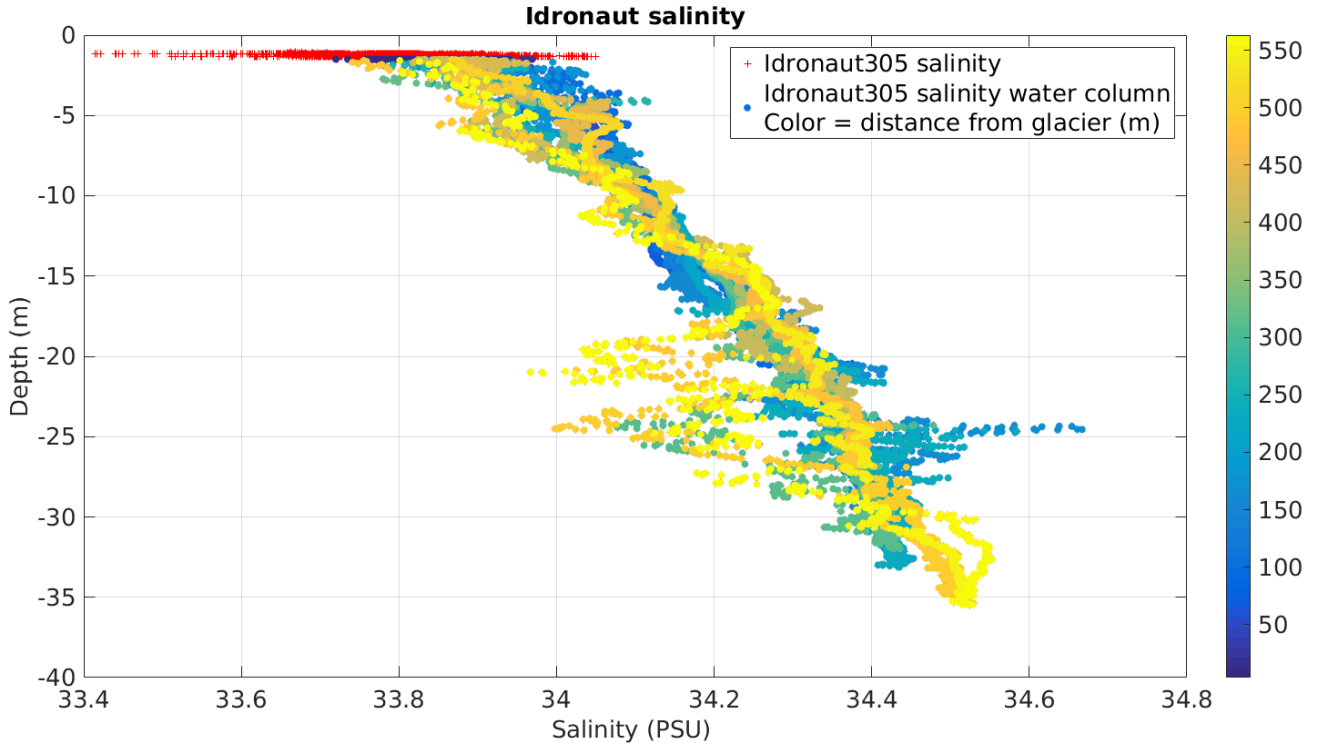


Figure 4.19 - Salinity trend (PSU, x-axis) as a function of the depth (m, y-axis); red cross represent data corresponding to the surface water masses; the scale of the colors (blue = near; yellow = far) indicates the distance from the front of the glacier.

Some small anomalies are observed in the salinity values in the range between -20 and -30 m of depth in correspondence with the data from vertical profiles number 2, 4, 6 and 7, at a distance from the front of the glacier of approximately 160 m, 300 m, 480 m and 543 m respectively. The changes are visible in the salinity graph while the temperature graph does not show anomalous trends. To understand if there is actually a mass of water different from the rest of the environment, the T-S graphs, that represent both variables (temperature and salinity), have been made as a function of the depth (Figure 4.20) while in the second the relation with the distance from the glacier front is highlighted (Figure 4.21).

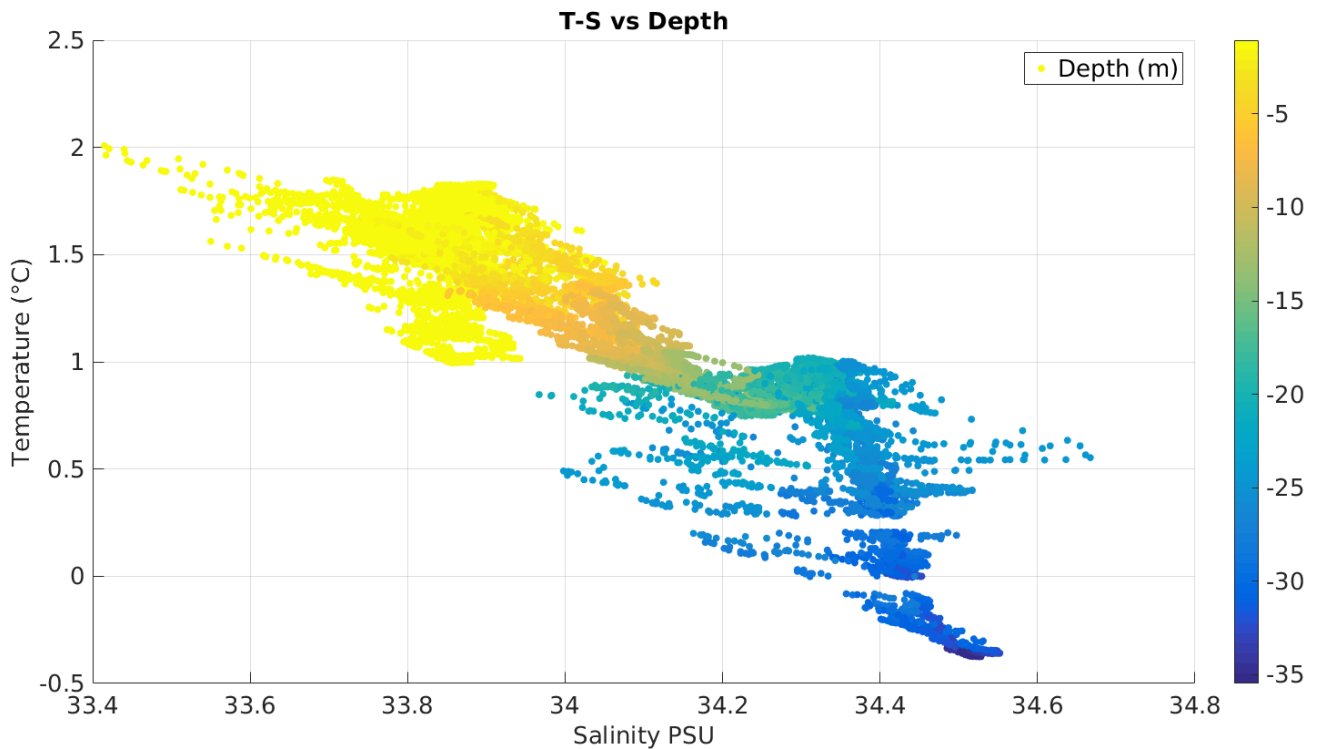


Figure 4.20 - T-S diagram: temperature (°C, y-axis) is plotted versus salinity (PSU, x-axis). The color scale is proportional to depth values (m): yellow = surface; blue = high depth.

In Figure 4.20, the vertical stratification of the water mass, consisting of a surface layer of warmer and less salty water and of a colder and saltier layer at greater depth, is clearly evident.

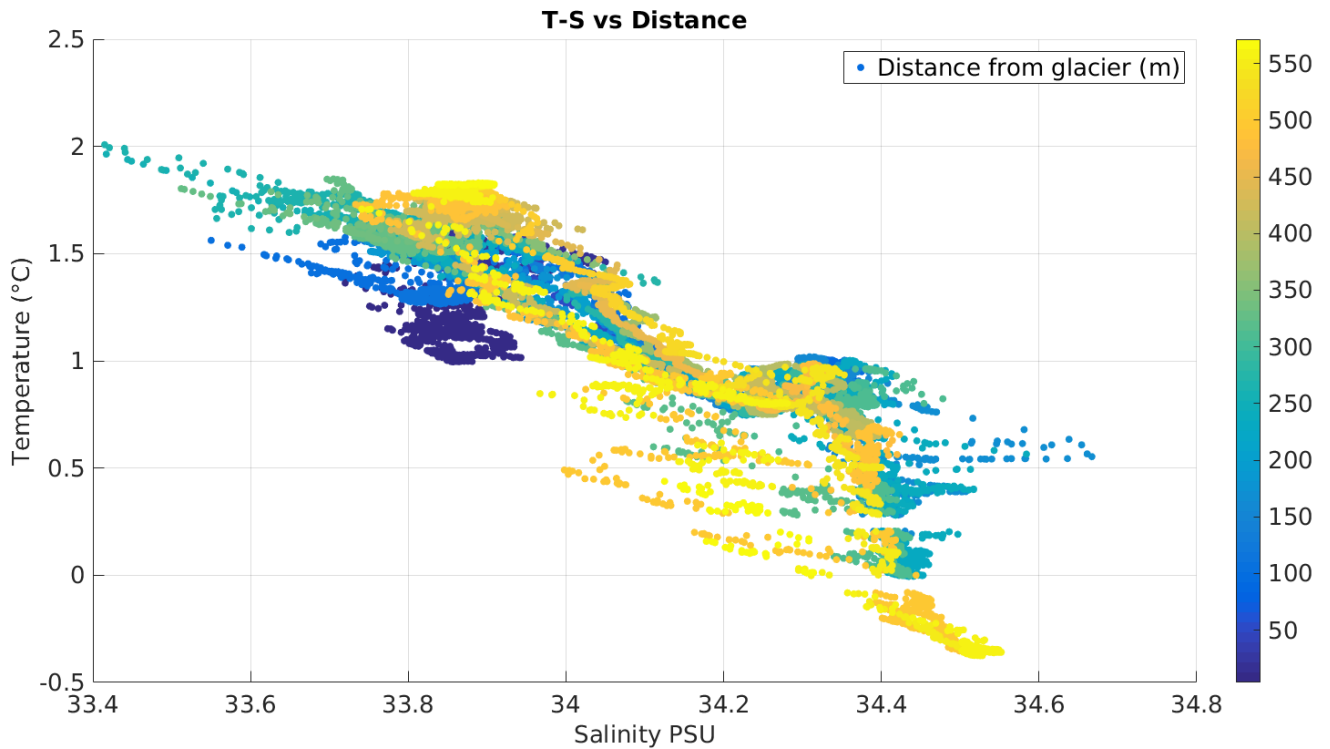


Figure 4.21 - T-S diagram: temperature (°C, y-axis) is plotted versus salinity (PSU, x-axis). The color scale is proportional to distance from the glacier front (m): yellow = far; blue = near.

The small changes compared to the expected salinity trend observed in certain points, already shown in Figure 4.18, are also visible in the graph of Figure 4.21. However, since these discrepancies are highlighted by salinity but not significantly by temperature, it is necessary to analyse other variables in order to determine whether they are actually due to the introduction of a mass of water of a different type than the water of the fjord in that area. In this case, the only two variables temperature and salinity are not sufficient to resolve the doubt.

To better understand the situation in the area, turbidity and chlorophyll-a data are analysed and showed in the following graphs.

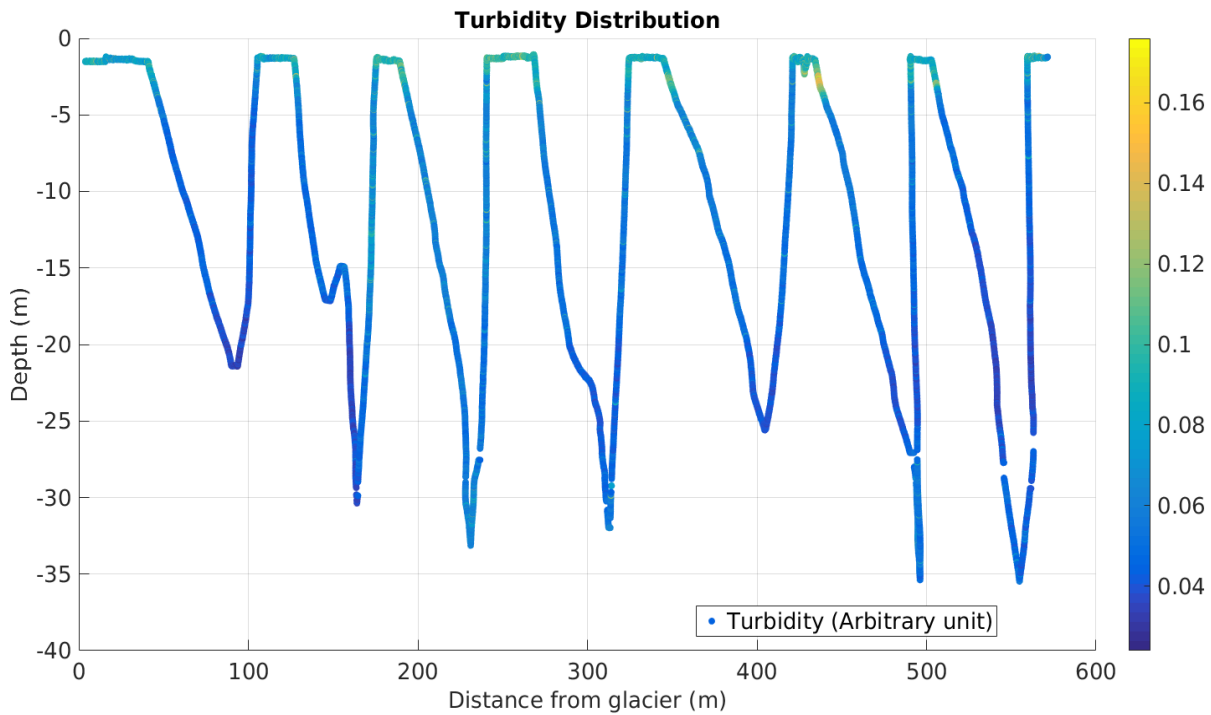


Figure 4.22 - Variation in Turbidity (arbitrary unit; yellow = high turbidity; blue = low turbidity) as a function of depth (m, y-axis) and distance from the front of the glacier (m, x-axis). The values of the turbidity are expressed in arbitrary units since they are raw data, read directly from the serial port of the sensors, not yet converted to values with a SI measurement unit.

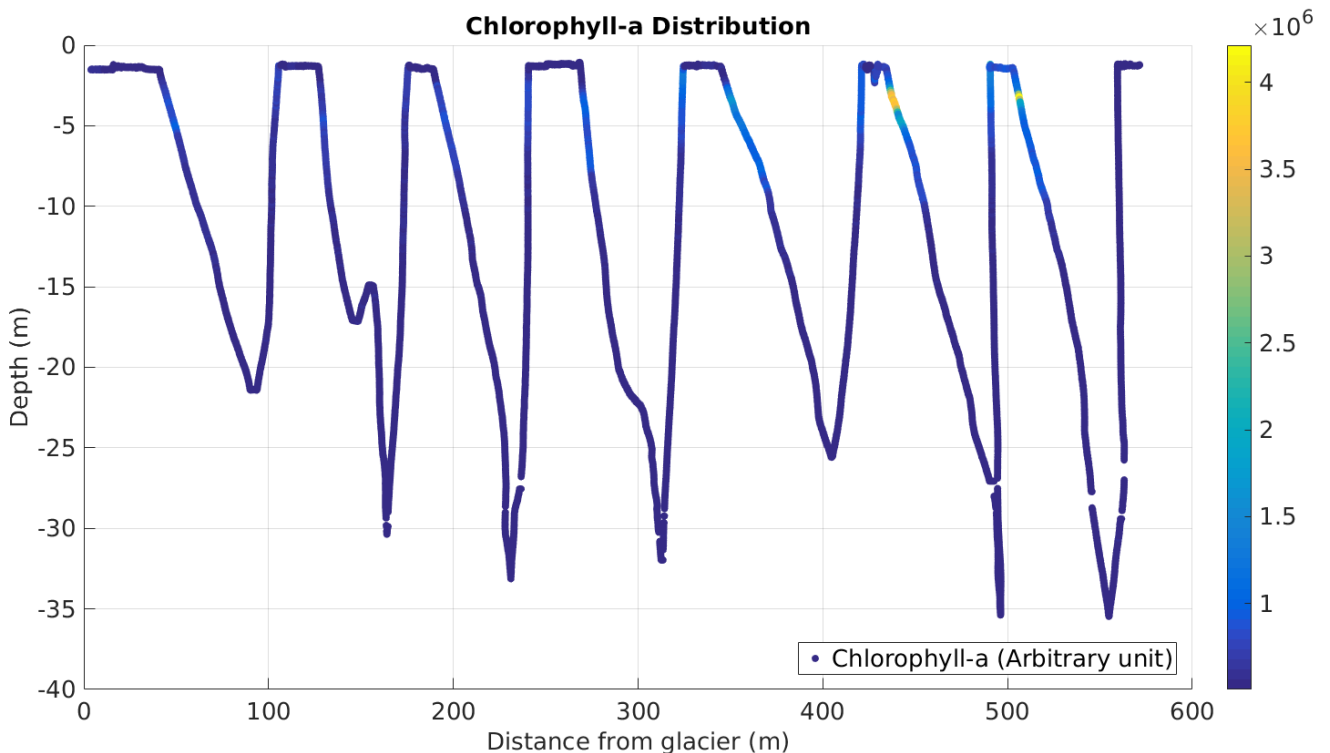


Figure 4.23 - Variation in Chlorophyll-a (arbitrary unit; yellow = high Chl-a; blue = low Chl-a) as a function of depth (m, y-axis) and distance from the front of the glacier (m, x-axis). The values of the Chl-a are expressed in arbitrary units since they are raw data, read directly from the serial port of the sensors, not yet converted to values with a SI measurement unit.

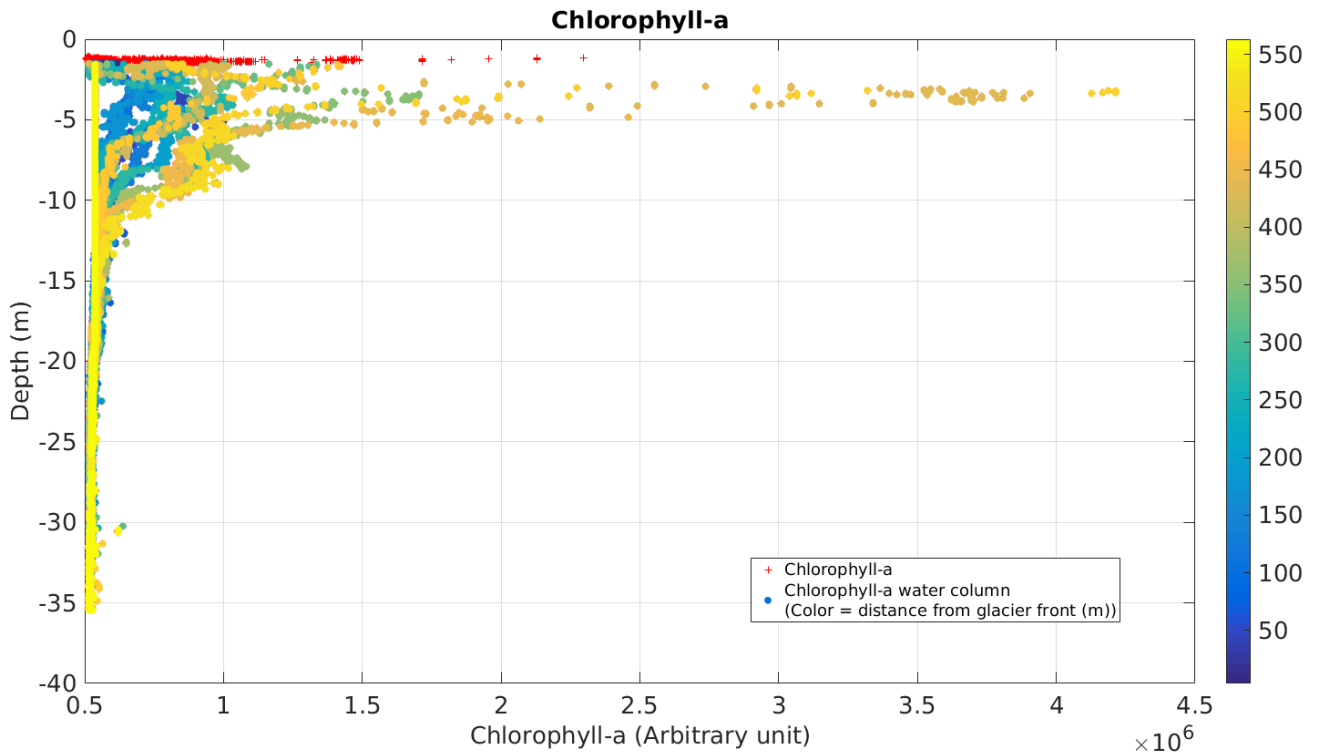


Figure 4.24 - Chlorophyll-a trend (arbitrary unit, x-axis) as a function of the depth (m, y-axis); red cross represent data corresponding to the surface water masses; the scale of the colors (blue = near; yellow = far) indicates the distance from the front of the glacier. The values of the Chl-a are expressed in arbitrary units since they are raw data, read directly from the serial port of the sensors, not yet converted to values with a SI measurement unit.

The turbidity graph in Figure 4.22 shows a gradual decreasing trend with depth, with highest values on the surface. Moreover, a spot of high turbidity is observed at about 450 m from the front of the glacier and in the superficial layer of the water. From figure 4.23 it can be seen that in the same position there is also a spot of high chlorophyll-a values, also visible in the graph in figure 4.24 (orange points at about -5 m). Apart from this situation very localized in space, from these graphs we can say that the plume is not present near the Conwaybreen glacier at the moment of the sampling. This could be due to different factors: during the early ice melting season (late Spring) the discharge flux is not strong enough to reach the surface; an elevated presence of sediment might affect the density of the plume, preventing it from reaching the surface and stratifying at an intermediate depth; the transept with PROTEUS samples only a tiny part of the glacier front so the subglacial plume may have originated elsewhere. However, the area close to the front of this glacier is interesting as regards the distribution of water masses and the possible relationship of this with the morphology of the seabed. In this regard, a graph of the various descent profiles of the CTD (blue dots) as a function of the distance from the glacier is done, showing the trend of the seabed (orange dots) obtained from the data of the altimeter mounted on board PROTEUS (Figure 4.25).

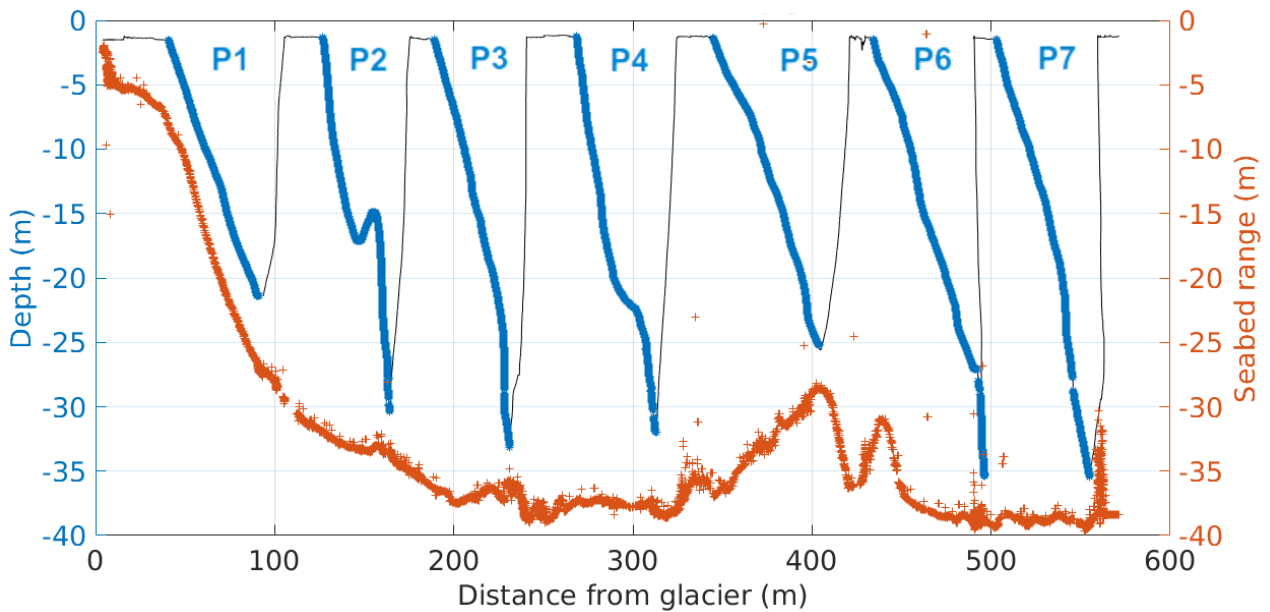


Figure 4.25 - Graph of the descent profiles of the CTD (blue dots) as a function of the distance from the glacier, showing the trend of the seabed (orange dots) obtained from the data of the altimeter mounted on board PROTEUS. P1 is the CTD profile near to the glacier front (the first on the left side) and P7 is the CTD profile far from the glacier front (the last on the right)

Observing the data of the seabed, about 400 m away from the front of the glacier, a morphology can be seen that could create a boundary effect in the distribution of the water masses, distinguishing between an area closer to the front and a more distant one. To study this phenomenon in detail, the variables Temperature, Salinity, Chlorophyll-a and Turbidity of each vertical profile are analyzed.

The following graph (figure 4.26) shows the Temperature data for the different profiles (in logarithmic scale) as a function of the depth with respect to the water surface. The logarithmic scale allows to better highlight small effects on the general trend of the data. From this graph it is possible to observe two inflections with respect to the decreasing trend, positioned at approximately -25 / -30 m.

Moreover it is possible to see that the P4 profile (purple) located about 300 m from the front constitutes the delimitation of the waters closest to the front of the glacier. The P5 profile (green) is a mixed water profile and then the P6 and P7 profiles have a different trend than the others, being more influenced by the water of the fjord.

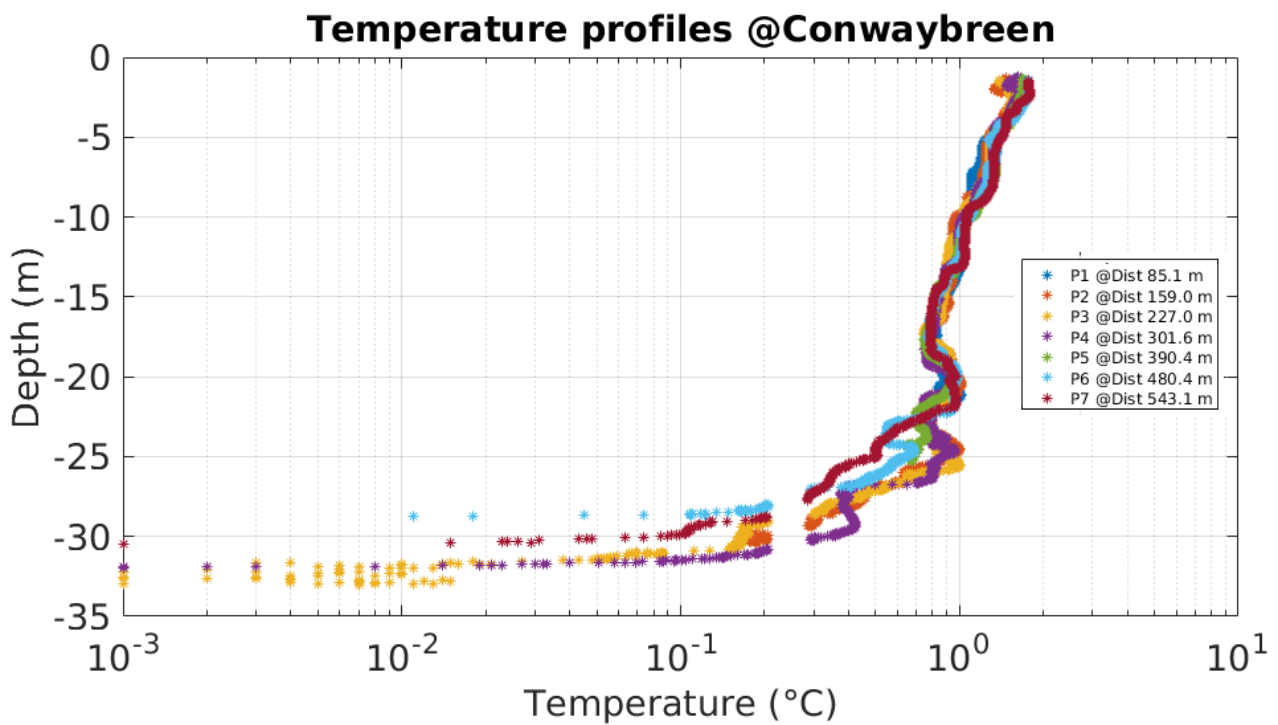


Figure 4.26 - Graph of the Temperature ($^{\circ}\text{C}$) for the descent profiles of the CTD as a function of the Depth (m) from the water surface. The temperature values are drawn using the logarithmic scale to highlight small variations in the trends.

The graphs of the other variables examined also confirm the distinction between the different water masses. For example, the Chlorophyll-a graph (figure 4.27) is particularly significant. The following figure clearly shows the difference between the data of the profiles closest to the glacier front (profiles P1 to P4), the presence of a transition zone which is represented by the data of the profile P5 and then the different trend of profiles P6 and P7. This differentiation between the Chlorophyll-a values occurs in the most superficial part of the water mass, at a depth between the surface and -10 m.

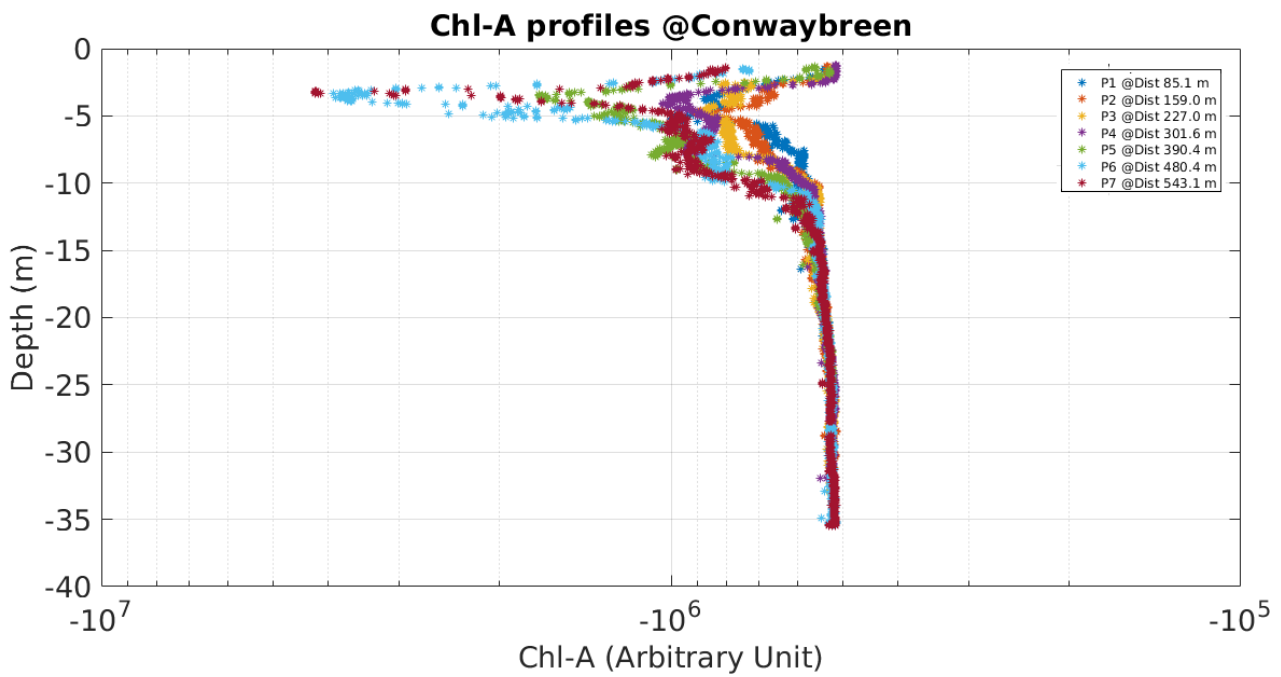


Figure 4.27 - Graph of the Chlorophyll-a (Arbitrary units) for the descent profiles as a function of the Depth (m) from the water surface. The Chlorophyll-a values are drawn using the logarithmic scale to highlight small variations in the trends.

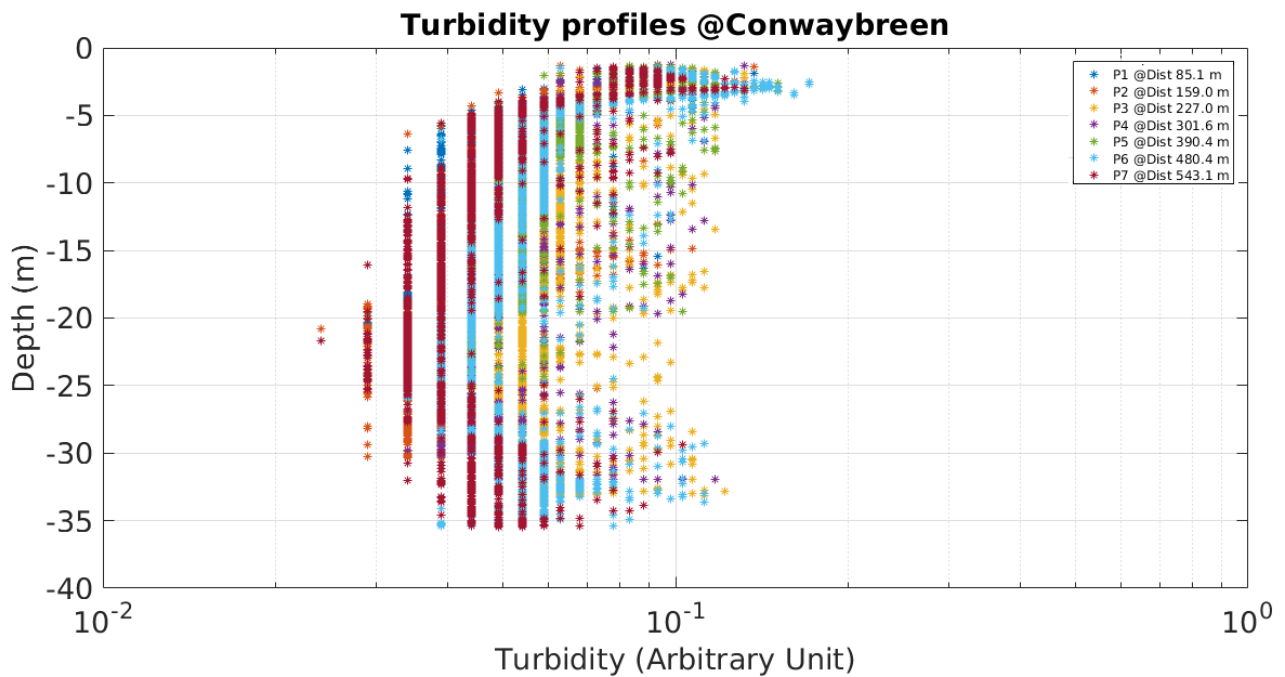


Figure 4.28 - Graph of the Turbidity (Arbitrary units) for the descent profiles as a function of the Depth (m) from the water surface. The Turbidity values are drawn using the logarithmic scale to highlight small variations in the trends.

The turbidity trend (figure 4.28) also confirms the distinction between the water closest to the glacier front, at higher turbidity values due to the influence of the ice melt water, and the water beyond the boundary region, less turbid because influenced by the water of the fjord. It is also

noted, as already seen from the low Chlorophyll-a values, that the surface layer is characterized by more turbid and dense water.

4.3 Blomstrandbreen Glacier

Unlike the two previous glaciers (Kongsbreen and Conwaybreen), the Blomstrandbreen is more exposed to the influence of the Atlantic current due to its position, in the North-East part of the fjord. The area near the front of the glacier can therefore present considerable complexity as the water of the fjord can be mixed with ocean water and also with freshwater due to the melting of the glacier. For this reason, it is extremely important to study and analyse this area in detail (high spatial and temporal resolution) and systematically, with the use of a robotic platform.

During the 2018 campaign carried out by the CNR-INM, samplings were made near the front of this glacier. The operating procedures followed are slightly different from those described for the other two glaciers: in this case PROTEUS performed a first transept starting far from the glacier and gradually approaching it and a second transept starting from a position close to the front of the glacier (up right in the following graph) and gradually increasing its distance; in both cases PROTEUS was moving in a direction approximately perpendicular to the front of the glacier. The Figure 4.29 shows the track recorded by the PROTEUS positioning system (latitude and longitude in WGS84, EPSG 4326 reference system) and the color, from light to dark blue, is proportional to the depth (m) with respect to the water surface.

It is important to underline that in this case the depth of the water column profiles is lower than in the other two cases (maximum depth about -9 m instead of -20 m and -35 m in the previous cases): this is due to the particular morphology of the seabed near the front of the Blomstrandbreen glacier, characterised by low range values, as it is possible to see in the graph of Figure 4.30 which represents the value of the range of the seabed measured using an altimeter mounted on PROTEUS: for each position (latitude, longitude) the corresponding value of the range is shown with a different color, ranging from light blue for low range to dark blue for deeper range.

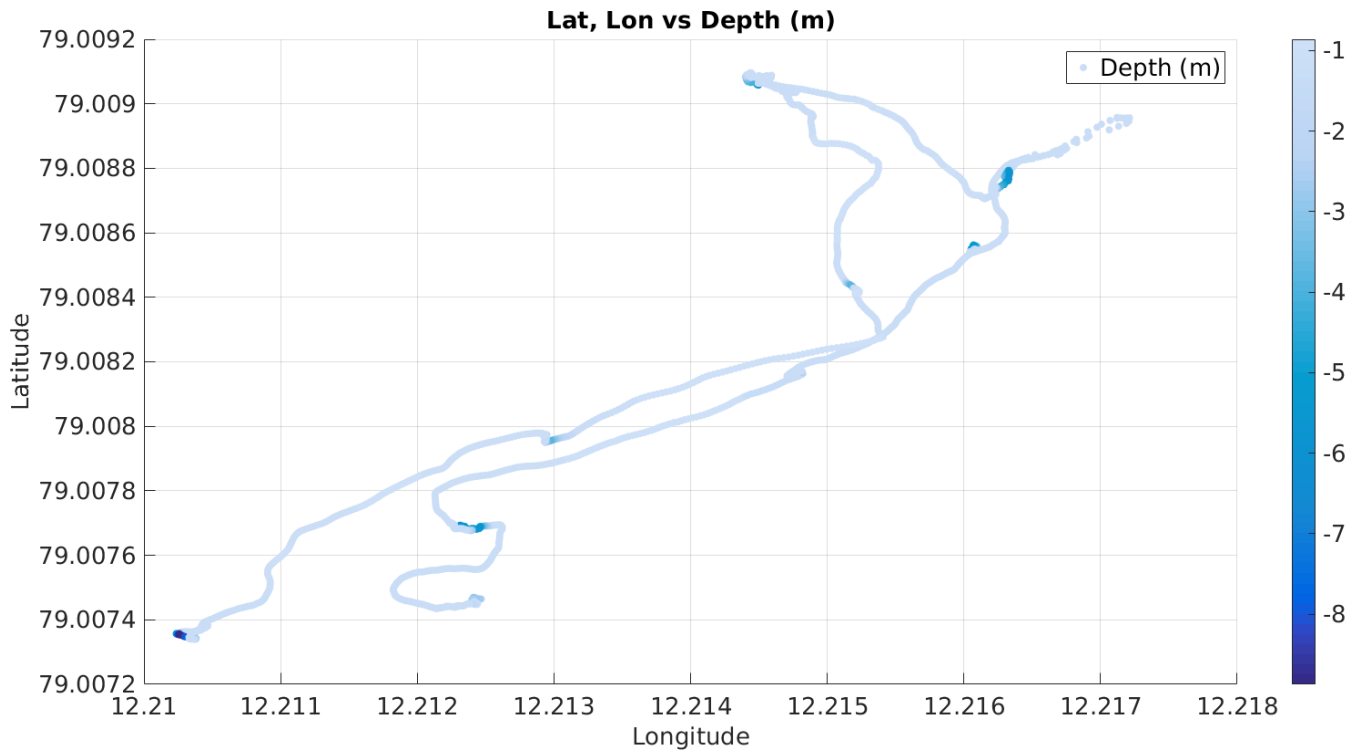


Figure 4.29 - Latitude and longitude (WGS84, EPSG 4326 reference system) positions of PROTEUS. The color is proportional to the depth (m) with respect to the surface of the water. The front of Blomstrandbreen glacier is in the up-right part of the graph.

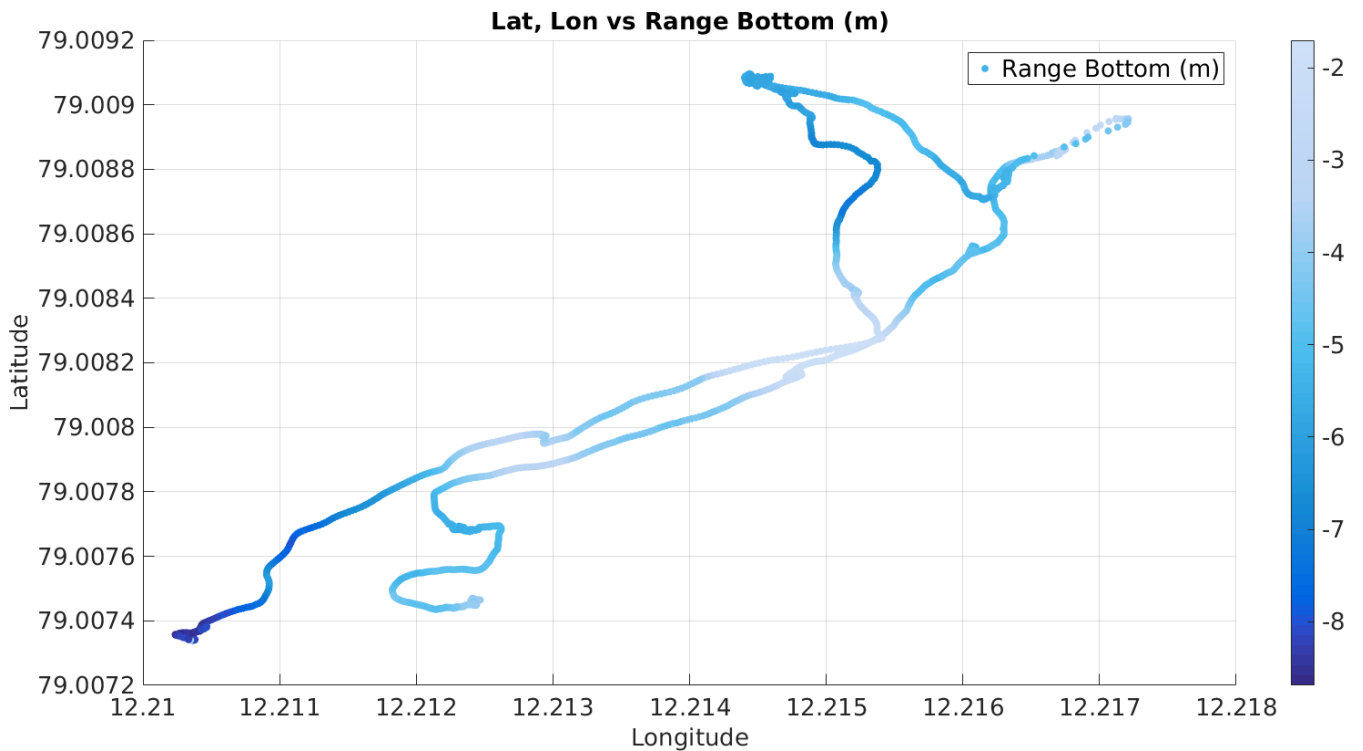


Figure 4.30 - Range of the seabed measured using an altimeter mounted on PROTEUS: for each position (latitude, longitude) the corresponding value of the range is shown with a different color, ranging from light blue for low range to dark blue for deeper range.

The goal of the samplings is to study the distribution of different parameters as a function of the distance from the glacier front. The distance data are calculated applying the haversine formula between each position of PROTEUS and the position of the front of the glacier obtained from satellite images acquired in the same day of the samplings.

The following two graphs represent the water column profiles registered at different depth and distances from the glacier. It is possible to see that the area sampled extends in depth from the surface down to about 9 m and that the distances from the glacier front range from 30 m to 230 m.

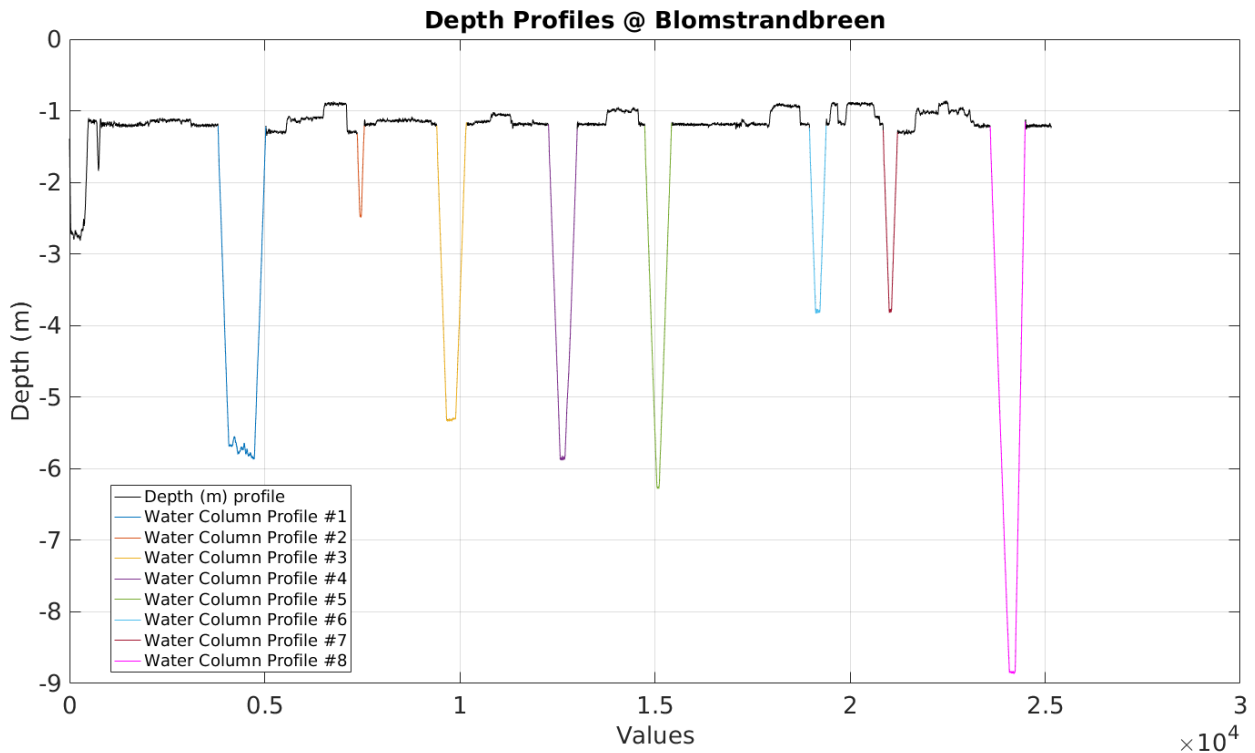


Figure 4.31 - Sequence of recorded values on the x-axis and depth (m) values on the y-axis. The different colors highlight the different water column profiles made.

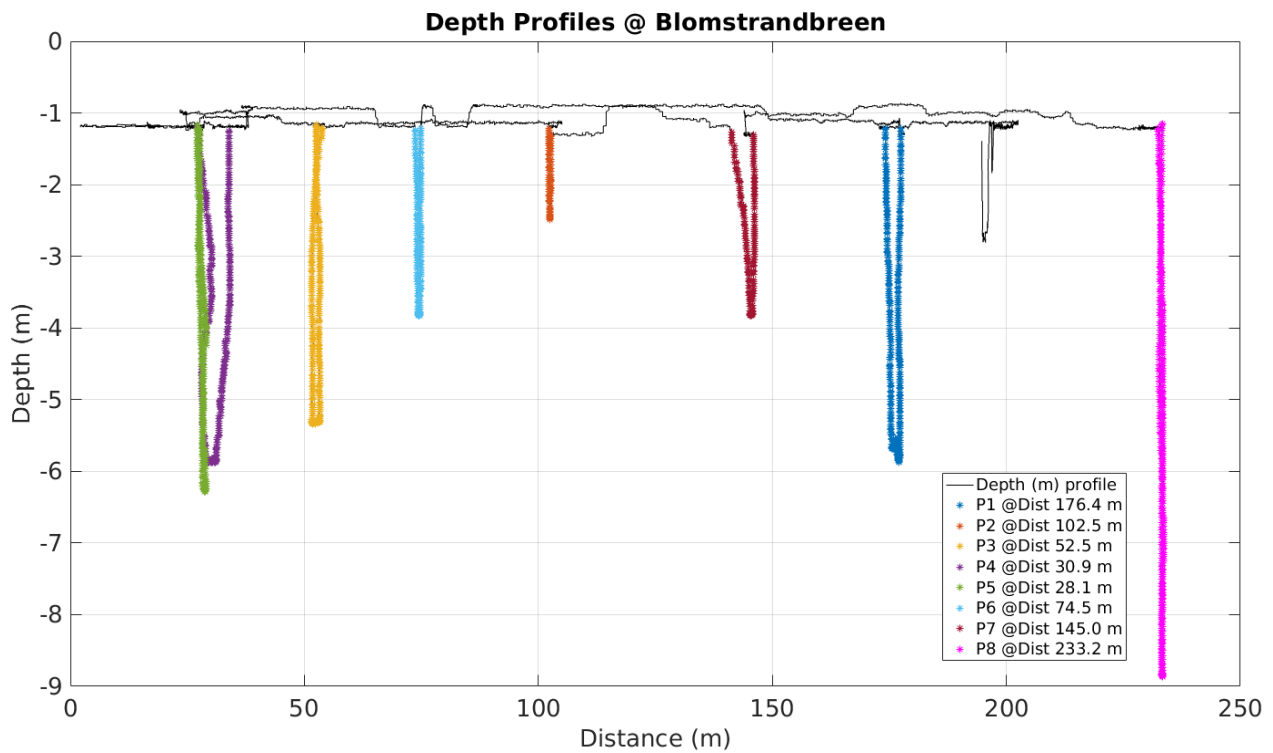


Figure 4.32 - Variation of the depth (m, y-axis) as a function of the distance from the front of the glacier (m, x-axis). The average distance from the front of the glacier for each profile is calculated and indicated in the legend.

In Figures 4.33 and 4.34 the temperature and salinity parameters are analysed in order to identify the distribution of the water masses in the area.

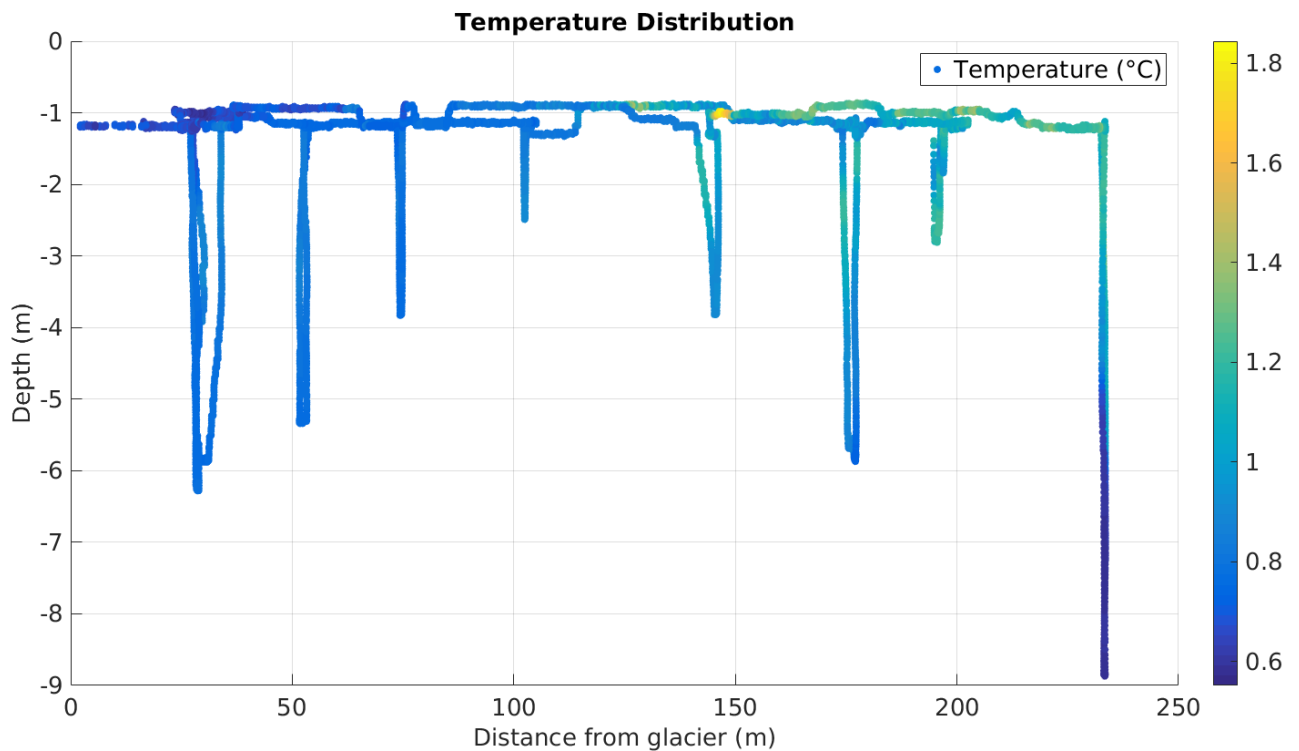


Figure 4.33 - Variation in temperature (°C; yellow = warm; blue = cold) as a function of depth (m, y-axis) and distance from the front of the glacier (m, x-axis).

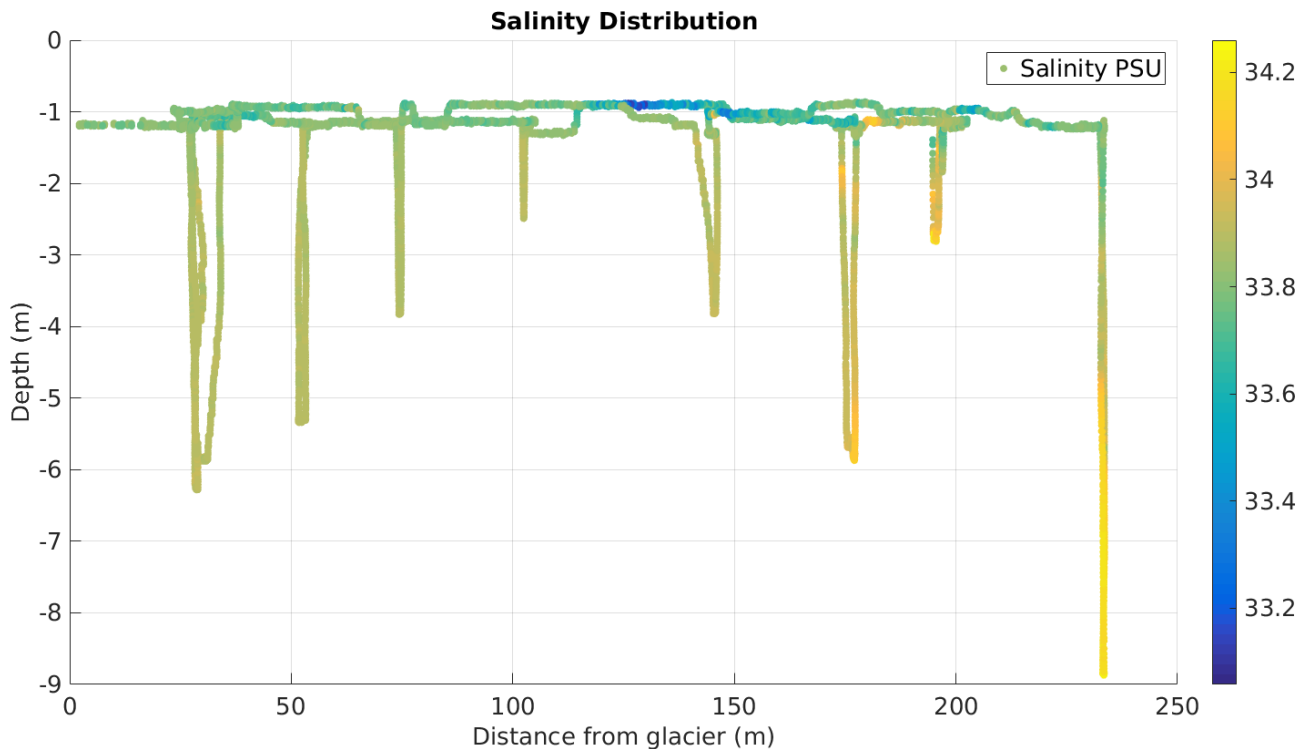


Figure 4.34 - Variation in Salinity (PSU; yellow = high salinity; blue = low salinity) as a function of depth (m, y-axis) and distance from the front of the glacier (m, x-axis).

The graph in Figure 4.33 shows the variation in temperature ($^{\circ}\text{C}$; yellow = warm; blue = cold) as a function of depth (m, y-axis) and distance from the front of the glacier (m, x-axis) while the graph in figure 4.34 represents the variation of salinity (PSU; yellow = high salinity; blue = low salinity) as a function of the depth (m, y-axis) and the distance from the front of the glacier (m, x-axis).

From the observation of the graphs of these two parameters, we can see an area around 130-150 m away from the glacier front and at the water surface which is characterised by higher temperature and lower salinity.

To better understand the situation, the distribution of the temperature trend ($^{\circ}\text{C}$, x-axis) as a function of the depth (m, y-axis), indicating with red color the data corresponding to the surface water masses and with the scale of the colors (blue = near; yellow = far) the distance from the front of the glacier, is shown in Figure 4.35.

A similar graph, which shows the salinity trend (PSU, x-axis) as a function of the depth (m, y-axis), indicating with red color the data corresponding to the surface water masses and with the color scale (blue = near; yellow = far) the distance from the front of the glacier, is displayed in Figure 4.36.

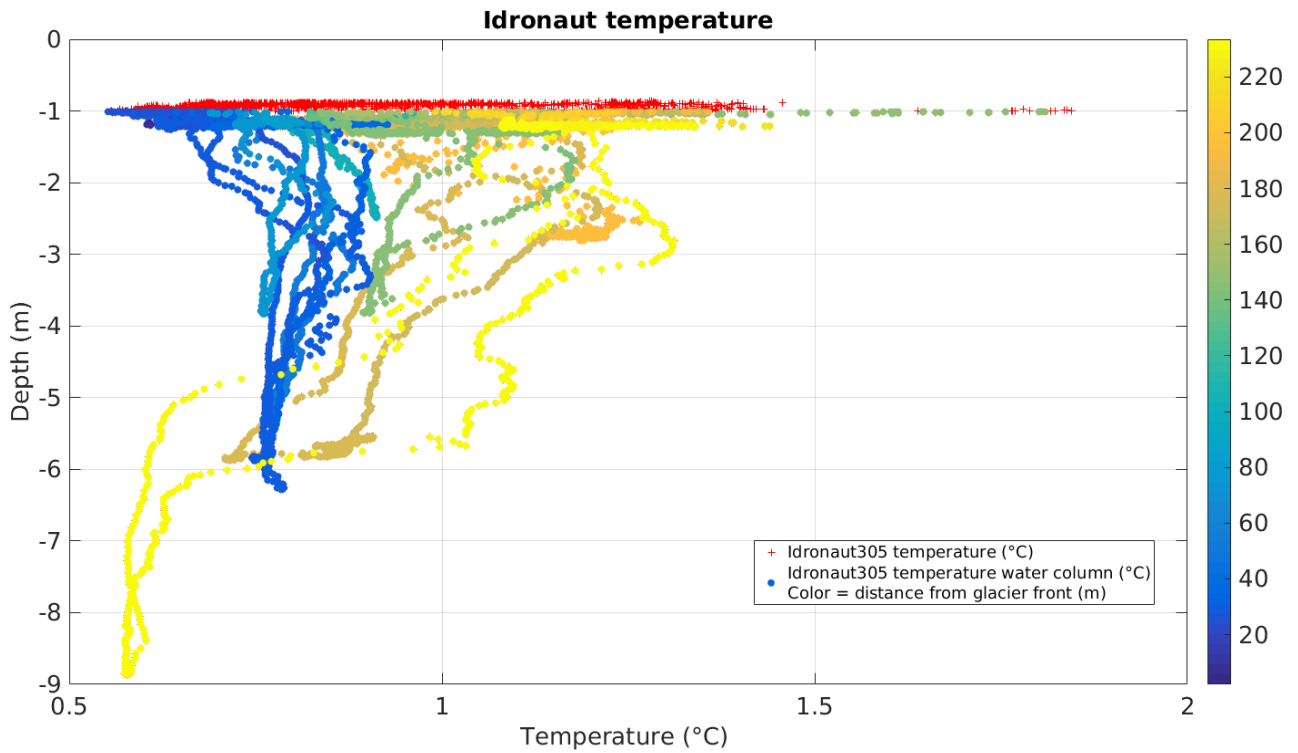


Figure 4.35 - Temperature trend ($^{\circ}\text{C}$, x-axis) as a function of the depth (m, y-axis); red cross represent data corresponding to the surface water masses; the scale of the colors (blue = near; yellow = far) indicates the distance from the front of the glacier.

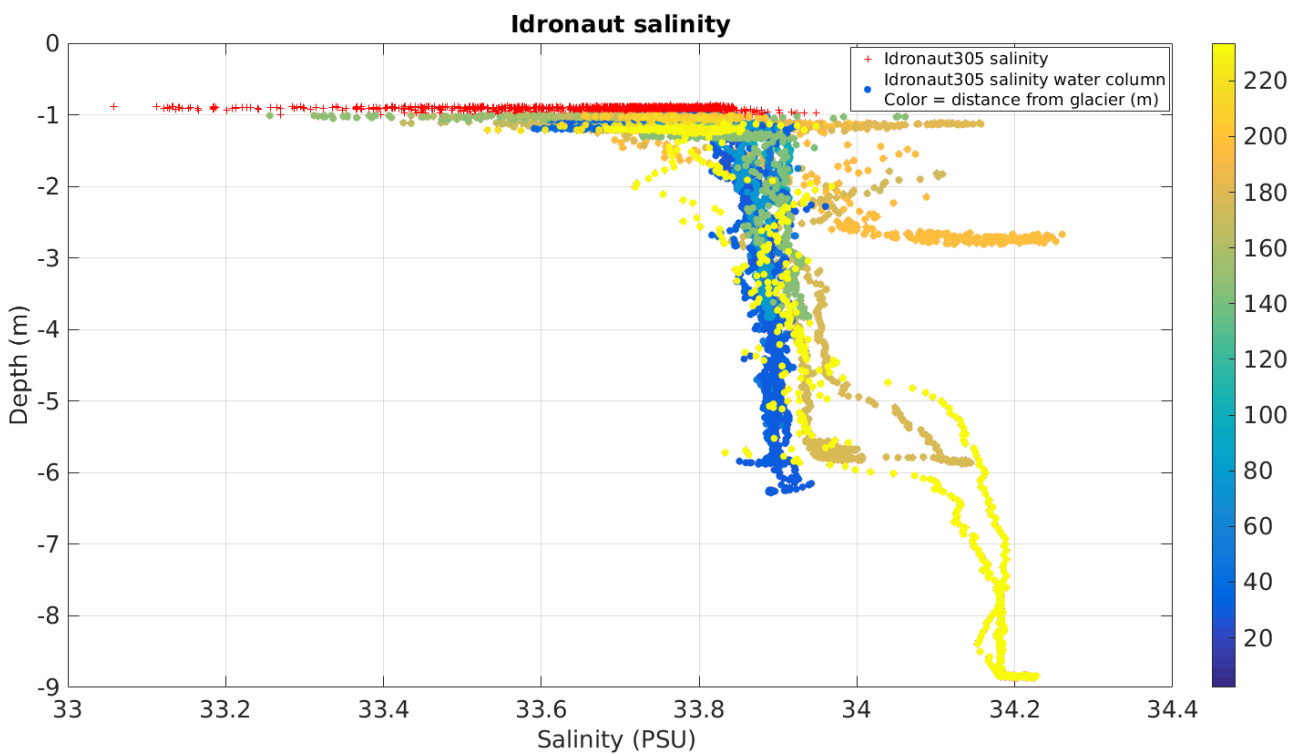


Figure 4.36 - Salinity trend (PSU, x-axis) as a function of the depth (m, y-axis); red cross represent data corresponding to the surface water masses; the scale of the colors (blue = near; yellow = far) indicates the distance from the front of the glacier.

From these graphs it is possible to observe the presence of surface water at higher temperature and lower salinity with respect to the surrounding trend, as already visible in Figures 4.33 and 4.34.

In addition, analysing the trend of the two parameters as a function of depth, a clear separation between the mass of water closest to the front of the glacier and the more distant one is visible. It is also possible to notice at about 230 m from the glacier front an area characterised by decreasing temperature values and at the same time increasing salinity values. This fact could be explained assuming the presence of a different kind of water mass in this area.

The separation into distinct water masses is even more evident analysing the T-S graphs that represent both variables (temperature and salinity) as a function of the depth in Figure 4.37 and of the distance from the glacier front in Figure 4.38.

In Figure 4.37, the vertical stratification of the water mass, consisting of a surface layer of warmer and less salty water and of a colder and saltier layer at greater depth, is clearly evident.

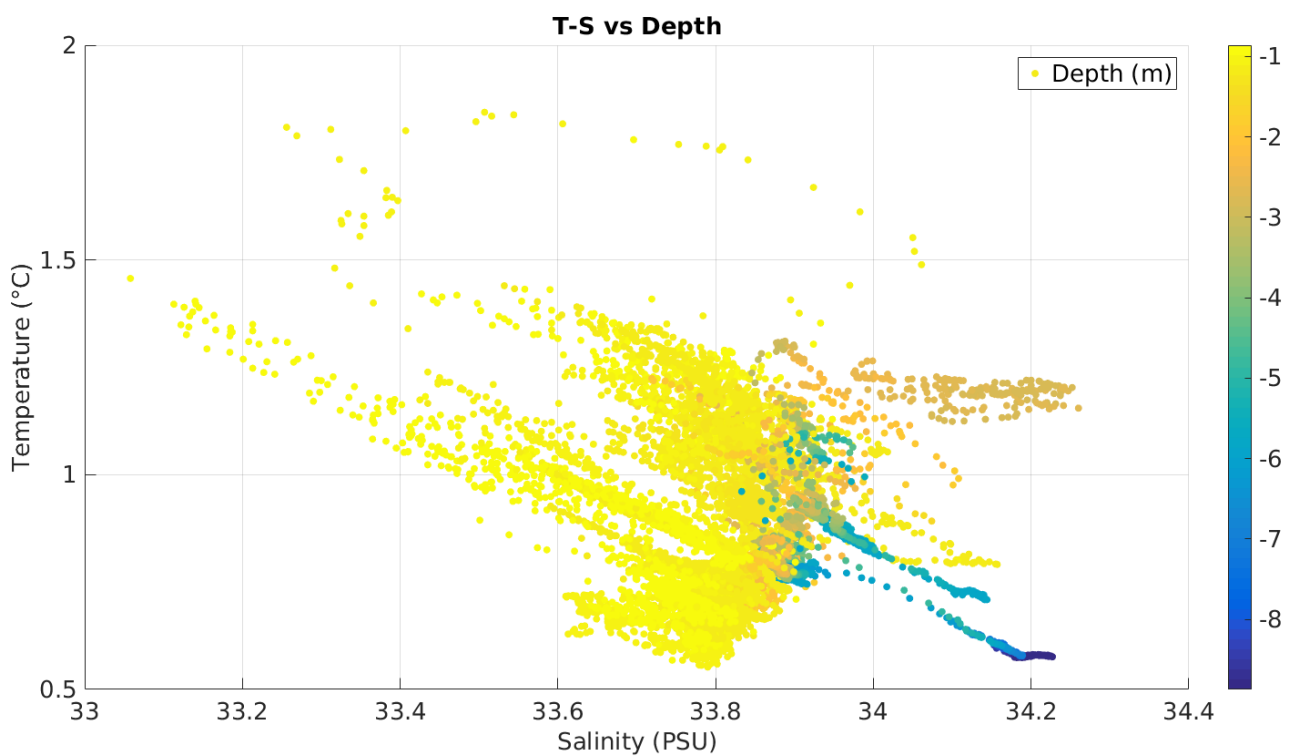


Figure 4.37 - T-S diagram: temperature (°C, y-axis) is plotted versus salinity (PSU, x-axis). The color scale is proportional to depth values (m): yellow = surface; blue = high depth.

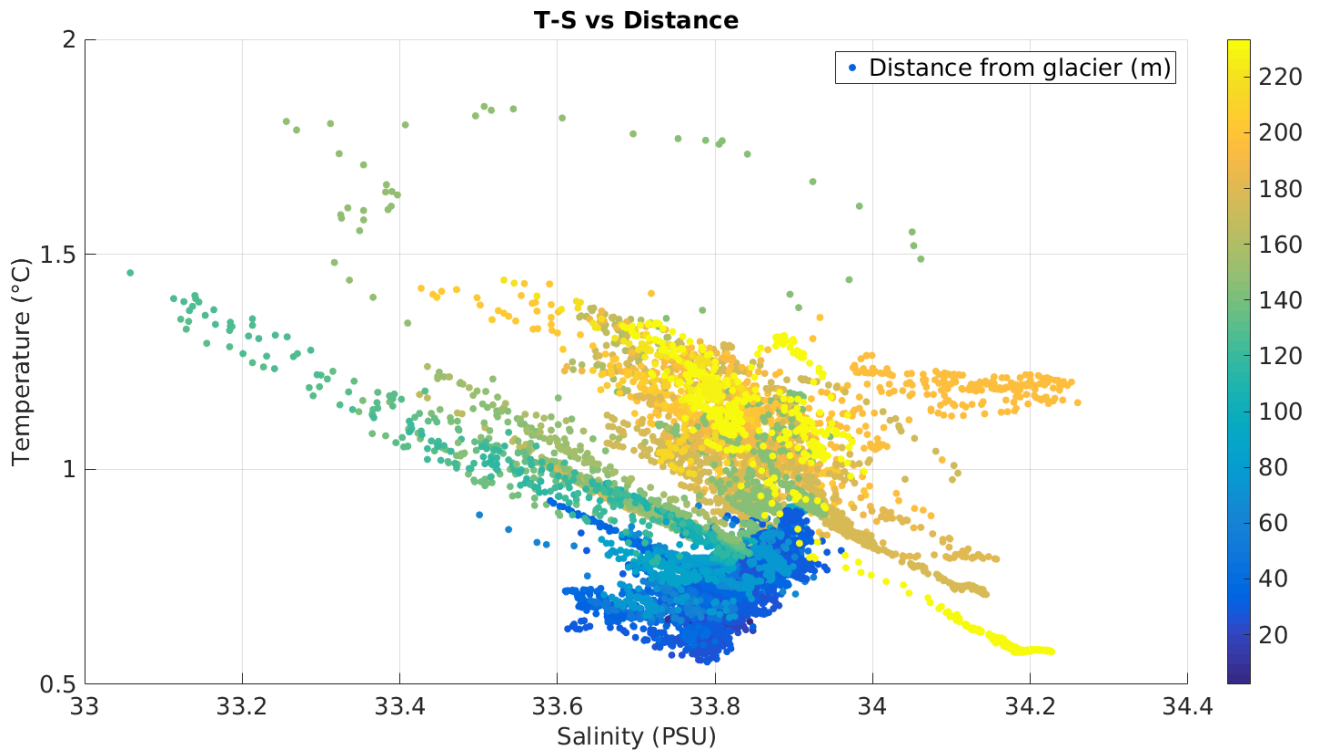


Figure 4.38 - T-S diagram: temperature (°C, y-axis) is plotted versus salinity (PSU, x-axis). The color scale is proportional to distance from the glacier front (m): yellow = far; blue = near.

In Figure 4.38 it is perfectly distinguishable an area close to the front of the glacier (blue-green dots), characterised by water mass at an average temperature below 1 °C and salinity around 33.8 PSU and a second area (orange-yellow dots) at a greater distance from the glacier, characterised by mass of water on average above 1 °C and salinity values slightly higher than the other mass. Still in this graph, the presence of at least two areas where the parameters' values stand out from the rest and which have already been highlighted by some previous graphs, is visible:

- at about 130-150 m from the glacier there is a surface mass with low salinity and slightly higher temperature than the average in that area;
- at about 230 m from the front of the glacier the presence of a deeper water mass characterised by low temperature and high salinity is noted.

To understand what type of water mass is observed, it is necessary to study also other chemical-physical parameters of the water. The area near the Blomstrandbreen front is confirmed as a complex and interesting area, due to the presence of freshwater from the melting glacier, of water from the inner fjord and also of water from the Atlantic current. This mix of different types of water, the balance of which varies according to the season, has a significant influence on life in the marine environment and consequently on the entire ecosystem. For these reasons, turbidity and chlorophyll-a values are also analysed.

The graph in Figure 4.39 show higher turbidity values in the area near the glacier front (distances < 150 m) and decreasing trend with the depth.